A PETROLOGICAL/GEOCHEMICAL STUDY

OF ROCKS FROM THE SÃO MIGUEL

DRILLHOLE, SÃO MIGUEL, AZORES

by

PATRICIA A. MCGRAW

Submitted in partial fulfillment of the

requirements of Master of Science Degree

at Dalhousie University, March, 1976.

EXAMINERS:

_____   ___   _____

_____   ___   _____

DALHOUSIE UNIVERSITY

Date____April, 1976____

Author____Patricia Ann McGraw_____

Title____A Petrological/Geochemical Study of Rocks From the_____

____São Miguel Drillhole, São Miguel, Azores, Portugal._____

_____

Department or School_____Geology Department_____

Degree___M.Sc.____ Convocation____Spring____ Year____1976____

Permission is herewith granted to Dalhousie University to circulate and to have copied for non-commercial purposes, at its discretion, the above title upon the request of individuals or institutions.

_____
Signature of Author

THE AUTHOR RESERVES OTHER PUBLICATION RIGHTS, AND NEITHER THE THESIS NOR EXTENSIVE EXTRACTS FROM IT MAY BE PRINTED OR OTHERWISE RE-PRODUCED WITHOUT THE AUTHOR'S WRITTEN PERMISSION.

(i)

TABLE OF CONTENTS

ABSTRACT

Thirty-six rock units sampled from a 980 m borehole drilled into the island of São Miguel, Azores were analysed for major and trace elements. Twenty-four basalts, two trachybasalts, four trachytes, two intrusives, and four pyroclastic units are represented. Electron microprobe analyses of olivine, clinopyroxene, and plagioclase phenocrysts were made.

The chemical and microprobe studies indicate that the rocks are of alkaline affinity. A lack of rocks of intermediate chemical compositions is demonstrated and is considered to represent a Daly Gap for the volcanic flow units. However, the pyroclastic units appear to have chemical compositions intermediate to the trachytes and trachybasalts.

Projections in the CMAS system show a probable equilibration of the basalts at one atmosphere pressure with an enrichment in plagioclase phenocrysts.

ACKNOWLEDGEMENTS

CHAPTER 1: INTRODUCTION

i) Location of Study

  In 1972, a program was initiated by the scientists
of Dalhousie University and Lamont-Doherty Geological
Observatory which involved deep drilling into oceanic
islands in order to better understand their structure,
petrology, and geochemistry. The initial project consisted
of the drilling of an 800 m. hole into the island of Ber-
muda. The Deep Drill Project for the summer of 1973
involved the drilling of a borehole into the island of
São Miguel, Azores, Portugal. This thesis is a study of
the rocks from that drillhole.

  The Azores consist of a group of nine islands
stretching from west to east across the Mid-Atlantic Ridge
between 37° and 40°N latitude and 32° and 25°W longitude.
Corvo and Flores are on the west flank of the Mid-Atlantic
Ridge, while Faial, São Jorge, Pico, Graciosa, Terceira,
São Miguel and Santa Maria trend from northwest to south-
east across the eastern flank of the Ridge (Figure 1).

  The drillhole was located at 25°31.4'W, 37°48.9'N,
approximately 5 km from the main crater on the northwest
flank of the volcano of Agua de Pau (Figure 3, Chapter 2).
The surface area immediately around the borehole is covered
with trachytic ash. The core consisted of 981 m of sub-
aerial and submarine lavas and pyroclastics.
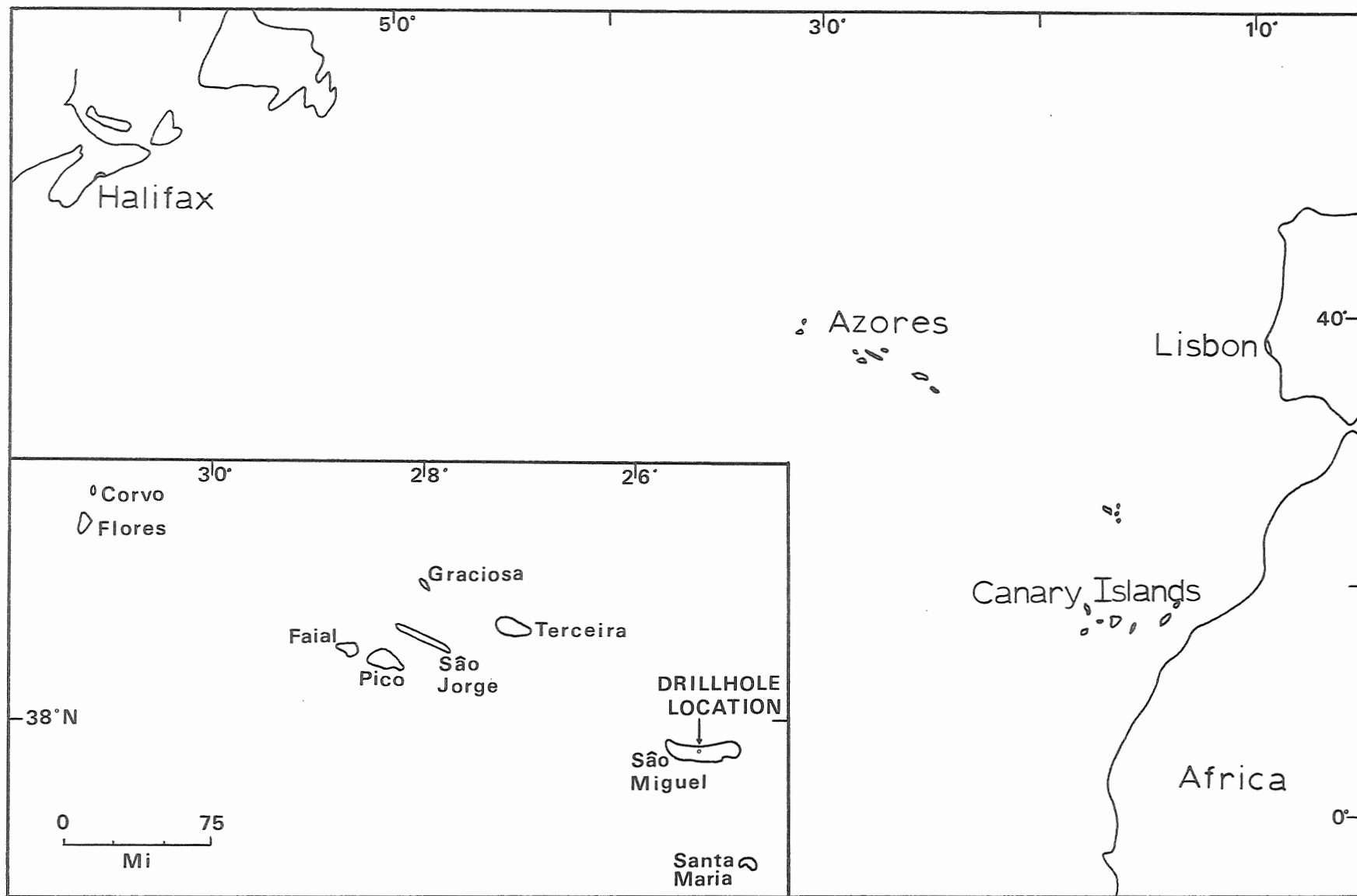
FIGURE 1: Location map.

ii) Purpose of the Thesis

This thesis includes petrological, mineralogical, and geochemical studies of the rock units recovered from the borehole, with major interest centred on the volcanic flow units. Forty-three rock units consisting of four pyroclastics, two intrusives, and thirty-seven lavas were chosen for major and trace element geochemical analysis. Petrographic descriptions of the volcanic flow units and of the intrusive units were also made.

The data obtained have been studied for chemical variations with depth in the core, and have been compared with available data from other oceanic islands, including others in the Azores Group.

CHAPTER 2: GEOLOGICAL SETTING

i) Regional Tectonics

The position of the Azores as an island group astride the volcanically active Mid-Atlantic Ridge makes their tectonic setting particularly pertinent to a discussion of their geology in terms of present theories about plate tectonics. The tectonic features in the region are of importance in understanding the occurrence and nature of the magmatism at this particular spot within the ocean basin.

Krause and Watkins (1970) have recognized five morphological features in the Azores area (Figure 2): (1) the presence of the East Azores Fracture Zone, which is seismically active; (2) the presence of the West Azores Fracture Zone, which is seismically inactive; (3) the Azores island chain which extends transversely across the Mid-Atlantic Ridge; (4) the change of trend of the Mid-Atlantic Ridge just south of its intersection with the Azores; and (5) the broadening of the Mid-Atlantic Ridge into the Azores Platform on the eastern flank of the ridge. These features are important in terms of the igneous and tectonic history of the area, and will be discussed briefly in the following paragraphs.

(1),(2) The East Azores Fracture Zone is part of the Alpide Tectonic Zone which extends through the Mediterranean Sea westward from Gibralter to connect with the Mid-

3
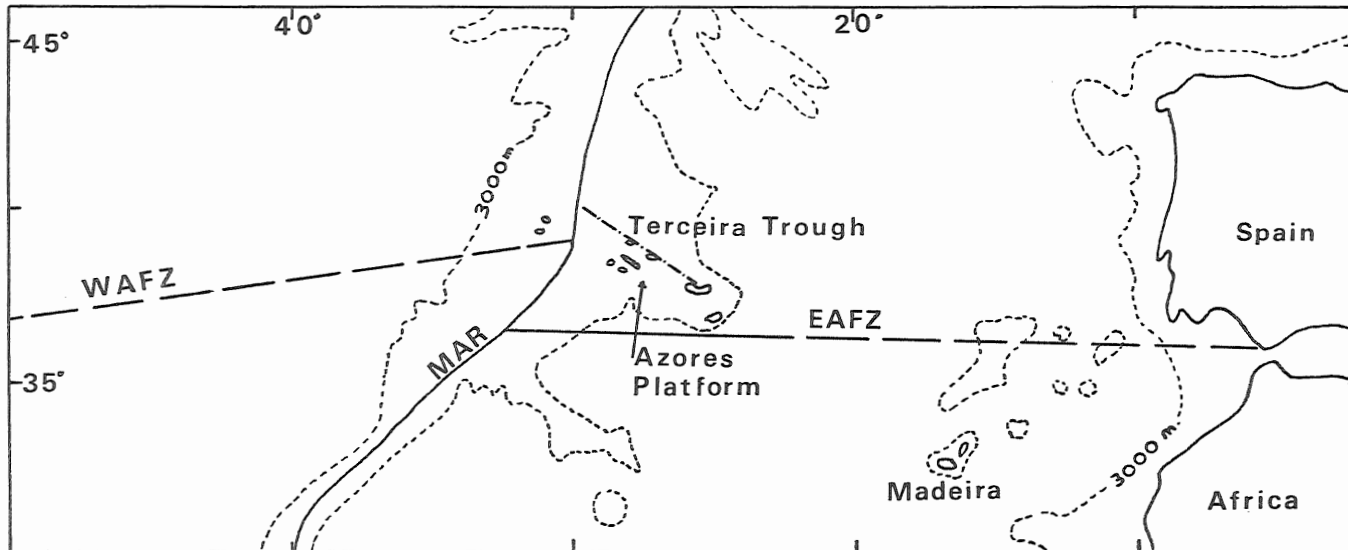
FIGURE 2: Tectonic features of Azores area showing the Mid-Atlantic Ridge [MAR], the East Azores Fracture Zone [EAFZ], and the West Azores Fracture Zone [WAFZ]. The 3000 m submarine contour line is included.

Atlantic Ridge in the vicinity of the Azores. The Fracture
Zone is offset northwards at the Ridge, continues westward
as the West Azores Fracture Zone, and terminates at 38°N
latitude at Corner Rise in the Kelvin Seamounts (Krause,
1965). The East Azores Fracture Zone is seismically active;
the West Azores Fracture Zone is aseismic (Heezen, 1962;
Krause and Watkins, 1970).

(3) The nine islands of the Azores Group are separated
into two groups by the Mid-Atlantic Ridge. Corvo and Flores
are on the west flank of the Ridge and the remaining islands
stretch across the east side of the Ridge. The line of
islands has been interpreted by Krause and Watkins (1970)
as representing a linear tensional axis. They see the
Terceira Trough, which extends from the Ridge through
Terceira towards Sao Miguel (Figure 2) as a secondary spread-
ing centre to the Mid-Atlantic Ridge.

(4),(5) The Mid-Atlantic Ridge changes direction
from trending north-south above approximately 38°N latitude
to trending northeast-southwest below 38°N latitude. There
is also a broadening of the Ridge known as the Azores Plat-
form represented on Figure 2 by the 3000 m depth contour, in
the area of the Azores (Krause, 1965). This area is charac-
terized by a positive free air gravity anomaly relative to
hydrostatic equilibrium (Kaula, 1972).

The tectonic features described above have been inter-
preted by Krause and Watkins (1970) and by others as a triple
junction in which the two sections of the Mid-Atlantic Ridge

act as spreading centres, and the East and West Azores

Fracture Zones are transform faults. The Terceira Trough

is viewed as a secondary spreading centre. Morgan (1971)

has proposed the existence of a mantle plume located under-

neath the Azores; Schilling (1975) has inferred the existence

of a mantle "blob". The evidence for such a plume or blob

will be discussed in a later chapter.

ii) Geology of São Miguel

São Miguel is composed of volcanic rocks, with pumice

and ash comprising the greater area of surface covering on

the island. As shown on the geological map of São Miguel

(Figure 3), the major volcanic centres are: Sete Cidades,

Agua de Pau, Furnas, and Provoacao of the Nordeste Complex.

Historic eruptions have been recorded for all but

Provoaçao. Numerous volcanic events, both subaerial and

submarine that have occurred in the area of the Azores are

presented as Figure 4 after Ridley et al. (1974, Figure 5,

p. 450). The locations and dates of these eruptions are

shown. The data were based on a compilation made by Weston

(1964).

Sete Cidades is composed chiefly of a large composite

cone with a summit caldera. The slopes of the volcano are

made up chiefly of trachytic pumice. The smaller cinder

cones are basaltic in nature. The lavas of the main cone

are classed as "olivine andesites" in Portuguese usage, but

they appear to have the chemical composition of basalts.
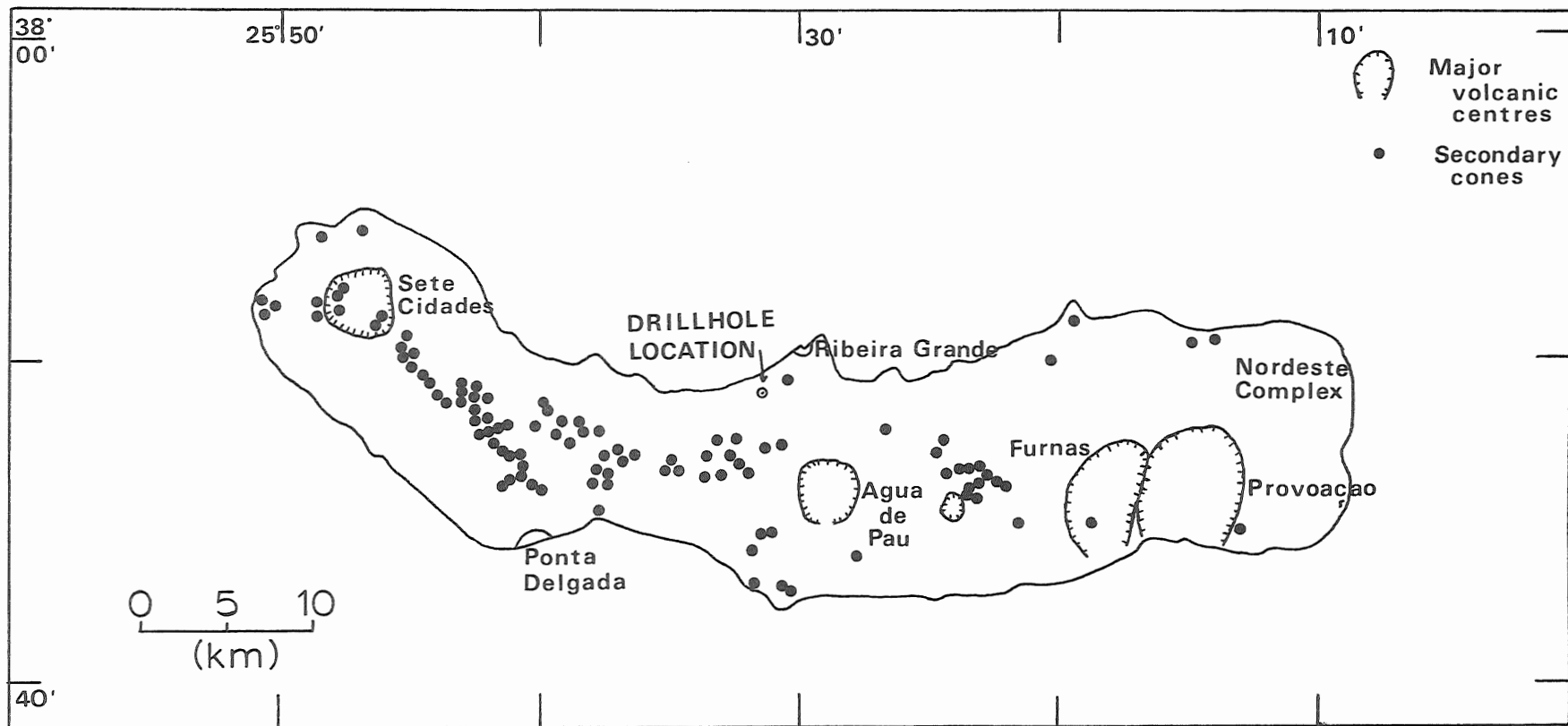
FIGURE 3: Primary and secondary volcanic centres on São Miguel (after Ridley et al [1974]).
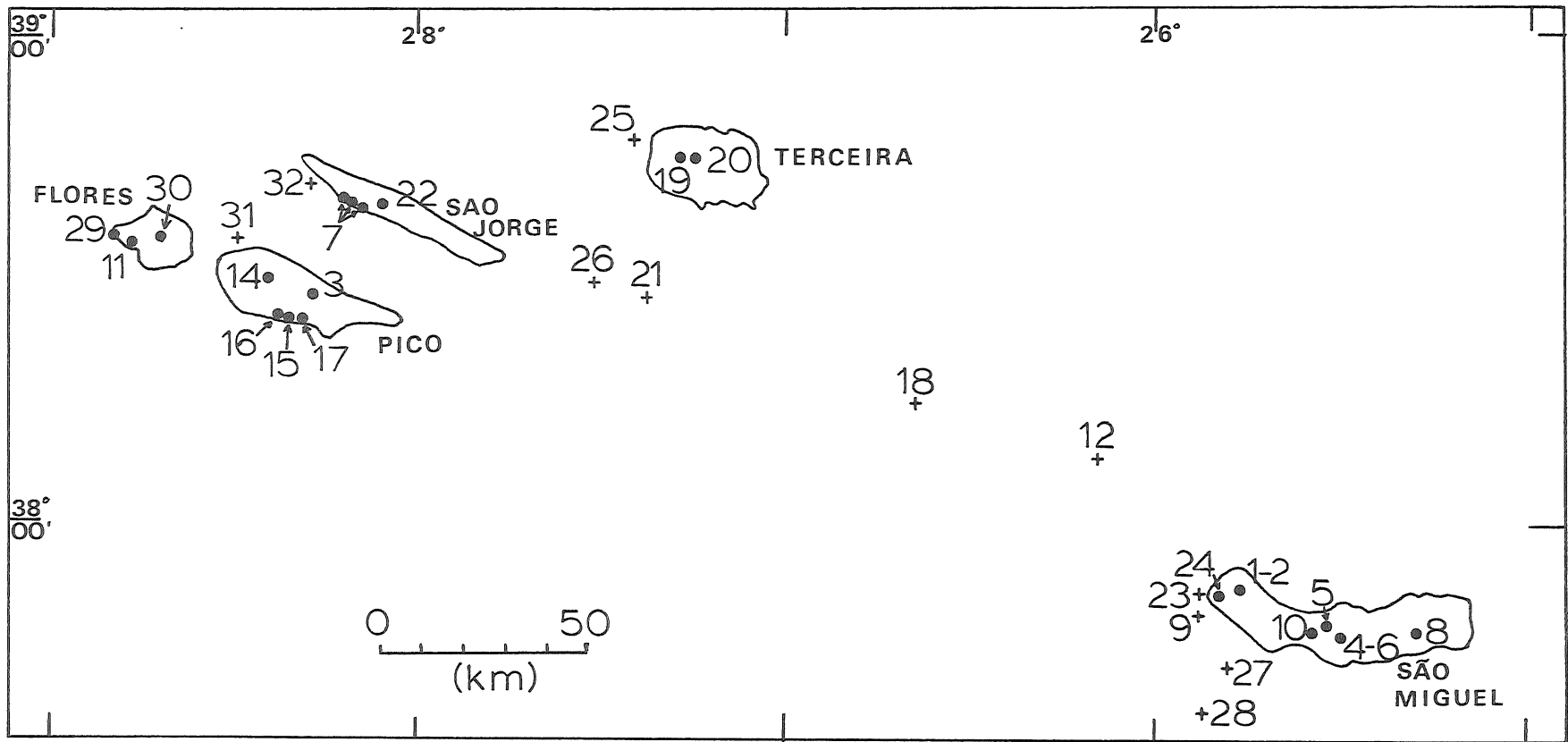
FIGURE 4: Recorded volcanic eruptions in the central Azores area from Ridley et al [1974] after Weston[1964].

Dates of the eruptions: 1439[1], 1460[2], 1562[3], 1563[4,5], 1564[6], 1580[7], 1630[8], 1638[9], 1652[10], 1672[11], 1682[12], 1713[13], 1718[14,15,16], 1720[17,18], 1761[19,20], 1800[21], 1808[22], 1811[23], 1861[24], 1867[25], 1902[26], 1907[27], 1911[28], 1957[29], 1958[30], 1963[31], 1964[32].

There are also some alkaline trachytes and younger basaltic lavas.

Agua de Pau is centrally located on the island of São Miguel. It is in the form of a composite volcano with a summit caldera. An historic eruption occurred in 1563 with a Plinian cloud which covered much of the island with ash before lava erupted from the northwest flank (Machado, 1967). A lava eruption also occurred in 1652. The lavas which form the main cone are basaltic and are covered by trachytic flows. Basaltic lavas are present in the younger vents. Walker and Croasdale (1970) have studied four trachytic pumice layers, the oldest dated at 4600 years B.P. obtained by the dating of a carbonized wood sample.

Furnas and Provoaçao are found adjacent to each other on the southeast end of São Miguel. Provoaçao is considered extinct since there have been no recorded eruptions from this site. Furnas erupted in 1630 with a violent pumice explosion (Machado, 1967). The older lavas of these volcanoes are basalts which are covered in places by trachytic flows. Abdel Monem et al. (1968) have dated the basalt flows of the Nordeste complex on the east end of São Miguel at ages between 1.92 and 2.15 m.y.

In addition to the major volcanic centres noted above, a feature noticeable on Figure 3 is the presence of many smaller volcanic cones located both within the larger calderas and on their flanks. Much of the surface character of

São Miguel consists of these smaller volcanic cones which form lineaments, apparently along fissures extending out from the main volcanic centres. A photograph of the Agua de Pau area illustrates this feature (Plate 1).

Fumarolic activity is another notable volcanic feature of São Miguel. Hot springs are found in the north central section of the island in the region of Agua de Pau, and also on the southeastern section at Furnas (Plate 2). Sulphur is deposited at both locations.

Geological correlation of the volcanic units on the island are hindered by the use of every available plot of land for agriculture (Plate 3). In the absence of cultivation, the land is covered by natural vegetation which grows profusely in response to the extremely humid climate. Thus, there is very little outcrop of lavas in the vicinity of Agua de Pau and very little outcrop other than pyroclastic material on the island as a whole. Some flows are visible on the eastern side of the island in the Nordeste Complex, but it is impossible to trace rock units from one area to another. Alternating basic flows and pyroclastic units are exposed in the cliffs on the western end of the island (Plate 4), but they are inaccessible. In addition, there is exposure on the north and south coasts, but it is not readily accessible in all cases.

The rock units which are exposed on the island are both trachytic and basaltic in nature. The trachytic flows

PLATE 1:   Secondary volcanic cones forming lineaments.

Photograph looking west from Agua de Pau.

PLATE 2: Fumarolic activity at Furnas.

PLATE 3:   Natural vegetation and cultivation of the

island of Sao Miguel.   Photograph of the

east end of the island.

PLATE 4:   Alternating flows and pyroclastics in a cliff

exposure on the west end of Sao Miguel.

are in most cases porphyritic with feldspar laths up to 1 cm length present. On the eastern end of the island in the Nordeste Complex, several basic lavas containing aggregates of green pyroxene phenocrysts are exposed. There are several flow units in the core which show similar pyroxene aggregates, but they are present at a greater depth than the surface outcrops, and are of different ages (Muecke et al., 1974; Abdel-Monem et al., 1968).

At Serra Agua de Pau, 15 km east of the town of Ponta Delgada, ejected syenitic blocks have been reported to occur (Cann, 1967). These blocks contain mineral assemblages of sanidine-arfvedsonite-quartz-aegirine-fayalite-astrophyllite-dalyite-pyrrhite, and sometimes with biotite-zircon replacing the astrophyllite-dalyite.

It is apparent from this brief outline that the surface geology of São Miguel shows a variety of volcanic activity. The sampling of rocks from just one drillhole can obviously provide only the minimum indication of the vertical distribution of the varied and multitudinous volcanic products present on the island, but it does augment our knowledge about the evolution of this volcanic island.

CHAPTER 3: PETROLOGY/PETROGRAPHY

i) A Summary of the Rock Sequence

The rocks retrieved from the borehole comprise a complex sequence of lava flows, pyroclastics, agglomerates, and breccias, which are denoted by the letters AUL, AUA, AUG, and AUB, respectively. Several intrusive units have also been recognized and are labelled with the letters AUS. Much of the descriptive material in the following section has been taken from the core log, with additional observations and interpretations added as necessary.

The rock units are numbered according to the core box in which they first appear. For example, AUL 006.1 means that the unit is a flow which starts in core box number 6 as the first new recognizable unit in that core box. The second recognizable unit in core box 6 would be labelled AUL 006.2, if it were a flow unit, or AUA 006.2 if it were a pyroclastic unit, etc.

The volcanic flows are massive basaltic or trachytic rock units which may have autobrecciated or vesicular tops. They are usually separated from one another by ash beds or brecciated tops. They have a limited colour range from grey-brown to green.

The units which are labelled pyroclastics consist chiefly of fine-grained to medium-grained ash material, sometimes containing flattened pumice fragments.

Bedding is rarely seen, although size gradations are sometimes visible. The category "pyroclastics" also includes ignimbrites.

The agglomerate units consist of pebble-sized, slightly rounded to subangular trachytic or basaltic rock fragments which are contained in a matrix of fine-grained ash. Some of the units are graded.

The intrusives are recognized by the occurrence of chilled margins in abrupt contact with the flow units into which they intrude. The contacts dip steeply in some places. The intrusives are fine-grained, green-grey in colour, and some contain large feldspar phynocrysts. Subsequent analyses have shown them to have trachybasaltic compositions.

Basaltic breccia units are recognized to consist of brown, grey, and maroon angular basalt fragments contained in a chloritic matrix. The matrix can also be calcitic, hematitic, or clayey in nature. Subhorizontal bedding is recognized in some units and is indicated by the presence of size grading. AUB 118.2 is striking in that it consists of basalt fragments contained in a lithic sand-stone matrix with a carbonate-quartz cement.

Muecke et al. (1974) have noted the following divisions within the core (Figure 5): Subaerial Sequence III, 0 - 268.4 m; Subaerial Sequence II, 268.4 - 428.6 m; Subaerial Sequence I, 428.6 - 762.8 m; Transition Sequence,
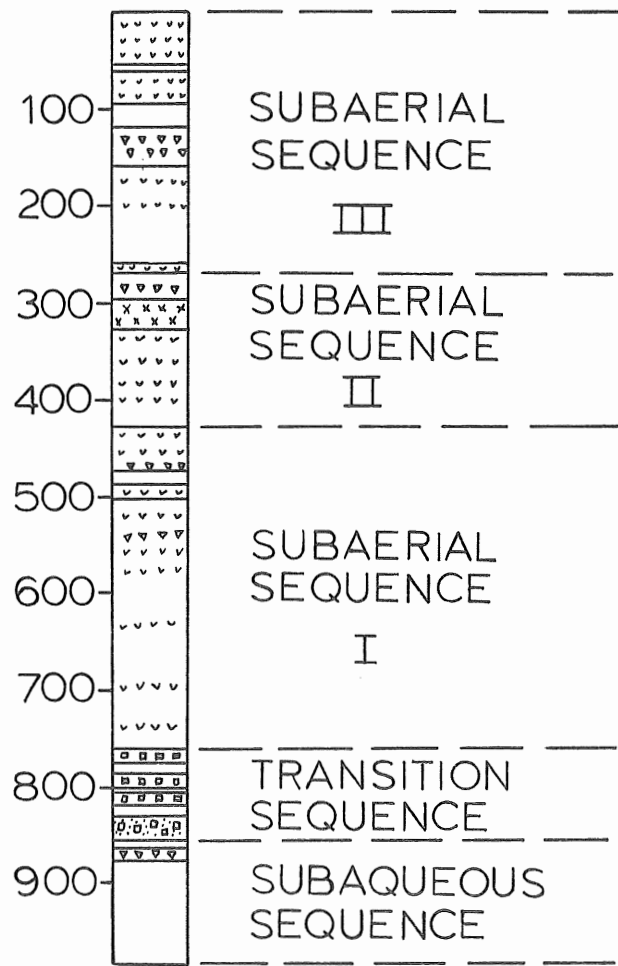
LEGEND

Ash, Ignimbrites
Basalt
Agglomerate
Trachytic Lavas
Basalt Breccia
Basalt Breccia and "Sandstone"

FIGURE 5: Core log showing major units and recognized sequences.

762.8 - 856.8 m; and Subaqueous Sequence, 856.8 - 980.5 m.
Possible changes suggested from the study of the opaque
minerals (Abdel-Aal, personal communication) would increase
the thickness of the Transition Sequence. The subaerial
material is distinguished from the submarine rocks by the
lack of pillow structures, the absence of evidence indi-
cating re-working of the pyroclastic units, the presence
of some lateritic horizons, and the occurrence of vesicular
and auto-brecciated flow tops. The subaerial sequences are
separated from each other by the presence of thick pyro-
clastic units (Figure 5). The transition series is unique
in containing sedimentary-type rocks interbedded with
basaltic flow units. The submarine sequence contains pillow
basalts and exhibits a lack of pyroclastic units.

In Subaerial Sequence III, 25 flow units have been
recognized as well as 15 pyroclastic units and 5 agglomerate
units. With the exception of the first flow unit (AUL001.2),
the flows appear to be basaltic in nature. Pyroxene pheno-
crysts, both singly and as glomeroporphyritic aggregates,
are visible in some flow units (AUL's 020.1, 020.3, 022.2,
024.1, 025.5). The pyroclastic units vary in nature from
trachytic to red or green altered ash material. Some of the
pyroclastics are ignimbrites (AUA 025.1, 025.2, 025.3,
025.4). A notable increase in temperature of 3 - 5° C
above the ambient temperature was noted at the time of
extraction of the core at 217.5 m, at flow unit AUL 014.3,

which was noted to be highly brecciated with slickensides
visible on the surfaces of the fragments, indications of
the occurrence of a fault in this area. This suggests that
the rise in temperature and the faulting could be related.
A 5° C elevation in temperature was recorded at 261.1 m
in the vicinity of flow units AUL 022.2 and 024.1. It
must be noted that these temperatures are not reliable
indicators of in situ temperatures.

Subaerial Sequence II contains the remaining 3
trachytic flow units uncovered in the core. AUL 030.4,
031.1, and 036.1 occur in sequence between 290.8 m and
327.9 m at the top of Subaerial Sequence II. There are 28
volcanic flows in this direction, 25 of which are basaltic
in appearance and chemistry. There are 17 pyroclastic units
in Subaerial Sequence II, most of which are trachytic.
AUA 026.1, 026.2 and 049.2 are ignimbrites. Two agglomerates,
AUG 027.3 and AUG 030.3, are present, both of which contain
trachytic fragments.

Subaerial Sequence I is the thickest (333.7 m)
sequence in the core. According to the core log this
sequence contains 68 flow units, 36 pyroclastic units, 4
agglomerates, 6 intrusives, and 1 breccia unit. However,
AUS 097.1 and AUS 097.4, and, AUS 098.4 and AUS 098.5,
could represent the same unit cut twice by the core, re-
ducing the number of intrusives to 4. The flow units are
mainly basaltic, but trachybasalts were analysed from the

section between 650 and 700 m. The pyroclastics are mostly trachytic, and 15 of these have been identified as ignim-brites. This is the only section in which intrusive units have been recognized. The intrusives are thin units, with plagioclase phenocrysts present. Chemical analysis have revealed these intrusives to be close in composition to the trachybasalts.

The Transition Sequence starts at 762.8 m and extends to 867.3 m. This section consists of 12 breccia units, 8 flow units, 1 pyroclastic unit, and 1 agglomerate unit. The breccia units consist of angular basalt fragments in matrices of either chloritic or reddish hematitic material, with some localized sections of calcitic or clayey matrix. Some of the material is sedimentary in appearance, with a matrix of sand-sized particles which are volcanic in origin.

The Subaqueous Sequence begins at 867.3 m and extends to the bottom of the drillhole (980.5 m). This sequence is notable for its lack of pyroclastic units and in the presence of pillowed basalts with chilled margins. Most of the 13 flow units are porphyritic, containing pheno-crysts of plagioclase, olivine, and pyroxene.

ii) Hand Specimen/Thin Section Study

The rock units which were chosen for chemical analysis have been listed in Table 1, and only these units have been studied in detail in thin section. Since there

TABLE 1: Units chosen for chemical analysis.

SUBAERIAL SEQUENCE III: 0-268.4 m

ANALYSED UNIT	DEPTH	THICKNESS
AUL 001.2	56.7- 59.5 m	2.8 m
AUL 006.1	159.4-169.5	10.1
AUL 008.5	171.9-185.6	13.7
AUL 014.3	205.6-220.3	14.7
AUL 020.3	240.8-247.8	7.0
AUL 022.1	247.8-251.1	3.3
AUL 025.5	263.4-265.9	2.5

SUBAERIAL SEQUENCE II: 268.4-428.6 m

AUA 026.4	270.5-272.9	2.4
AUL 030.4	290.8-292.3	1.5
AUL 031.1	292.3-317.4	25.1
AUL 036.1	317.4-327.9	10.5
AUL 046.2	370.8-381.0	10.2
AUL 048.1	381.0-382.9	11.9
AUL 051.2	396.3-399.1	2.8

SUBAERIAL SEQUENCE I: 428.6-762.8 m

AUA 058.9	433.2-436.1	2.9
AUL 062.2	454.0-458.7	4.7
AUL 066.4	475.2-480.3	5.1
AUL 068.1	481.8-486.8	5.0
AUL 071.3	498.6-501.6	3.0
AUA 080.5	550.2-557.8	7.6
AUL 082.1	563.8-568.3	4.5
AUL 087.2	598.3-602.2	1.9
AUL 094.1	641.0-646.3	5.3
AUL 096.1	651.1-658.2	7.1
AUL 098.2	662.1-664.5	2.4
AUS 098.5	665.5-665.9	0.4
AUL 099.1	665.9-668.1	2.2
AUL 108.1	726.2-734.6	8.4
AUS 111.2	739.9-744.2	4.3
AUL 112.1	745.5-753.1	7.6
AUL 114.1	758.0-762.8	4.8

TRANSITION SEQUENCE: 762.8-856.8 m

AUL 124.1	821.7-829.5	7.8

SUBAEQUEOUS SEQUENCE: 856.8-980.5 m

AUL 134.1	884.3-894.1	9.8
AUL 136.1	900-4-907.4	7.0
AUL 138.1	913.2-939.7	26.5
AUL 143.1	947.3-952.5	5.2

are many similarities in thin section between the rocks of a given type, detailed petrographic descriptions of each flow unit would serve no purpose. Therefore, each rock unit which was sampled for analysis was summarized as to rock type, type of phenocrysts, type of groundmass grains, and texture of the groundmass. This information has been included as Table 2 which can be used to get an overall view of how each sample differs, and of how the mineralogy varies with depth in the core.

The basaltic flow units in the core are generally porphyritic with a fine-grained groundmass. Their colour varies from medium-grey to greenish-grey to brown. Plagioclase, olivine, and pyroxene are present as phenocrysts and occur as euhedral to subhedral grains both singly and as glomeroporphyritic aggregates. The amount of phenocrysts varies, and all three minerals are not present as phenocrysts in every flow unit.

The trachytes are generally fine-grained, grey, and porphyritic with feldspar phenocrysts. The intrusives are fine-grained, green to grey in colour, and show distinct, chilled margins where they are in contact with the volcanic flows into which they intrude. The intrusives are porphyritic, with feldspar phenocrysts which are up to 2 cm in length.

In thin section, five distinct rock types can be recognized: 1) subaerial basalts, 2) submarine basalts, 3) trachytes (alkali feldspar porphyries), 4) trachy-

basalts, and 5) intrusives.

a) Subaerial Basalts

The subaerial basalts generally possess a ground-
mass of feldspar microlites which are predominantly plagio-
clase. The microlites appear to be labradorite in composition,
varying from approximately An_{50} to An_{65}. Numerous small
irregular opaque grains and varying amounts of clinopyroxene
and olivine are also present as groundmass minerals. Apatite
almost always occurs as an accessory mineral. Some glass is
found in the groundmass. An X-ray study of the secondary
minerals found in vugs and fractures and in the groundmass
has been conducted, and has revealed that in altered samples,
most of the olivines have been replaced by Mg-rich mont-
morillonite which has subsequently been replaced by chlorite
(P. Sarkar, personal communication). No zeolites were found,
but various other phases including Ca-rich and Fe-rich mont-
morillonites, kaolinite, barite, anhydrite, fluorite,
hematite, limonite, calcite, and quartz were present as
secondary minerals in the vugs and fractures of some highly
altered samples.

The phenocrysts found in the subaerial basalts vary
in size and type. The clinopyroxenes are present as pheno-
crysts in just about every subaerial basalt. The most common
type found is a faint brown-coloured augite showing cleavage
traces, sometimes good euhedral outlines, and quite often,

zoning. Where zoning occurs, the rims of the pyroxene are darker brown, an indication of the increase of TiO_2 in the rims as noted in the microprobe analyses. Sometimes simple twinning is present, and even more rarely, hourglass structure. In basalt sample AUL 112.1, two types of pyroxene are present: a brown-coloured augite and a pale green pleochroic aegirine-augite. The aegirine-augite occurs only as phenocrysts, whereas the augite is present as phenocrysts and as small grains in the groundmass. Aegirine-augite is rerely seen in the other subaerial basalts.

Olivine is rarely found in these basalts as fresh grains. In general, the presence of olivine is inferred from relict grain outlines and the presence of chlorite. In several samples, iddingsite is present as an alteration product of olivine.

Plagioclase is frequently present as a phenocryst phase. It occurs as generally lath-shaped grains exhibiting polysynthetic twinning, and quite often occurs as aggregates of randomly-oriented individual plagioclase grains. In some cases, the plagioclase is mildly sericitized. The grains are found to vary in composition from labradorite to bytownite (approximately An_{60} to An_{75}). Normal zoning is found in some grains, but is not a very common feature.

The texture of the subaerial basalts varies from fluidal to sub-fluidal, showing an alignment of feldspar

microlites in the groundmass. In most cases, the flows are vesicular in parts, with the vesicles filled mainly with calcite and/or chlorite. Where chlorite is present, it is common for calcite to rim the vesicle and chlorite to fill the centre. Quartz is found in some of the vesicles of the flow units, but was present in only AUL 046.2 of the analysed units, and was of such small concentration that it was not seen as greatly contributing to the contamination of the sample.

b) Submarine Basalts

The submarine basalts vary little macroscopically from the subaerial basalts. In thin section, the opaque minerals of the submarine basalts occur as very fine needles in the groundmass, in direct contrast to the small, subequant grains found in the groundmass of the subaerial basalts. The presence of the needle-like opaques is first seen in AUL 131.1, the first submarine basalt encountered in the core. All of the basalts below AUL 131.1 (below 867.3 m) show this same feature.

In other respects, the submarine basalts appear to have a smaller grain size than the subaerial basalts, both in the phenocrysts and in the groundmass. There are no visible signs of a change in pyroxene composition, although the grains of clinopyroxene are more common in the groundmass of the submarine basalts. The

clinopyroxene appears to be slightly darker brown in colour in the submarine basalts. No pyroxenes of aegirine-augite composition were observed in the submarine flow units.

In general, the submarine basalts tend to be non-porphyritic. The phenocrysts tend to be small, where present, and composed of plagioclase, olivine, or clinopyroxene. In these basalts, as in the subaerial lavas, the presence of olivine is inferred from relict grains.

Submarine basalts rarely show good fluidal texture although, in some cases, the feldspar microlites in the groundmass are somewhat aligned. Vesicles are rare in the submarine basalts.

c) Trachybasalts

The trachybasalts differ from the basalts in having few phenocrysts of olivine or pyroxene, although some completely serpentinized relict grains of olivine were observed. Plagioclase is a common phenocryst in these trachybasalts. The composition of the plagioclase in both AUL 098.2 and AUL 099.1 varies between An_{50} (andesine-labradorite) and An_{66} (labradorite). There are some plagioclase phenocrysts which show much lower extinction angles, indicating the presence of two types of plagioclase, one more sodic than the other. Many plagioclase phenocrysts show normal zoning, making it difficult to obtain an accurate extinction angle. Some

of the grains have been partially sericitized.

The trachybasalts are porphyritic in texture, and also show fluidal texture of the groundmass feldspar microlites. Not all of the feldspar grains of the groundmass are twinned, possibly indicating that some potassium feldspar is present as a groundmass constituent. Some vesicles were observed, and were seen to vary in the amount of calcite and chlorite filling.

In summary, in comparison with basalts, trachybasalts are characterized by the occurrence of plagioclase as the common phenocryst phase, by the small amount of pyroxene and olivine both as phenocrysts and in the groundmass, and by a fluidal texture.

d) Trachytes

The trachytes (AUL 0012, 030.4, 031.1, and 0.36.4) differ from the basalts and the trachybasalts in having phenocrysts that are essentially all potassium feldspar rather than plagioclase, pyroxene, or olivine. Plagioclase is present only as a groundmass phase. Olivine and pyroxenes are lacking, except in the case of AUL 001.2, in which a large phenocryst of aegirine-augite was found, and small clinopyroxene grains were present in the groundmass.

All of the large phenocrysts appear to be potassium

feldspar present as the minerals sanidine and/or anortho-
clase. The sanidine is present as grey, subhedral feature-
less grains with very small axial angle ($2V = 0 - 4^{\circ}$), and
optically negative. In some cases, the sanidine phenocrysts
show square grain outlines, and very striking normal zoning.
Anorthoclase is also present, and in some cases exhibits
tartan twinning. Anorthoclase has been found as a secondary
mineral (P. Sarkar, personal communication).

The groundmass consists of feldspar microlites
which appear to be both potassium feldspar and plagioclase.
Small irregularly-shaped opaques are common as a ground-
mass constituent, as is a yellow material, probably
palagonite. Apatite grains are extremely uncommon.

The trachyte units show a trachytic to subtrachytic
texture in the alignment of the feldspar microlites in
the groundmass. The trachytes are vuggy in places, but in
general, they tend to be massive rather than vesicular.

e) Intrusives

The intrusives are distinctly different from the
extrusive lavas in that they have a very small grain
size, giving them almost a granular appearance. This
feature probably reflects a rapid cooling of these
units during intrusion since the intrusives with the
exception of AUS 111.2 are thinner than the basaltic flows.
In the groundmass, the feldspars occur as small

rectangular or square grains rather than as the needle-like and lath-shaped microlites of the volcanic rocks. The intrusives are porphyritic, with plagioclase comprising the phenocryst phase.

The intrusives, AUS 098.5 and 111.2 are close in composition to the trachybasalts, and as such, do not have phenocrysts of clinopyroxene or of olivine, although AUS 098.5 appears to contain some remnants of olivine grains. Some small grains of potassium feldspar appear to be present also.

TABLE 2: Summary of Thin Section Study

Note: The rock names used in this table and in the text of this thesis
were determined on the basis of thin section identification.
The nomenclature used is that of Borley (1974) and Wilkinson (1974).
The term "trachyandesite" is the potassic equivalent of a mugearite
and implies that the plagioclase contains less than 50% An. The term
"trachybasalt" implies that the plagioclase has An greater than 50%,
and is used as an equivalent to andesine basalt, olivine andesite, and
hawaiite, although hawaiite is usually used to denote a sodic nature,
and can have SiO_2 less than 50%.

| Sample & Depth | Rock Type | Phenocrysts | | Groundmass | | Texture |
		Common	Rare	Common	Rare	
AUL 001.2 56.7-59.5 m	TRACHYTE	Anortho- clase Sanidine	Aegirine- Augite Placio- clase	Feldspar Microlites Palagonite Opaques Hornblende	Biotite	Porphyritic
AUL 006.1 159.4-169.5 m	BASALT		Plagio- clase Augite	Opaques Feldspar Microlites Palagonite	Augite Chlorite Apatite	Subfluidal Amygdaloidal
AUL 008.5 171.9-185.6 m	BASALT	Plagioclase Augite	Biotite	Glass Palagonite Opaques Plagioclase Microlites	Hematite Apatite	Porphyritic Amygdaloidal
AUL 014.3 205.6-220.3 m	BASALT		Plagio- clase Olivine	Opaques Plagio- clase Microlites Palagonite	Apatite	Aphanitic

TABLE 2: Continued

Sample & Depth	Rock Type	Phenocrysts		Groundmass		Texture
		Common	Rare	Common	Rare	
AUL 020.3 240.8-247.8 m	BASALT	Plagio-clase Olivine Augite		Palagonite Opaques Plagioclase Microlites Augite	Apatite	Highly Porphyritic
AUL 022.1 247.8-251.2 m	BASALT	Olivine Augite		Opaques Augite Olivine Plagioclase Microlites Palagonite	Apatite	Porphyritic
AUL 025.5 263.4-265.9 m	BASALT	Olivine Augite		Olivine Apatite Opaques Palagonite Iddingsite Plagioclase Microlites	Augite	Subfluidal Vesicular
AUL 030.4 290.8-292.3	TRACHYTE	Sanidine	Anortho-clase	Opaques Feldspar Microlites Feldspar Laths	Hematite Biotite	Trachytic Porphyritic
AUL 031.1 292.3-317.4 m	TRACHYTE	Sanidine	Anortho-clase	Feldspar Microlites Opaques Chlorite	Hematite Quartz	Trachytic Porphyritic

TABLE 2: Continued

Sample & Depth	Rock Type	Phenocrysts		Groundmass		Texture
		Common	Rare	Common	Rare	
AUL 036.1 317.4-327.9 m	TRACHYTE	Sanidine	Anortho-clase	Opaques Feldspar Microlites	Calcite	Trachytic Porphyritic
AUL 046.2 370.8-381.0 m	BASALT		Olivine Augite Plagio-clase	Feldspar Microlites Opaques Hematite Palagonite Calcite Augite	Apatite	Subfluidal Vesicular
AUL 051.2 396.3-399.1 m	BASALT	Augite Olivine	Plagio-clase	Apatite Plagioclase Microlites Chlorite Opaques		Highly Porphyritic
AUL 062.2 454.0-458.7 m	BASALT	Augite	Olivine	Feldspar Microlites Opaques Palagonite Augite	Apatite	Porphyritic
AUL 066.4 475.4-480.3 m	BASALT		Augite Olivine	Opaques Plagio-clase Microlites Augite	Apatite	Aphanitic
AUL 068.1 481.8-486.8 m	BASALT	Augite	Aegirine-Augite	Opaques Augite Plagio-clase Microlites	Chlorite Hematite Apatite	Porphyritic Vesicular

TABLE 2: Continued

Sample & Depth	Rock Type	Phenocrysts		Groundmass		Texture
		Common	Rare	Common	Rare	
AUL 071.3 498.6-501.6 m	BASALT		Olivine Augite Plagio- clase	Plagio- clase Microlites Opaques Hematite Chlorite Augite	Apatite	Aphanitic Vesicular
AUL 082.1 563.8-568.3 m	BASALT	Augite	Olivine Plagio- clase	Opaques Augite Plagio- clase Microlites Chlorite	Olivine Apatite	Fluidal Vesicular
AUL 087.2 598.3-602.2 m	BASALT	Augite Olivine		Opaques Plagioclase Microlites Hematite Calcite Chlorite	Apatite	Fluidal Vesicular
AUL 094.1 641.0-646.3 m	BASALT	Plagio- clase Augite	Biotite Olivine	Feldspar Microlites Opaques Chlorite	Apatite	Porphyritic Vesicular
AUL 096.1 651.1-658.2 m	BASALT		Olivine Augite	Feldspar Microlites Chlorite Palagonite Glass	Augite Hematite	Aphanitic Vesicular

TABLE 2: Continued

Sample & Depth	Rock Type	Phenocrysts		Groundmass		Texture
		Common	Rare	Common	Rare	
AUL 098.2 662.1-664.5 m	TRACHY-BASALT	Plagio-clase	Olivine K-spar	Opaques Hematite Plagioclase Microlites K-spar	Chlorite Apatite	Trachytic Porphyritic
AUS 098.5 665.5-665.9 m	INTRUSIVE		Olivine Plagio-clase	Opaques Plagioclase Glass		Aphanitic
AUL 099.1 665.9-668.1 m	TRACHY-BASALT	Plagio-clase	Olivine K-spar	Plagioclase Microlites Opaques Chlorite	Apatite K-spar	Trachytic Porphyritic
AUL 108.1 726.2-734.6 m	BASALT	Augite	Olivine	Opaques Plagio-clase Microlites Augite Apatite	Chlorite	Porphyritic
AUS 111.2 739.9-744.2 m	INTRUSIVE		Plagioclase	Opaques Chlorite Calcite	Apatite	Aphanitic
AUL 112.1 745.5-753.1 m	BASALT		Augite Plagioclase Olivine	Opaques Plagio-clase Microlites Augite Chlorite	Apatite Biotite	Vesicular Fluidal

TABLE 2: Continued

Sample & Depth	Rock Type	Phenocrysts		Groundmass		Texture
		Common	Rare	Common	Rare	
AUL 114.1 758.0-762.8 m	BASALT		Olivine Augite Plagioclase	Opaques Plagio- clase Microlites Augite Chlorite	Apatite	Aphanitic Fluidal
AUL 124.1 821.7-829.5 m	BASALT		Plagio- clase	Plagio- clase Microlites Augite Palagonite Opaques	Apatite	Aphanitic Fluidal
AUL 134.1 884.3-894.1 m	SUBMARINE BASALT		Plagioclase Olivine Augite	Plagio- clase Microlites Opaques Chlorite Augite	Hematite Apatite	Aphanitic Slightly Vesicular
AUL 136.1 900.4-907.4 m	SUBMARINE BASALT		Plagioclase Olivine Augite	Opaques Plagio- clase Microlites Chlorite Augite	Hematite Apatite	Aphanitic
AUL 138.1 913.2-939.7 m	SUBMARINE BASALT		Plagioclase Olivine Augite	Opaques Plagio- clase Microlites Chlorite Augite	Apatite	Aphanitic

TABLE 2: Continued

Sample & Depth	Rock Type	Phenocrysts		Groundmass		Texture
		Common	Rare	Common	Rare	
AUL 143.1 947.3-952.5 m	SUBMARINE BASALT		Plagioclase	Plagio-clase Microlites Opaques Augite	Apatite	Aphanitic Fluidal

CHAPTER 4:   CHEMICAL STUDY

i) <u>Sample Selection</u>

a) Volcanic Flows and Intrusives

The volcanic flows selected for major and trace element analysis were chosen to try to represent the divisions of the core noted in the core log descriptions: Subaerial Sequences I, II, and III, the Transition Sequence, and the Subaqueous Sequence. Much of the core was sampled by G.K. Muecke for analysis for K, U, and Th. These sample powders, with the exception of the pyroclastics and AUL 001.1, AUL 030.4, and AUL 036.1 were used for the major and trace element analyses. Each sample represents 4 to 6 transverse cores spaced over the thickness of the unit. Two intrusive units, AUS 098.5 and AUS 111.2 were also analysed. The method of sample preparation is included in Appendix I.

Table 1, which was presented in Chapter 3, lists the rock units which were selected for analysis. Each division of the core has been represented as presented in Table 3. Only those chemical analyses whose totals are within the range 98.5 to 101.5 are included in Tables 1 and 3.

b) Pyroclastic Units

The pyroclastic units present in the core are almost completely altered to clays, and as such, are not

TABLE 3: Number of Analyses from each division of the core.

Division of the Core	Number of Analyses
Subaerial Sequence III 0-268.4 m	1 trachyte, 6 basalts
Subaerial Sequence II 268.4-428.6 m	3 trachytes, 2 basalts, 2 pyroclastics
Subaerial Sequence I 428.6-762.8 m	2 trachybasalts, 11 basalts, 2 intrusives, 2 pyroclastics
Transition Sequence 762.8-856.8 m	1 basalt
Submarine Sequence 856.8-980.5 m	4 basalts

particularly useful for major element analysis. However, since a large number of the pyroclastics are trachytic, it was thought important to at least represent them in the analytical work carried out. Four pyroclastics units taken from the thicker of the pyroclastic sequences encountered in the core were sampled and analysed, and are also represented in Table 1 in Chapter 3.

ii) <u>Elements Analysed</u>

The major oxides which were analysed were as follows: SiO_2, TiO_2, Al_2O_3, Fe_2O_3, FeO, MgO, K_2O, Na_2O, MnO, H_2O^+, H_2O^-, P_2O_5, and CO_2.

The trace elements which were analysed were as follows: Nb, Y, Sr, Rb, Zr, Cr, and Ni. The analyses were performed by Dr. Ian Gibson of Bedford College, London.

The methods of analysis and a discussion of errors are presented in Appendices I and II.

iii) <u>Tables of Results</u>

a) Major Elements

The analyses of the major elements have been presented along with their C.I.P.W. norms in six Tables numbers 4 to 9 under the following headings:

      1) Table 4: "As Is"

      2) Table 5: $CaCO_3$-free

      3) Table 6: CO_2-free

TABLE 4:   Analyses "As Is".

	AUL 001.2	AUL 006.1	AUL 008.5	AUL 014.3	AUL 020.3	AUL 022.1	AUL 025.5	AUL 030.4	AUL 031.1	AUL 036.1
SIO2	64.36	42.64	45.47	44.17	43.05	43.43	43.41	69.96	66.03	65.83
TIO2	.67	4.86	4.57	4.72	3.87	3.44	3.31	.50	.73	.55
AL2O3	16.75	13.26	14.79	13.93	13.59	14.55	15.63	14.41	15.80	16.37
CR2O3	0.00	0.00	0.00	0.00	0.00	0.00	0.00	0.00	0.00	0.00
FE2O3	1.01	3.38	.43	2.99	1.26	3.90	5.94	2.90	.81	3.35
FEO	2.56	9.89	11.54	9.82	10.72	7.63	5.48	.30	2.59	.33
MNO	.16	.25	.18	.20	.25	.21	.17	.07	.21	.09
NIO	0.00	0.00	0.00	0.00	0.00	0.00	0.00	0.00	0.00	0.00
MGO	.48	5.22	4.84	5.39	6.46	4.48	2.43	.09	.20	.41
CAO	.39	11.14	9.91	10.95	11.36	10.46	10.61	.22	.73	.44
NA2O	7.02	2.23	2.68	2.39	2.31	2.71	2.75	5.94	5.20	5.57
K2O	5.81	1.54	1.56	1.64	1.23	1.46	1.60	4.79	6.22	5.80
P2O5	.12	.90	.65	.76	.47	.54	.46	.03	.06	.06
CO2	.03	2.83	1.30	2.19	4.19	5.30	6.88	0.00	1.05	0.00
H2O	.03	.86	.92	.55	1.47	1.84	1.78	.71	.24	.88
S	0.00	0.00	0.00	0.00	0.00	0.00	0.00	0.00	0.00	0.00
TOTAL	99.33	99.00	98.84	99.60	100.23	99.95	100.45	99.90	99.84	99.72

	AUL 001.2	AUL 006.1	AUL 008.5	AUL 014.3	AUL 020.3	AUL 022.1	AUL 025.5	AUL 030.4	AUL 031.1	AUL 036.1
Q	.71	.98	0.00	0.00	0.00	6.60	15.21	17.54	10.23	9.86
OR	34.61	9.28	9.42	9.79	7.37	8.80	9.59	28.56	37.14	34.71
AB	54.16	19.22	23.16	20.41	19.79	23.37	23.58	47.81	44.41	47.68
AN	0.00	22.03	24.22	22.65	23.37	15.14	6.22	0.00	0.00	2.01
NS	.54	0.00	0.00	0.00	0.00	0.00	0.00	0.00	0.00	0.00
AC	2.94	0.00	0.00	0.00	0.00	0.00	0.00	2.51	0.00	0.00
WO	0.00	0.00	0.00	0.00	0.00	0.00	0.00	.07	0.00	0.00
DI	.83	8.18	11.01	10.75	3.09	0.00	0.00	.49	0.00	0.00
HY	4.59	17.22	10.74	15.48	22.77	16.98	6.14	0.00	3.81	1.03
OL	0.00	0.00	7.39	.83	3.57	0.00	0.00	0.00	0.00	0.00
MT	0.00	4.99	.64	4.23	1.85	5.76	8.73	0.00	1.19	0.00
HM	0.00	0.00	0.00	0.00	0.00	0.00	0.00	2.06	0.00	3.39
IL	1.28	9.41	8.86	9.05	7.44	6.66	6.37	.79	1.41	.9
RU	0.00	0.00	0.00	0.00	0.00	0.00	0.00	.09	0.00	.08
AP	.28	2.13	1.54	1.78	1.10	1.28	1.08	.07	.14	.14
C	0.00	0.00	0.00	0.00	0.00	0.00	0.00	0.00	.51	.20
CC	.07	6.56	3.02	5.03	9.65	12.29	15.86	0.00	1.17	0.00
TOTAL	100.00	100.00	100.00	100.00	100.00	100.00	100.00	100.00	100.00	100.00

	AUL 046.2	AUL 051.2	AUL 062.2	AUL 066.4	AUL 068.1	AUL 071.3	AUL 082.1	AUL 087.2	AUL 094.1	AUL 096.1
SIO2	45.84	45.71	42.86	42.06	43.16	42.57	48.58	43.60	45.42	43.22
TIO2	4.93	3.54	3.67	4.11	4.37	4.93	3.00	4.43	4.32	4.3
AL2O3	15.45	13.77	14.01	12.21	11.64	13.69	14.45	14.16	13.47	13.97
CR2O3	0.00	0.00	0.00	0.00	0.00	0.00	0.00	0.00	0.00	0.00
FE2O3	7.49	4.30	6.31	5.65	5.47	6.37	5.98	6.54	8.26	0.0
FEO	5.43	6.62	6.19	7.20	5.91	7.81	4.42	6.16	4.61	7.79
MNO	.19	.19	.16	.21	.19	.18	.18	.16	.14	.17
NIO	0.00	0.00	0.00	0.00	0.00	0.00	0.00	0.00	0.00	0.00
MGO	2.95	5.76	8.06	8.04	9.13	5.36	3.80	5.26	5.48	5.58
CAO	8.32	11.16	9.96	11.59	11.66	9.44	8.42	9.67	7.10	8.67
NA2O	2.57	2.35	1.82	1.73	1.72	1.82	2.31	2.14	2.56	2.37
K2O	1.91	.89	.57	1.13	.95	.84	2.00	.91	1.57	1.5
P2O5	1.76	.62	.54	.83	.47	.82	.50	.71	.65	.57
CO2	2.14	3.49	3.04	2.51	1.98	3.05	3.63	4.67	2.86	3.72
H2O	1.27	2.05	2.64	1.81	2.84	2.47	2.06	2.14	2.55	2.58
S	0.00	0.00	0.00	0.00	0.00	0.00	0.00	0.00	0.00	0.00
TOTAL	100.25	100.45	99.83	99.08	99.49	99.35	99.33	100.55	98.99	99.23

	AUL 046.2	AUL 051.2	AUL 062.2	AUL 066.4	AUL 068.1	AUL 071.3	AUL 082.1	AUL 087.2	AUL 094.1	AUL 096.1
Q	12.29	7.16	6.57	2.15	2.27	10.96	15.52	14.09	11.18	8.86
OR	11.41	5.35	3.47	6.87	5.81	5.13	12.16	5.47	9.63	9.18
AB	21.97	20.21	15.84	15.05	15.06	15.89	20.09	18.40	22.46	20.75
AN	16.39	24.79	27.43	22.84	21.97	22.90	15.99	14.03	13.36	16.31
DI	0.00	3.92	0.00	11.32	16.93	0.00	0.00	0.00	0.00	0.00
HY	7.42	15.88	21.05	17.49	15.68	15.09	9.73	13.31	14.15	14.39
MT	3.87	6.34	9.41	8.42	7.25	9.53	6.31	7.66	2.90	3.65
HM	4.90	0.00	0.00	0.00	.66	0.00	1.80	1.36	6.57	5.54
IL	9.46	6.83	7.17	8.03	8.59	9.67	5.86	8.55	8.51	8.45
AP	4.13	1.46	1.29	1.98	1.13	1.96	1.19	1.67	1.56	1.37
C	3.24	0.00	.65	0.00	0.00	0.00	1.71	2.86	4.67	1.37
CC	4.92	8.07	7.11	5.87	4.66	7.16	8.49	10.79	6.74	8.73
TOTAL	100.00	100.00	100.00	100.00	100.00	100.00	100.00	100.00	100.00	100.00

TABLE 4:   Cont'd.

	AUL 098.2	AUS 098.5	AUL 099.1	AUL 108.1	AUS 111.2	AUL 112.1	AUL 114.1	AUL 124.1	AUL 134.1	AUL 136.1
SIO2	54.27	51.77	53.29	45.22	51.65	48.36	45.04	47.61	43.85	43.67
TIO2	2.27	2.61	2.21	3.90	2.70	2.90	3.82	3.53	4.34	4.17
AL2O3	17.47	17.00	17.56	12.06	16.22	14.98	13.55	16.15	15.04	14.65
CR2O3	0.30	0.00	0.00	0.00	0.00	0.00	0.00	0.00	0.00	0.00
FE2O3	3.39	2.39	1.66	7.79	2.33	4.14	5.24	2.24	2.45	2.91
FEO	3.00	5.18	4.07	4.02	5.60	5.25	5.37	7.55	9.08	8.74
MNO	.09	.09	.15	.13	.12	.16	.17	.18	.20	.19
NIO	0.00	0.00	0.00	0.00	0.00	0.00	0.00	0.00	0.00	0.00
MGO	3.01	3.87	2.08	6.99	5.31	4.76	5.42	3.16	3.93	4.21
CAO	5.11	4.96	6.41	8.40	5.26	8.59	11.18	8.49	10.18	10.11
NA2O	3.27	3.05	3.79	3.00	3.13	3.21	2.45	2.98	2.21	2.39
K2O	3.80	3.70	3.41	1.18	3.82	2.55	1.75	2.37	1.97	1.89
P2O5	.89	.65	.89	.54	.54	.68	.54	.75	.63	.57
CO2	.56	1.40	2.28	3.49	.85	2.15	2.92	2.94	3.40	3.57
H2O	1.47	2.46	1.40	2.67	1.82	1.22	1.54	1.53	2.22	1.38
S	0.00	0.00	0.00	0.00	0.00	0.00	0.00	0.00	0.00	0.00
TOTAL	98.60	99.13	99.20	99.39	99.35	98.95	98.99	99.45	99.48	98.25

	AUL 098.2	AUS 098.5	AUL 099.1	AUL 108.1	AUS 111.2	AUL 112.1	AUL 114.1	AUL 124.1	AUL 134.1	AUL 136.1
Q	9.58	7.83	9.04	6.12	1.63	2.70	4.40	5.59	3.41	2.94
OR	23.14	22.64	20.62	7.22	23.17	15.43	10.62	14.31	11.98	11.54
AB	28.48	26.69	32.79	26.24	27.15	27.79	21.27	25.74	19.22	20.87
AN	16.46	11.90	11.82	16.50	17.62	19.37	21.35	19.01	25.59	24.12
DI	0.00	0.00	0.00	0.00	.19	4.56	10.12	0.00	0.00	0.00
HY	7.72	13.48	8.09	17.95	17.79	11.75	9.16	14.69	13.05	18.34
MT	3.48	3.59	2.46	2.15	3.46	6.14	6.97	3.32	3.67	4.36
HM	1.09	0.00	0.00	6.57	0.00	0.00	.57	0.00	0.00	0.00
IL	4.44	5.13	4.29	7.66	5.26	5.64	7.45	6.85	8.48	7.98
AP	2.13	1.56	2.11	1.30	1.28	1.61	1.29	1.78	1.50	1.37
C	2.18	3.89	3.47	0.00	.65	0.00	0.00	1.89	.16	.11
CC	1.31	3.29	5.30	8.21	1.98	5.00	6.81	6.83	7.95	8.38
TOTAL	100.00	100.00	100.00	100.00	100.00	100.00	100.00	100.00	100.00	100.00

	AUL 138.1	AUL 143.1
SIO2	45.39	45.64
TIO2	4.32	3.59
AL2O3	15.45	15.49
CR2O3	0.00	0.00
FE2O3	1.07	2.70
FEO	10.37	9.77
MNO	.17	.18
NIO	0.00	0.00
MGO	4.17	3.19
CAO	8.27	8.65
NA2O	2.75	2.83
K2O	2.04	2.39
P2O5	.67	.75
CO2	2.53	3.18
H2O	1.76	1.60
S	0.00	0.00
TOTAL	98.96	98.87

	AUL 138.1	AUL 143.1
Q	1.32	4.01
OR	12.41	14.53
AB	23.94	24.62
AN	21.24	18.40
HY	22.35	16.45
MT	1.60	4.03
IL	8.44	7.01
AP	1.60	1.79
C	1.18	1.73
CC	5.92	7.44
TOTAL	100.00	100.00

TABLE 5:   Analyses CaCO$_3$-free.

	AUL 001.2	AUL 006.1	AUL 008.5	AUL 014.3	AUL 020.3	AUL 022.1	AUL 025.5	AUL 030.4	AUL 031.1	AUL 036.1
SIO2	64.38	45.61	46.87	46.49	47.57	49.38	51.52	69.96	66.98	65.83
TIO2	.67	5.20	4.71	4.97	4.28	3.91	3.93	.50	.74	.55
AL2O3	16.76	14.18	15.25	14.66	15.02	16.54	18.55	14.41	16.03	16.37
CR2O3	0.00	0.00	0.00	0.00	0.00	0.00	0.00	0.00	0.00	0.00
FE2O3	1.01	3.62	.44	3.04	1.39	4.43	5.86	2.90	.82	3.35
FEO	2.50	10.58	11.90	10.34	11.85	8.68	6.50	.30	2.63	.33
MNO	.16	.27	.19	.21	.28	.24	.20	.07	.21	.19
NIO	0.00	0.00	0.00	0.00	0.00	0.00	0.00	0.00	0.00	0.00
MGO	.48	5.58	4.99	5.67	7.14	5.09	2.88	.09	.20	.41
CAO	.39	8.05	8.50	8.59	6.65	4.22	2.18	.20	.00	.43
NA2O	7.02	2.38	2.76	2.52	2.55	3.08	3.26	5.94	5.28	5.57
K2O	5.81	1.65	1.61	1.73	1.36	1.66	1.90	4.79	6.31	5.80
P2O5	.12	.96	.67	.80	.52	.61	.55	.03	.06	.06
CO2	0.00	0.00	0.00	0.00	0.00	0.00	0.00	0.00	.49	0.00
H2O	.03	.92	.96	.58	1.62	2.09	2.11	.71	.24	.88
S	0.00	0.00	0.00	0.00	0.00	0.00	0.00	0.00	0.00	0.00
TOTAL	99.33	99.00	98.85	99.60	100.23	99.93	99.44	99.90	99.99	99.72

	AUL 001.2	AUL 006.1	AUL 008.5	AUL 014.3	AUL 020.3	AUL 022.1	AUL 025.5	AUL 030.4	AUL 031.1	AUL 036.1
Q	.66	1.08	0.00	0.00	0.00	7.51	17.90	17.54	10.37	9.86
OR	34.61	9.95	9.73	10.33	8.16	10.04	11.55	28.56	37.63	34.71
AB	54.21	20.53	23.85	21.53	21.88	26.63	28.34	47.81	45.03	47.68
AN	0.00	23.59	24.99	23.81	25.88	17.32	7.41	0.00	0.00	2.01
NS	.53	0.00	0.00	0.00	0.00	0.00	0.00	0.00	0.00	0.00
AC	2.94	0.00	0.00	0.00	0.00	0.00	0.00	2.51	0.00	0.00
WO	0.00	0.00	0.00	0.00	0.00	0.00	0.00	.07	0.00	0.00
DI	.99	8.73	11.31	11.35	3.39	0.00	0.00	.49	0.00	0.00
HY	4.50	18.43	11.12	16.16	25.25	19.36	8.37	0.00	3.85	1.03
OL	0.00	0.00	7.62	.96	3.94	0.00	0.00	0.00	0.00	0.00
MT	0.00	5.35	.65	4.45	2.04	6.57	8.73	0.00	1.20	0.00
HM	0.00	0.00	0.00	0.00	0.00	0.00	0.00	2.06	0.00	3.39
IL	1.28	10.07	9.14	9.53	8.24	7.59	7.67	.79	1.42	.9
RU	0.00	0.00	0.00	0.00	0.00	0.00	0.00	.09	0.00	.08
AP	.28	2.27	1.59	1.87	1.22	1.45	1.31	.07	.14	.14
C	0.00	0.00	0.00	0.00	0.00	3.54	8.72	0.00	.51	.20
CC	0.00	0.00	0.00	0.00	0.00	0.00	0.00	0.00	.14	0.00
TOTAL	100.00	100.00	100.00	100.00	100.00	100.00	100.00	100.00	100.00	100.00

	AUL 046.2	AUL 051.2	AUL 062.2	AUL 066.4	AUL 068.1	AUL 071.3	AUL 082.1	AUL 087.2	AUL 094.1	AUL 096.1
SIO2	48.18	49.63	46.05	44.63	45.20	45.77	52.98	48.48	48.61	47.25
TIO2	5.18	3.84	3.94	4.36	4.58	5.30	3.27	4.93	4.62	4.7
AL2C3	16.24	14.95	15.05	12.96	12.19	14.72	15.76	15.75	14.42	15.27
CR2O3	0.00	0.00	0.00	0.00	0.00	0.00	0.00	0.00	0.00	0.00
FE2O3	7.97	4.67	6.78	6.00	5.73	6.85	6.52	7.27	8.84	8.52
FEO	5.71	7.19	6.65	7.64	6.19	8.40	4.82	6.85	4.93	5.24
MNO	.20	.21	.17	.22	.20	.19	.20	.18	.15	.19
NIO	0.00	0.00	0.00	0.00	0.00	0.00	0.00	0.00	0.00	0.00
MGO	3.10	6.25	8.66	8.53	9.56	5.76	4.14	5.85	5.87	6.10
CAO	5.88	7.29	6.54	8.30	9.57	5.97	4.14	4.14	4.3	4.3
NA2O	2.70	2.55	1.95	1.84	1.80	1.96	2.52	2.38	2.74	2.59
K2O	2.01	.97	.61	1.20	.99	.90	2.18	1.01	1.68	1.64
P2O5	1.85	.67	.58	.88	.49	.88	.55	.79	.76	.62
CO2	0.00	0.00	0.00	0.00	0.00	0.00	0.00	0.00	0.00	0.00
H2O	1.33	2.22	2.84	1.92	2.97	2.66	2.25	2.38	2.73	2.82
S	0.00	0.00	0.00	0.00	0.00	0.00	0.00	0.00	0.00	0.00
TOTAL	100.25	100.44	99.82	99.08	99.47	99.36	99.33	100.01	98.99	99.24

	AUL 046.2	AUL 051.2	AUL 062.2	AUL 066.4	AUL 068.1	AUL 071.3	AUL 082.1	AUL 087.2	AUL 094.1	AUL 096.1
Q	12.93	7.78	7.11	2.26	2.41	11.80	16.98	15.79	11.99	9.7
OR	12.02	5.84	3.72	7.31	6.07	5.51	13.28	6.12	10.32	10.06
AB	23.09	21.97	17.01	16.02	15.78	16.00	21.96	20.63	24.08	22.73
AN	17.25	26.96	29.54	24.25	23.06	24.67	17.45	15.74	14.31	17.92
DI	0.00	4.29	0.00	12.02	17.76	0.00	0.00	0.00	0.00	0.00
HY	7.80	17.27	22.67	18.57	16.44	16.25	10.62	14.92	15.19	15.76
MT	4.09	6.89	10.14	8.95	7.59	10.27	6.91	8.58	3.11	4.03
HM	5.14	0.00	0.00	0.00	.70	0.00	1.95	1.53	7.04	6.06
IL	9.95	7.43	7.72	8.52	9.01	10.41	6.40	9.59	9.12	9.26
AP	4.34	1.58	1.39	2.10	1.18	2.11	1.31	1.88	1.69	1.49
C	3.41	0.00	.70	0.00	0.00	1.84	3.14	5.23	3.16	3.01
TOTAL	100.00	100.00	100.00	100.00	100.00	100.00	100.00	100.00	100.00	100.00

TABLE 5: Cont'd.

	AUL 098.2	AUS 098.5	AUL 099.1	AUL 108.1	AUS 111.2	AUL 112.1	AUL 114.1	AUL 124.1	AUL 134.1	AUL 136.1
SIO2	55.76	53.49	56.22	49.15	52.67	50.87	48.28	51.04	47.54	48.71
TIO2	2.13	2.70	2.33	4.24	2.75	3.45	4.09	3.78	4.71	4.49
AL2O3	17.95	17.56	18.53	13.11	16.54	15.76	14.52	17.31	16.31	16.17
CR2O3	0.00	0.00	0.00	0.00	0.00	0.00	0.00	0.00	0.00	0.00
FE2O3	3.48	2.47	1.75	8.47	2.38	4.36	5.64	2.40	2.69	3.33
FEO	3.09	5.35	4.29	4.37	5.71	5.52	5.76	8.09	9.84	10.01
MNO	.09	.09	.16	.14	.12	.17	.18	.19	.22	.21
NIO	0.00	0.00	0.00	0.00	0.00	0.00	0.00	0.00	0.00	0.00
MGO	3.09	4.00	2.20	7.60	5.42	5.01	5.81	3.39	4.23	4.65
CAO	4.52	3.29	3.70	4.29	4.26	6.15	8.00	5.08	6.34	6.03
NA2O	3.36	3.15	4.00	3.26	3.19	3.38	2.63	3.20	2.40	2.64
K2O	3.90	3.82	3.60	1.28	3.90	2.68	1.88	2.54	2.14	2.09
P2O5	.91	.67	.94	.59	.55	.71	.58	.80	.68	.63
CO2	0.00	0.00	0.00	0.00	0.00	0.00	0.00	0.00	0.00	0.00
H2O	1.51	2.54	1.48	2.90	1.86	1.29	1.65	1.61	2.41	1.52
S	0.00	0.00	0.00	0.00	0.00	0.00	0.00	0.00	0.00	0.00
TOTAL	99.99	99.13	99.20	99.40	99.35	98.95	99.02	99.43	99.51	100.48

	AUL 098.2	AUS 098.5	AUL 099.1	AUL 108.1	AUS 111.2	AUL 112.1	AUL 114.1	AUL 124.1	AUL 134.1	AUL 136.1
Q	9.70	8.10	9.52	6.68	1.65	2.83	4.69	5.97	3.66	3.39
OR	23.42	23.39	21.79	7.85	23.66	16.23	11.42	15.36	13.04	12.49
AB	28.87	27.59	34.63	28.58	27.68	29.28	22.85	27.68	20.91	22.57
AN	16.72	12.36	12.49	17.99	17.99	20.39	22.86	20.41	27.81	26.06
DI	0.00	0.00	0.00	.15	0.00	4.81	10.90	0.00	0.00	0.00
HY	7.81	13.93	8.56	19.59	18.15	12.36	9.81	15.77	19.58	20.40
MT	3.55	3.71	2.60	2.33	3.54	6.47	7.49	3.56	4.02	4.88
HM	1.08	0.00	0.00	7.17	0.00	0.00	.62	0.00	0.00	0.00
IL	4.49	5.31	4.53	8.35	5.36	5.93	7.98	7.34	9.21	8.62
AP	2.14	1.61	2.23	1.42	1.31	1.69	1.38	1.90	1.62	1.48
C	2.20	4.00	3.66	0.00	.66	0.00	0.00	0.00	.15	.11
TOTAL	100.00	100.00	100.00	100.00	100.00	100.00	100.00	100.00	100.00	100.00

	AUL 138.1	AUL 143.1
SIO2	48.19	49.24
TIO2	4.59	3.87
AL2O3	16.40	16.71
CR2O3	0.00	0.00
FE2O3	1.14	2.91
FEO	11.01	9.46
MNO	.18	.19
NIO	0.00	0.00
MGO	4.43	3.34
CAO	5.36	4.96
NA2O	2.92	3.05
K2O	2.17	2.58
P2O5	.71	.91
CO2	0.00	0.00
H2O	1.87	1.73
S	0.00	0.00
TOTAL	98.97	98.85

	AUL 138.1	AUL 143.1
Q	1.37	4.36
OR	13.22	15.71
AB	25.44	26.57
AN	22.60	19.88
HY	23.75	17.76
MT	1.70	4.34
IL	8.98	7.57
AP	1.70	1.94
C	1.24	1.88
TOTAL	100.00	100.00

4) Table 7: CO_2-free, $Fe_2O_3 = TiO_2 + 1.5$ wt. %

5) Table 8: CO_2-free, $Fe_2O_3 = $ maximum 1.5 wt. %

6) Table 9: CO_2-free, $Fe_2O_3/(FeO + Fe_2O_3) = 0.15$

Table 4 presents the analyses "As Is", i.e., as they were obtained with only H_2O^- removed from the totals in order to allow SiO_2, a water-free analysis, to be added to the remaining oxide concentrations. When CO_2 is included in the calculation of the norms, some analyses generate normative corundum (C). Presenting the analyses as $CaCO_3$-free as in Table 5 does not solve the problem, since corundum still appears in the norms of some analyses. In neither Table 4 nor Table 5 are the analyses suitable for projection in the basalt tetrahedron (nepheline-olivine-quartz-clinopyroxene).

However, by calculating the analyses on a CO_2-free basins, "reasonable"-looking norms, i.e., norms that conform to usually fresh basalt compositions and can be projected within the basalt tetrahedron are obtained (Table 6). By presenting the results as CO_2-free, it is assumed that all of the CaO present as carbonate in the vesicles has come from the rocks and all of the CO_2 was added from sea water, juvenile water, or groundwater. This is partially justified by the fact that removing CaO as carbonate (Table 5) results in a deficit of CaO in the norms. One must still, however, be aware of a possible error in CaO concentrations in accepting the results as CO_2-free.

TABLE 6: Analyses CO_2-free.

	AUL 001.2	AUL 006.1	AUL 008.5	AUL 014.3	AUL 020.3	AUL 022.1	AUL 025.5	AUL 030.4	AUL 031.1	AUL 036.1
SIC2	64.38	43.89	46.08	45.16	44.93	45.86	46.64	69.96	66.70	65.83
TIO2	.67	5.00	4.63	4.83	4.04	3.63	3.56	.50	.74	.55
AL2C3	16.76	13.65	14.99	14.24	14.18	15.36	16.79	14.41	15.97	16.37
CR2C3	0.00	0.00	0.00	0.00	0.00	0.00	0.00	0.00	0.00	0.00
FE2O3	1.01	3.48	.44	2.96	1.32	4.12	5.06	2.90	.32	3.35
FEO	2.50	10.18	11.69	10.04	11.19	8.06	6.12	.30	2.62	.33
MNC	.16	.26	.18	.20	.26	.22	.18	.07	.21	.09
NIO	0.00	0.00	0.00	0.00	0.00	0.00	0.00	0.00	0.00	0.00
MGO	.48	5.37	4.91	5.51	6.74	4.73	2.61	.09	.20	.41
CAO	.39	11.47	10.04	11.20	11.86	11.05	11.40	.20	.74	.48
NA2O	7.02	2.30	2.72	2.44	2.41	2.86	2.95	5.94	5.25	5.57
K2O	5.91	1.59	1.58	1.68	1.28	1.54	1.72	4.79	6.29	5.80
P2O5	.12	.93	.66	.78	.49	.57	.49	.03	.06	.06
CO2	0.00	0.00	0.00	0.00	0.00	0.00	0.00	0.00	0.00	0.00
H2O	.03	.89	.93	.56	1.53	1.94	1.91	.71	.24	.58
S	0.00	0.00	0.00	0.00	0.00	0.00	0.00	0.00	0.00	0.00
TOTAL	99.33	99.01	98.85	99.60	100.23	99.94	99.43	99.90	99.84	99.72

	AUL 001.2	AUL 006.1	AUL 008.5	AUL 014.3	AUL 020.3	AUL 022.1	AUL 025.5	AUL 030.4	AUL 031.1	AUL 036.1
Q	.66	0.00	0.00	0.00	0.00	0.00	.88	17.54	9.29	9.86
OR	34.61	9.59	9.54	10.03	7.67	9.30	10.43	28.56	37.35	34.71
AB	54.21	19.22	23.50	20.17	14.78	23.08	25.59	47.81	44.60	47.68
AN	0.00	22.65	24.53	23.16	24.41	25.02	28.19	0.00	1.42	2.01
NE	0.00	.33	0.00	.37	3.19	.87	0.00	0.00	0.00	0.00
NS	.53	0.00	0.00	0.00	0.00	0.00	0.00	0.00	0.00	0.00
AC	2.94	0.00	0.00	0.00	0.00	0.00	0.00	2.51	0.00	0.00
WO	0.00	0.00	0.00	0.00	0.00	0.00	1.99	.07	0.00	0.00
DI	.99	23.72	18.21	22.63	26.24	21.94	17.30	.49	1.63	0.00
HY	4.50	0.00	.30	0.00	0.00	0.00	0.00	0.00	2.97	1.03
OL	0.00	7.48	12.72	8.22	12.86	5.31	0.00	0.00	0.00	0.00
MT	0.00	5.14	.65	4.33	1.94	6.10	7.52	0.00	1.19	0.00
HM	0.00	0.00	0.00	0.00	0.00	0.00	0.00	2.06	0.00	3.39
IL	1.28	9.58	8.98	9.26	7.77	7.04	6.93	.79	1.41	.96
RU	0.00	0.00	0.00	0.00	0.00	0.00	0.00	0.00	0.00	.08
AP	.28	2.20	1.56	1.83	1.15	1.35	1.17	.07	.14	.14
C	0.00	0.00	0.00	0.00	0.00	0.00	0.00	0.00	0.00	.24
TOTAL	100.00	100.00	100.00	100.00	100.00	100.00	100.00	100.00	100.00	100.00

	AUL 046.2	AUL 051.2	AUL 062.2	AUL 066.4	AUL 068.1	AUL 071.3	AUL 082.1	AUL 087.2	AUL 094.1	AUL 096.1
SIC2	46.84	47.35	44.21	43.15	44.04	43.92	50.42	45.72	46.77	44.90
TIO2	5.04	3.67	3.79	4.22	4.46	5.09	3.11	4.65	4.45	4.47
AL2C3	15.79	14.27	14.45	12.53	11.88	14.12	15.00	14.86	13.87	14.51
CR203	0.00	0.00	0.00	0.00	0.00	0.00	0.00	0.00	0.00	0.00
FE2O3	6.54	4.45	5.29	5.72	5.58	6.57	4.61	6.86	5.95	5.97
FEO	6.55	6.86	7.48	7.46	6.03	8.07	6.03	6.46	7.05	6.83
MNC	.19	.20	.16	.22	.19	.19	.19	.17	.14	.18
NIO	0.00	0.00	0.00	0.00	0.00	0.00	0.00	0.00	0.00	0.00
MGO	3.01	5.97	8.31	8.25	9.31	5.53	3.94	5.52	5.64	5.80
CAO	8.50	11.56	10.27	11.89	11.90	9.74	8.74	10.14	7.31	9.01
NA2O	2.63	2.43	1.88	1.78	1.75	1.88	2.40	2.24	2.64	2.46
K2O	1.95	.92	.59	1.16	.97	.87	2.08	.95	1.62	1.56
P2O5	1.80	.64	.56	.85	.48	.85	.52	.74	.67	.59
CO2	0.00	0.00	0.00	0.00	0.00	0.00	0.00	0.00	0.00	0.00
H2O	1.30	2.12	2.72	1.86	2.90	2.55	2.14	2.24	2.63	2.68
S	0.00	0.00	0.00	0.00	0.00	0.00	0.00	0.00	0.00	0.00
TOTAL	100.14	100.44	99.71	99.09	99.49	99.38	99.18	100.55	98.74	99.02

	AUL 046.2	AUL 051.2	AUL 062.2	AUL 066.4	AUL 068.1	AUL 071.3	AUL 082.1	AUL 087.2	AUL 094.1	AUL 096.1
Q	7.60	2.41	.57	0.00	0.00	5.81	7.91	5.11	5.11	1.74
OR	11.57	5.54	3.60	7.06	5.94	5.31	12.68	5.72	9.97	9.58
AB	22.51	20.91	16.40	15.49	15.33	16.43	20.93	19.28	23.24	21.60
AN	25.82	25.74	30.16	23.42	22.46	28.42	24.74	28.16	22.07	24.85
DI	3.84	22.51	14.71	24.83	27.56	12.37	13.09	14.08	8.70	13.72
HY	5.81	7.73	17.90	6.66	9.54	9.80	6.44	7.46	11.53	5.29
OL	0.00	0.00	0.00	3.74	1.18	0.00	0.00	0.00	0.00	0.00
MT	7.21	6.56	7.91	8.53	7.38	9.84	6.89	8.03	8.98	8.99
HM	1.65	0.00	0.00	0.00	.69	0.00	0.00	1.44	0.00	0.00
IL	9.68	7.09	7.42	8.24	8.77	9.98	6.09	8.98	8.79	8.81
AP	4.22	1.51	1.34	2.03	1.15	2.04	1.24	1.75	1.62	1.42
TOTAL	100.00	100.00	100.00	100.00	100.00	100.00	100.00	100.00	100.00	100.00

TABLE 6: Cont'd.

	AUL 098.2	AUS 098.5	AUL 099.1	AUL 108.1	AUS 111.2	AUL 112.1	AUL 114.1	AUL 124.1	AUL 134.1	AUL 136.1
SIO2	54.58	52.51	54.54	46.87	52.10	49.43	46.41	49.06	45.40	45.79
TIO2	2.28	2.65	2.26	4.04	2.72	2.96	3.94	3.64	4.49	4.22
AL2O3	17.57	17.24	17.97	12.50	16.36	15.31	13.96	16.64	15.57	15.20
CR2O3	0.00	0.00	0.00	0.00	0.00	0.00	0.00	0.00	0.00	0.00
FE2O3	3.41	2.42	1.70	5.54	2.35	4.23	5.40	2.31	2.55	3.02
FEO	3.02	5.25	4.17	6.45	5.65	5.37	5.53	7.78	9.40	9.07
MNO	.09	.09	.15	.13	.12	.16	.18	.18	.21	.23
NIO	0.00	0.00	0.00	0.00	0.00	0.00	0.00	0.00	0.00	0.00
MGO	3.03	3.92	2.13	7.24	5.36	4.87	5.59	3.26	4.04	4.37
CAO	5.14	5.03	6.56	8.71	5.31	8.78	11.52	8.75	10.54	10.39
NA2O	3.29	3.09	3.88	3.11	3.16	3.28	2.52	3.07	2.29	2.48
K2O	3.82	3.75	3.49	1.22	3.85	2.61	1.80	2.44	2.04	1.96
P2O5	.89	.66	.91	.56	.55	.70	.56	.77	.65	.59
CO2	0.00	0.00	0.00	0.00	0.00	0.00	0.00	0.00	0.00	0.00
H2O	1.48	2.50	1.43	2.77	1.84	1.25	1.59	1.55	2.30	1.43
S	0.00	0.00	0.00	0.00	0.00	0.00	0.00	0.00	0.00	0.00
TOTAL	98.60	99.11	99.19	99.14	99.37	98.95	99.00	99.45	99.48	98.72

	AUL 098.2	AUS 098.5	AUL 099.1	AUL 108.1	AUS 111.2	AUL 112.1	AUL 114.1	AUL 124.1	AUL 134.1	AUL 136.1
Q	8.13	3.99	3.90	.85	.05	0.00	.35	.39	0.00	0.00
OR	23.27	22.96	21.12	7.49	23.35	15.80	10.93	14.74	12.42	11.92
AB	28.66	27.06	33.58	27.30	27.41	28.40	21.89	26.53	19.94	21.57
AN	20.26	21.36	21.79	17.17	19.56	19.79	22.03	24.94	26.94	25.23
DI	0.00	0.00	4.38	18.67	3.01	15.88	25.59	11.72	18.48	19.44
HY	7.77	13.66	6.16	10.87	16.52	5.66	2.43	9.37	3.91	2.96
OL	0.00	0.00	0.00	0.00	0.00	.77	0.00	0.00	4.20	4.73
MT	3.52	3.63	2.52	8.34	3.49	6.28	7.18	3.42	3.80	4.50
HM	1.08	0.00	0.00	0.00	0.00	0.00	.59	0.00	0.00	0.00
IL	4.46	5.21	4.39	7.96	5.30	5.75	7.68	7.06	8.78	8.24
AP	2.13	1.59	2.16	1.35	1.31	1.66	1.33	1.82	1.55	1.41
C	.83	.55	0.00	0.00	0.00	0.00	0.00	0.00	0.00	0.00
TOTAL	100.00	100.00	100.00	100.00	100.00	100.00	100.00	100.00	100.00	100.00

	AUL 138.1	AUL 143.1
SIO2	46.58	47.16
TIO2	4.43	3.71
AL2O3	15.85	16.00
CR2O3	0.00	0.00
FE2O3	1.10	2.79
FEO	10.64	9.06
MNO	.17	.19
NIO	0.00	0.00
MGO	4.28	3.20
CAO	8.49	8.94
NA2O	2.82	2.92
K2O	2.09	2.47
P2O5	.69	.77
CO2	0.00	0.00
H2O	1.81	1.65
S	0.00	0.00
TOTAL	98.95	98.86

	AUL 138.1	AUL 143.1
OR	12.73	15.03
AB	24.56	25.41
AN	25.13	23.92
DI	11.27	13.70
HY	5.95	4.45
OL	8.41	4.24
MT	1.64	4.16
IL	8.66	7.25
AP	1.65	1.84
TOTAL	100.00	100.00
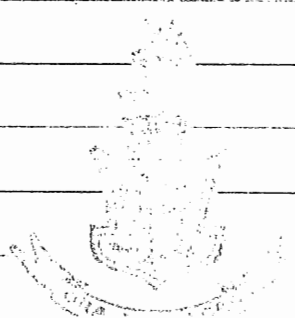
In Table 6, four of the flow units at the top of
the volcanic pile (AUL 006.1, 014.3, 020.3, and 022.1)
are nepheline (Ne) normative. However, three of these
have Ne small enough to be accounted for by analytical
error. The remainder of the analyses are either quartz (Q)
normative or hypersthene (Hy) normative, indicating that
from their present composition, the majority of the rocks
are tholeiitic, with only a small capping of alkali rocks
at the top of the drillhole. It must be remembered that
the norms for these samples could have resulted from
alteration, and thus, the younger rocks might be expected
to have retained more of their original chemical character.
The question of alkaline versus tholeiitic character for
the analysed rocks will be discussed in a later chapter.

One could accept the analyses as presented in
Table 6, but it is common practice to make an adjustment
for the oxidation of Fe^{2+} to Fe^{3+}, a process which occurs
readily during alteration. Since there is no doubt that
much of the core has been subjected to hydrothermal
influences, as attested to the high water temperatures
reached during the drilling of the hole, and from an
examination of polished sections (Abdel-Aal, personal
communication), a correction for iron oxidation is believed
to be justified.

Table 7 presents those analyses for which a
correction for the alteration of iron has been made. The
adjustment used was proposed by Irvine and Baragar (1971)

TABLE 7:   Analyses CO_2-free, Fe_2O_3 = TiO_2 + 1.5 wt. %.

	AUL 001.2	AUL 006.1	AUL 008.5	AUL 014.3	AUL 020.3	AUL 022.1	AUL 025.5	AUL 030.4	AUL 031.1	AUL 036.1
SIO2	64.38	43.89	46.08	45.16	44.93	45.86	46.64	69.96	66.73	65.83
TIO2	.67	5.00	4.63	4.83	4.04	3.63	3.56	.50	.74	.55
AL2O3	16.76	13.65	14.99	14.24	14.18	15.36	16.77	14.41	15.97	16.37
CR2O3	0.00	0.00	0.00	0.00	0.00	0.00	0.00	0.00	0.00	0.00
FE2O3	1.01	3.48	.44	2.96	1.32	4.12	5.06	2.00	.82	2.05
FEO	2.50	10.18	11.69	10.04	11.19	8.06	6.12	1.11	2.62	1.55
MNO	.16	.26	.18	.20	.26	.22	.18	.07	.21	.09
NIO	0.00	0.00	0.00	0.00	0.00	0.00	0.00	0.00	0.00	0.00
MGO	.48	5.37	4.91	5.51	6.74	4.73	2.61	.09	.20	.41
CAO	.39	11.47	10.04	11.20	11.86	11.05	11.40	.20	.74	.48
NA2O	7.02	2.30	2.72	2.44	2.41	2.86	2.95	5.94	5.25	5.57
K2O	5.81	1.59	1.58	1.68	1.28	1.54	1.72	4.79	6.29	5.80
P2O5	.12	.93	.66	.78	.49	.57	.49	.03	.06	.06
CO2	0.00	0.00	0.00	0.00	0.00	0.00	0.00	0.00	0.00	0.00
H2O	.03	.89	.93	.56	1.53	1.94	1.91	.71	.24	.88
S	0.00	0.00	0.00	0.00	0.00	0.00	0.00	0.00	0.00	0.00
TOTAL	99.33	99.01	98.85	99.60	100.23	99.94	99.41	99.81	99.84	99.59

	AUL 001.2	AUL 006.1	AUL 008.5	AUL 014.3	AUL 020.3	AUL 022.1	AUL 025.5	AUL 030.4	AUL 031.1	AUL 036.1
Q	.66	0.00	0.00	0.00	0.00	0.00	.89	17.38	3.29	9.72
OR	34.61	9.59	9.54	10.03	7.67	9.30	10.43	28.59	37.35	34.76
AB	54.21	19.22	23.50	20.17	14.78	23.08	25.60	47.86	44.60	47.74
AN	0.00	22.65	24.53	23.16	24.41	25.02	28.14	0.00	1.42	2.02
NE	0.00	.33	0.00	.37	3.19	.87	0.00	0.00	0.00	0.00
NS	.53	0.00	0.00	0.00	0.00	0.00	0.00	0.00	0.00	0.00
AC	2.94	0.00	0.00	0.00	0.00	0.00	0.00	2.52	0.00	0.00
WO	0.00	0.00	0.00	0.00	0.00	0.00	2.02	0.00	0.00	0.00
DI	.99	23.72	18.21	22.63	26.24	21.94	17.30	.68	1.63	0.00
HY	4.50	0.00	.30	0.00	0.00	0.00	0.00	.29	2.97	1.36
OL	0.00	7.48	12.72	8.22	12.86	5.31	0.00	0.00	0.00	0.00
MT	0.00	5.14	.65	4.33	1.94	6.10	7.52	1.67	1.19	3.01
IL	1.28	9.68	8.98	9.26	7.77	7.04	6.94	.96	1.41	1.06
AP	.28	2.20	1.56	1.83	1.15	1.35	1.17	.07	.14	.14
C	0.00	0.00	0.00	0.00	0.00	0.00	0.00	0.00	0.00	.20
TOTAL	100.00	100.00	100.00	100.00	100.00	100.00	100.00	100.00	100.00	100.00

	AUL 046.2	AUL 051.2	AUL 062.2	AUL 066.4	AUL 068.1	AUL 071.3	AUL 082.1	AUL 087.2	AUL 094.1	AUL 096.1
SIO2	46.84	47.35	44.21	43.15	44.04	43.92	50.42	45.72	46.77	44.90
TIO2	5.14	3.67	3.79	4.22	4.46	5.09	3.11	4.65	4.45	4.47
AL2O3	15.79	14.27	14.45	12.53	11.88	14.12	15.00	14.86	13.87	14.51
CR2O3	0.00	0.00	0.00	0.00	0.00	0.00	0.00	0.00	0.00	0.00
FE2O3	6.54	4.45	5.29	5.72	5.58	6.57	4.61	6.15	5.95	5.97
FEO	6.55	6.86	7.48	7.46	6.03	8.07	6.03	7.10	7.05	6.89
MNO	.19	.20	.16	.22	.19	.19	.19	.17	.14	.18
NIO	0.00	0.00	0.00	0.00	0.00	0.00	0.00	0.00	0.00	0.00
MGO	3.01	5.97	10.27	9.31	9.31	5.53	3.94	5.52	5.64	5.80
CAO	8.50	11.56	10.27	11.89	11.90	9.74	8.74	10.14	7.31	9.51
NA2O	2.63	2.43	1.88	1.78	1.75	1.88	2.40	2.24	2.64	2.46
K2O	1.95	.92	.59	1.16	.97	.87	2.08	.95	1.62	1.56
P2O5	1.80	.64	.56	.85	.48	.85	.52	.74	.67	.59
CO2	0.00	0.00	0.00	0.00	0.00	0.00	0.00	0.00	0.00	0.00
H2O	1.30	2.12	2.72	1.82	2.90	2.55	2.14	2.24	2.63	2.68
S	0.00	0.00	0.00	0.00	0.00	0.00	0.00	0.00	0.00	0.00
TOTAL	100.14	100.44	99.71	99.05	99.49	99.38	99.18	100.48	98.74	99.02

	AUL 046.2	AUL 051.2	AUL 062.2	AUL 066.4	AUL 068.1	AUL 071.3	AUL 082.1	AUL 087.2	AUL 094.1	AUL 096.1
Q	7.60	2.41	.57	0.00	0.00	5.81	7.91	4.84	5.11	1.74
OR	11.57	5.54	3.60	7.06	5.94	5.31	12.68	5.72	9.97	9.58
AB	22.51	20.91	16.40	15.49	15.33	16.43	20.93	19.29	23.24	21.60
AN	25.82	25.74	30.16	23.42	22.46	28.42	24.74	28.18	22.07	24.85
DI	3.84	22.51	14.71	24.83	27.56	12.37	13.09	14.15	8.70	13.72
HY	5.81	7.73	17.90	6.66	9.54	9.80	6.44	8.00	11.53	9.29
OL	0.00	0.00	0.00	3.74	1.18	0.00	0.00	0.00	0.00	0.00
MT	7.21	6.56	7.91	8.53	7.38	9.84	6.89	9.08	8.98	8.99
HM	1.65	0.00	0.00	0.00	.69	0.00	0.00	0.00	0.00	0.00
IL	9.68	7.09	7.42	8.24	8.77	9.98	6.09	8.99	8.79	8.81
AP	4.22	1.51	1.34	2.03	1.15	2.04	1.24	1.75	1.62	1.42
TOTAL	100.00	100.00	100.00	100.00	100.00	100.00	100.00	100.00	100.00	100.00

TABLE 7: Cont'd.

	AUL 098.2	AUS 098.5	AUL 099.1	AUL 108.1	AUS 111.2	AUL 112.1	AUL 114.1	AUL 124.1	AUL 134.1	AUL 136.1
SIO2	54.58	52.51	54.54	46.87	52.10	49.43	46.41	43.06	45.43	45.79
TIO2	2.28	2.65	2.26	4.14	2.72	2.96	3.94	3.64	4.49	4.22
AL2O3	17.57	17.24	17.97	12.50	16.36	15.31	13.96	16.64	15.57	15.20
CR2O3	0.00	0.00	0.00	0.00	0.00	0.00	0.00	0.00	0.00	0.00
FE2O3	3.41	2.42	1.70	5.54	2.35	4.23	5.40	2.31	2.55	3.02
FEO	3.02	5.25	4.17	6.45	5.65	5.37	5.53	7.78	9.40	9.07
MNO	.59	.09	.15	.13	.12	.16	.18	.18	.21	.20
NIO	0.00	0.00	0.00	0.00	0.00	0.00	0.00	0.00	0.00	0.00
MGO	3.03	3.92	2.13	7.24	5.36	4.87	5.59	3.26	4.04	4.37
CAO	5.14	5.03	6.56	8.71	5.31	8.78	11.52	8.75	10.54	10.39
NA2O	3.29	3.09	3.88	3.11	3.16	3.28	2.52	3.07	2.29	2.48
K2O	3.82	3.75	3.49	1.22	3.85	2.61	1.80	2.44	2.04	1.96
P2O5	.89	.66	.91	.56	.55	.70	.56	.77	.65	.59
CO2	0.00	0.00	0.00	0.00	0.00	0.00	0.00	0.00	0.00	0.00
H2O	1.48	2.50	1.43	2.77	1.84	1.25	1.59	1.55	2.30	1.43
S	0.00	0.00	0.00	0.00	0.00	0.00	0.00	0.00	0.00	0.00
TOTAL	98.60	99.11	99.19	99.14	99.37	98.95	99.00	99.45	99.48	98.72

	AUL 098.2	AUS 098.5	AUL 099.1	AUL 108.1	AUS 111.2	AUL 112.1	AUL 114.1	AUL 124.1	AUL 134.1	AUL 136.1
Q	8.03	3.99	3.90	.85	.05	0.00	.35	.39	0.00	0.00
OR	23.27	22.96	21.12	7.49	23.35	15.80	10.93	14.74	12.42	11.96
AB	28.66	27.06	33.58	27.30	27.41	28.40	21.89	26.53	19.94	21.57
AN	20.26	21.36	21.79	17.17	19.56	19.79	22.03	24.94	26.94	25.23
DI	0.00	0.00	4.38	18.67	3.01	15.88	25.59	11.72	18.48	19.44
HY	7.77	13.66	6.16	10.87	16.52	5.66	2.43	9.37	3.91	2.96
OL	0.00	0.00	0.00	0.00	0.00	.77	0.00	0.00	4.20	4.73
MT	3.52	3.63	2.52	8.34	3.49	6.28	7.18	3.42	3.80	4.55
HM	1.08	0.00	0.00	0.00	0.00	0.00	.59	0.00	0.00	0.00
IL	4.46	5.21	4.39	7.96	5.30	5.75	7.68	7.06	8.78	8.24
AP	2.13	1.59	2.16	1.35	1.31	1.66	1.33	1.82	1.55	1.41
C	.83	.55	0.00	0.00	0.00	0.00	0.00	0.00	0.00	0.00
TOTAL	100.00	100.00	100.00	100.00	100.00	100.00	100.00	100.00	100.00	100.00

	AUL 138.1	AUL 143.1
SIO2	46.58	47.16
TIO2	4.43	3.71
AL2O3	15.85	16.00
CR2O3	0.00	0.00
FE2O3	1.10	2.79
FEO	10.54	9.06
MNO	.17	.19
NIO	0.00	0.00
MGO	4.28	3.20
CAO	8.49	8.94
NA2O	2.82	2.92
K2O	2.09	2.47
P2O5	.66	.77
CO2	0.00	0.00
H2O	1.91	1.65
S	0.00	0.00
TOTAL	98.95	98.86

	AUL 138.1	AUL 143.1
OR	12.73	15.03
AB	24.56	25.41
AN	25.13	23.92
DI	11.27	13.73
HY	5.95	4.45
OL	8.41	4.24
MT	1.64	4.16
IL	8.66	7.25
AP	1.65	1.84
TOTAL	100.00	100.00

and is based on an observed relationship between Fe_2O_3 and TiO_2. The relationship used was:

$$Fe_2O_3 \text{ (wt. \%)} = TiO_2 + 1.5 \text{ (wt. \%)}.$$

Any Fe_2O_3 over this amount was converted to FeO. The difficulty in the use of this correction lies in the fact that these rocks have very high TiO_2 weight percentages, and thus the correction cannot be applied to most of the rocks.

By using Irvine and Baragar's relationship, only eight of the samples can be adjusted. This still leaves some samples which appear to be oxidized. For example, AUL 098.2 has not been adjusted, but the values for Fe_2O_3 and FeO are 3.41 and 3.02 weight per cent, respectively, probably indicating that this sample has had Fe^{2+} oxidized to Fe^{3+}. Thus another method of adjusting for this type of oxidation could be useful.

An adjustment for the oxidation of iron that is used by some petrologists (Coombs, 1963; Glassley, 1974) is:

$$Fe_2O_3 \text{ (wt. \%)} = 1.5 \text{ (wt. \%)}$$

i.e., Fe_2O_3 is set equal to a maximum of 1.5 weight per cent and any excess is converted to FeO. This has been calculated for the Azores rocks and is presented as Table 8.

The application of this adjustment to the Azores samples results in making an additional five samples nepheline normative, giving a total of nine nepheline

TABLE 8: Analyses CO_2-free, Fe_2O_3 = 1.5 wt. %.

	AUL 001.2	AUL 006.1	AUL 008.5	AUL 014.3	AUL 020.3	AUL 022.1	AUL 025.5	AUL 030.4	AUL 031.1	AUL 036.1
SIC2	64.18	43.89	46.08	45.16	44.93	45.86	46.64	69.96	66.70	65.83
TIO2	.67	5.09	4.63	4.83	4.04	3.63	3.56	.50	.74	.55
AL2O3	16.76	13.65	14.99	14.24	14.18	15.36	16.79	14.41	15.97	16.37
CR2O3	0.00	0.00	0.00	0.00	0.00	0.00	0.00	0.00	0.00	0.00
FE2O3	1.01	1.50	.44	1.50	1.32	1.50	1.50	1.50	.82	1.50
FEO	2.57	11.96	11.69	11.35	11.19	10.42	9.32	1.56	2.52	2.00
MNO	.16	.25	.18	.20	.26	.22	.18	.07	.21	.09
NIO	0.00	0.00	0.00	0.00	0.00	0.00	0.00	0.00	0.00	0.00
MGO	.48	5.37	4.91	5.51	6.74	4.73	2.61	.09	.20	.41
CAO	.39	11.47	10.04	11.20	11.86	11.05	11.40	.20	.74	.48
NA2O	7.02	2.30	2.72	2.44	2.41	2.86	2.95	5.94	5.25	5.57
K2O	5.81	1.59	1.58	1.68	1.28	1.54	1.72	4.79	6.29	5.80
P2O5	.12	.93	.66	.78	.49	.57	.49	.03	.06	.06
CO2	0.00	0.00	0.00	0.00	0.00	0.00	0.00	0.00	0.00	0.00
H2O	.03	.89	.93	.56	1.53	1.94	1.91	.71	.24	.88
S	0.00	0.00	0.00	0.00	0.00	0.00	0.00	0.00	0.00	0.00
TOTAL	99.33	98.81	98.85	99.45	100.23	99.68	99.07	99.76	99.84	99.54

	AUL 001.2	AUL 006.1	AUL 008.5	AUL 014.3	AUL 020.3	AUL 022.1	AUL 025.5	AUL 030.4	AUL 031.1	AUL 036.1
Q	.66	0.00	0.00	0.00	0.00	0.00	0.00	16.81	9.29	9.09
OR	34.61	9.60	9.54	10.05	7.67	9.32	10.47	28.60	37.35	34.77
AB	54.21	16.77	23.50	18.38	14.78	19.84	21.97	47.88	44.60	47.77
AN	0.00	22.69	24.53	23.20	24.41	25.09	28.29	0.00	1.42	2.02
NE	0.00	1.68	0.00	1.35	3.19	2.66	2.02	0.00	0.00	0.00
NS	.53	0.00	0.00	0.00	0.00	0.00	0.00	0.00	0.00	0.00
AC	2.34	0.00	0.00	0.00	0.00	0.00	0.00	2.52	0.00	0.00
DI	.99	24.14	18.21	22.92	26.24	22.52	22.37	.70	1.63	0.00
HY	4.50	0.00	.39	0.00	0.00	0.00	0.00	1.52	2.97	2.75
OL	0.00	11.00	12.72	10.80	12.86	9.93	4.52	0.00	0.00	0.00
MT	0.00	2.22	.65	2.20	1.94	2.23	2.24	.93	1.19	2.20
IL	1.28	9.70	8.98	9.28	7.77	7.05	6.96	.96	1.41	1.06
AP	.28	2.20	1.56	1.83	1.15	1.35	1.17	.07	.14	.14
C	0.00	0.00	0.00	0.00	0.00	0.00	0.00	0.00	0.00	.23
TOTAL	100.00	100.00	100.00	100.00	100.00	100.00	100.00	100.00	100.00	100.00

	AUL 046.2	AUL 051.2	AUL 062.2	AUL 066.4	AUL 068.1	AUL 071.3	AUL 082.1	AUL 087.2	AUL 094.1	AUL 096.1
SIC2	46.84	47.35	44.21	43.15	44.04	43.92	50.42	45.72	46.77	44.9?
TIO2	5.04	3.67	3.79	4.22	4.46	5.09	3.11	4.65	4.45	4.47
AL2O3	15.79	14.27	14.45	12.53	11.88	14.12	15.00	14.85	13.87	14.0?
CR2O3	0.00	0.00	0.00	0.00	0.00	0.00	0.00	0.00	0.00	0.00
FE2O3	1.50	1.50	1.50	1.50	1.50	1.50	1.50	1.50	1.50	1.50
FEO	11.09	9.51	10.89	11.26	9.70	12.63	8.83	11.28	11.05	10.91
MNO	.19	.20	.16	.22	.19	.19	.19	.17	.14	.18
NIO	0.00	0.00	0.00	0.00	0.00	0.00	0.00	0.00	0.00	0.00
MGO	3.01	5.97	8.31	8.25	9.31	5.53	3.94	5.52	5.64	5.80
CAO	8.50	11.56	10.27	11.89	11.90	9.74	8.74	10.14	7.31	9.61
NA2O	2.63	2.43	1.88	1.78	1.75	1.88	2.40	2.24	2.64	2.46
K2O	1.95	.92	.59	1.16	.97	.87	2.08	.95	1.62	1.56
P2O5	1.80	.64	.56	.85	.48	.85	.52	.74	.67	.59
CO2	0.00	0.00	0.00	0.00	0.00	0.00	0.00	0.00	0.00	0.00
H2O	1.30	2.12	2.72	1.86	2.90	2.55	2.14	2.24	2.63	2.68
S	0.00	0.00	0.00	0.00	0.00	0.00	0.00	0.00	0.00	0.00
TOTAL	99.64	100.14	99.33	98.67	99.08	98.87	98.87	100.00	98.29	98.57

	AUL 046.2	AUL 051.2	AUL 062.2	AUL 066.4	AUL 068.1	AUL 071.3	AUL 082.1	AUL 087.2	AUL 094.1	AUL 096.1
Q	2.47	0.00	0.00	0.00	0.00	0.00	4.30	0.00	0.00	0.00
OR	11.73	5.55	3.61	7.09	5.97	5.34	12.72	5.75	10.02	9.62
AB	22.63	20.97	16.46	14.44	15.39	16.51	20.99	19.39	23.35	21.71
AN	25.95	25.82	30.27	23.52	22.56	28.57	24.82	28.29	22.17	24.97
NE	0.00	0.00	0.00	.60	0.00	0.00	0.00	0.00	0.00	0.00
DI	4.15	23.25	15.21	25.81	28.64	13.09	13.66	15.00	9.18	14.48
HY	16.88	10.93	13.06	0.00	2.16	21.85	13.91	17.19	22.23	7.04
OL	0.00	2.63	10.33	15.98	13.05	.29	0.00	1.37	.32	9.64
MT	2.21	2.22	2.25	2.25	2.26	2.26	2.25	2.23	2.27	2.27
IL	9.73	7.11	7.45	8.28	8.81	10.04	6.11	9.03	8.84	8.85
AP	4.25	1.52	1.35	2.04	1.16	2.05	1.25	1.76	1.63	1.43
TOTAL	100.00	100.00	100.00	100.00	100.00	100.00	100.00	100.00	100.00	100.00

TABLE 8: Cont'd.

	AUL 098.2	AUS 098.5	AUL 099.1	AUL 108.1	AUS 111.2	AUL 112.1	AUL 114.1	AUL 124.1	AUL 134.1	AUL 136.1
SIO2	54.58	52.51	54.54	46.87	52.10	49.43	46.41	49.06	45.40	45.79
TIO2	2.28	2.65	2.26	4.04	2.72	2.96	3.94	3.64	4.49	4.22
AL2O3	17.57	17.24	17.97	12.50	16.36	15.31	13.96	16.64	15.57	15.20
CR2O3	0.00	0.00	0.00	0.00	0.00	0.00	0.00	0.00	0.00	0.00
FE2O3	1.50	1.50	1.50	1.50	1.50	1.50	1.50	1.50	1.50	1.50
FEO	4.74	6.08	4.35	10.09	6.42	7.83	9.04	8.51	10.34	10.44
MNO	.09	.09	.15	.13	.12	.16	.18	.18	.21	.20
NIO	0.00	0.00	0.00	0.00	0.00	0.00	0.00	0.00	0.00	0.00
MGO	3.03	3.92	2.13	7.24	5.36	4.87	5.59	3.26	4.04	4.37
CAO	5.14	5.03	6.56	8.71	5.31	8.78	11.52	8.75	10.54	10.39
NA2O	3.29	3.09	3.88	3.11	3.16	3.28	2.52	3.07	2.29	2.48
K2O	3.82	3.75	3.49	1.22	3.85	2.61	1.80	2.44	2.04	1.96
P2O5	.89	.66	.91	.56	.55	.70	.56	.77	.65	.59
CO2	0.00	0.00	0.00	0.00	0.00	0.00	0.00	0.00	0.00	0.00
H2O	1.48	2.50	1.43	2.77	1.84	1.25	1.59	1.55	2.30	1.43
S	0.00	0.00	0.00	0.00	0.00	0.00	0.00	0.00	0.00	0.00
TOTAL	98.41	99.02	99.17	98.74	99.29	98.68	98.61	99.37	99.37	98.57

	AUL 098.2	AUS 098.5	AUL 099.1	AUL 108.1	AUS 111.2	AUL 112.1	AUL 114.1	AUL 124.1	AUL 134.1	AUL 136.1
Q	6.23	2.91	3.67	0.00	0.00	0.00	0.00	0.00	0.00	0.00
OR	23.31	22.98	21.12	7.52	23.37	15.85	10.97	14.75	12.43	11.93
AB	28.72	27.09	33.59	27.42	27.44	28.48	19.62	26.55	19.96	21.42
AN	20.30	21.38	21.80	17.24	19.58	19.85	22.12	24.96	26.97	25.27
NE	0.00	0.00	0.00	0.00	0.00	0.00	1.28	0.00	0.00	.10
DI	0.00	0.00	4.41	19.51	3.04	16.49	26.95	11.83	18.67	19.73
HY	11.77	16.04	6.65	6.28	15.29	.24	0.00	9.26	1.66	0.00
OL	0.00	0.00	0.00	10.42	2.45	9.43	7.77	1.53	7.73	9.65
MT	2.24	2.25	2.23	2.27	2.23	2.23	2.24	2.22	2.24	2.34
IL	4.47	5.21	4.39	8.00	5.30	5.77	7.71	7.07	8.79	8.25
AP	2.13	1.59	2.16	1.35	1.31	1.67	1.34	1.83	1.55	1.41
C	.84	.55	0.00	0.00	0.00	0.00	0.00	0.00	0.00	0.00
TOTAL	100.00	100.00	100.00	100.00	100.00	100.00	100.00	100.00	100.00	100.00

	AUL 138.1	AUL 143.1
SIO2	46.58	47.16
TIO2	4.43	3.71
AL2O3	15.85	16.00
CR2O3	0.00	0.00
FE2O3	1.10	1.50
FEO	10.64	10.22
MNO	.17	.19
NIO	0.00	0.00
MGO	4.28	3.20
CAO	8.49	8.94
NA2O	2.92	2.92
K2O	2.09	2.47
P2O5	.59	.77
CO2	0.00	0.00
H2O	1.81	1.65
S	0.00	0.00
TOTAL	98.95	98.73

	AUL 138.1	AUL 143.1
OR	12.73	15.05
AB	24.56	25.45
AN	25.13	23.95
DI	11.27	13.87
HY	5.95	1.63
OL	8.41	8.72
MT	1.64	2.24
IL	8.66	7.26
AP	1.65	1.84
TOTAL	100.00	100.00

normative samples. Also, many samples which were quartz
normative become hypersthene and/or olivine normative.

An alternative to the two adjustments presented
above is to express iron as:

$$\frac{Fe_2O_3}{FeO + Fe_2O_3} = 0.15$$

Since fresh, i.e., unaltered basalts have frequently
been found to have Fe_2O_3 /(FeO + Fe_2O_3) = 0.15, this
adjustment is a further attempt to determine the unaltered
state of these rocks.

This iron adjustment has been calculated for these
Azores samples and is presented as Table 9. Its effect
on the analyses is, generally, to increase Ne in the norms
and to decrease Q, i.e., to make the rocks appear more
undersaturated relative to the analyses "As Is" as
presented in Table 6.

It must now be decided which form of iron adjustment
is most valid. The effect on the placement of the samples
within the normative basalt tetrahedron is shown in
Figures 6, 7, 8, and 9. Figure 6 shows samples with no
iron correction. Figure 7 shows the effect of making Fe_2O_3 /
(FeO + Fe_2O_3) = 0.15. Figures 8 and 9 illustrate the
effects of setting Fe_2O_3 equal to TiO_2 + 1.5 weight per
cent and Fe_2O_3 equal to a maximum of 1.5 weight per cent,
respectively.

In general, the effect of converting Fe^{3+} to Fe^{2+}

TABLE 9: Analyses CO_2-free, $Fe_2O_3/(FeO + Fe_2O_3) = 0.15$.

Trace elements included.

	AUL 001.2	AUL 006.1	AUL 008.5	AUL 014.3	AUL 020.3	AUL 022.1	AUL 025.5	AUL 030.4	AUL 031.1	AUL 036.1
SIO2	64.38	43.89	46.08	45.16	44.93	45.86	46.64	69.96	66.70	65.83
TIO2	.67	5.00	4.63	4.83	4.04	3.63	3.56	.50	.74	.55
AL2O3	16.76	13.65	14.99	14.24	14.18	15.36	16.79	14.41	15.97	16.37
CR2O3	0.00	0.00	0.00	0.00	0.00	0.00	0.00	0.00	0.00	0.00
FE2O3	.52	2.04	1.85	1.90	1.89	1.80	1.64	.44	.51	.51
FEO	2.94	11.48	10.43	10.75	10.68	10.15	9.20	2.51	2.90	2.88
MNO	.16	.26	.18	.20	.26	.22	.18	.07	.21	.09
NIO	0.00	0.00	0.00	0.00	0.00	0.00	0.00	0.00	0.00	0.00
MGO	.48	5.37	4.91	5.51	6.74	4.73	2.61	.09	.20	.41
CAO	.39	11.47	10.04	11.20	11.86	11.05	11.40	.20	.74	.48
NA2O	7.02	2.30	2.72	2.44	2.41	2.86	2.95	5.94	5.25	5.57
K2O	5.81	1.59	1.58	1.68	1.28	1.54	1.72	4.79	6.29	5.80
P2O5	.12	.93	.66	.78	.49	.57	.49	.03	.06	.06
CO2	0.00	0.00	0.00	0.00	0.00	0.00	0.00	0.00	0.00	0.00
H2O	.03	.89	.93	.56	1.53	1.94	1.91	.71	.24	.88
S	0.00	0.00	0.00	0.00	0.00	0.00	0.00	0.00	0.00	0.00
TOTAL	99.28	98.87	99.00	99.25	100.29	99.71	99.09	99.65	99.81	99.43

	AUL 001.2	AUL 006.1	AUL 008.5	AUL 014.3	AUL 020.3	AUL 022.1	AUL 025.5	AUL 030.4	AUL 031.1	AUL 036.1
Q	.84	0.00	0.00	0.00	0.00	0.00	0.00	16.27	8.94	7.98
OR	34.63	9.60	9.53	10.07	7.67	9.32	10.47	28.64	37.37	34.81
AB	54.24	17.43	23.47	19.14	15.48	20.21	22.13	47.94	44.61	47.82
AN	0.00	22.68	24.50	23.24	24.39	25.08	20.29	0.00	1.42	2.02
NE	0.00	1.32	0.00	.96	2.80	2.46	1.92	0.00	0.00	0.00
NS	.90	0.00	0.00	0.00	0.00	0.00	0.00	.33	0.00	0.00
AC	1.52	0.00	0.00	0.00	0.00	0.00	0.00	1.29	0.00	0.00
DI	1.00	24.03	18.01	22.88	26.13	22.47	22.34	.71	1.64	0.00
HY	5.31	0.00	3.32	0.00	0.00	0.00	0.00	3.81	3.73	5.22
OL	0.00	10.03	7.92	9.79	11.84	9.39	4.27	0.00	0.00	0.00
MT	0.00	3.02	2.74	2.79	2.78	2.67	2.45	0.00	.74	.75
IL	1.28	9.69	8.97	9.30	7.77	7.05	6.96	.96	1.41	1.06
AP	.28	2.20	1.56	1.83	1.15	1.35	1.17	.07	.14	1.06
C	0.00	0.00	0.00	0.00	0.00	0.00	0.00	0.00	0.00	.20
TOTAL	100.00	100.00	100.00	100.00	100.00	100.00	100.00	100.00	100.00	100.00

Nb	163	48	52	55	45	49	51	202	216	198
Y	64	36	36	37	28	28	35	56	74	88
Sr	18	838	720	843	636	663	640	6	18	57
Rb	147	34	35	43	28	24	41	189	212	214
Zr	823	229	256	255	186	204	209	1182	1360	1363
Cr	N.D.	77	87	-	326	332	134	N.D.	N.D.	N.D.
Ni	2	25	39	-	99	125	51	2	1	2

	AUL 046.2	AUL 051.2	AUL 062.2	AUL 066.4	AUL 068.1	AUL 071.3	AUL 082.1	AUL 087.2	AUL 094.1	AUL 096.1
SIO2	46.84	47.35	44.21	43.15	44.04	43.92	50.42	45.72	46.77	44.90
TIO2	5.04	3.67	3.79	4.22	4.46	5.09	3.11	4.65	4.45	4.47
AL2O3	15.79	14.27	14.45	12.53	11.88	14.12	15.00	14.86	13.87	14.51
CR2O3	0.00	0.00	0.00	0.00	0.00	0.00	0.00	0.00	0.00	0.00
FE2O3	1.90	1.66	1.87	1.93	1.69	2.14	1.56	1.93	1.89	1.87
FEO	10.73	9.37	10.56	10.88	9.53	12.06	8.78	10.90	10.70	10.58
MNO	.19	.20	.16	.22	.19	.19	.19	.17	.14	.18
NIO	0.00	0.00	0.00	0.00	0.00	0.00	0.00	0.00	0.00	0.00
MGO	3.01	5.97	8.31	8.25	9.31	5.53	3.94	5.52	5.64	5.80
CAO	8.50	11.56	10.27	11.89	11.90	9.74	8.74	10.14	7.31	9.01
NA2O	2.63	2.43	1.88	1.78	1.75	1.88	2.40	2.24	2.64	2.46
K2O	1.95	.92	.59	1.16	.97	.87	2.08	.95	1.62	1.56
P2O5	1.80	.64	.56	.85	.48	.85	.52	.74	.67	.59
CO2	0.00	0.00	0.00	0.00	0.00	0.00	0.00	0.00	0.00	0.00
H2O	1.30	2.12	2.72	1.86	2.90	2.55	2.14	2.24	2.63	2.68
S	0.00	0.00	0.00	0.00	0.00	0.00	0.00	0.00	0.00	0.00
TOTAL	99.68	100.16	99.37	98.72	99.10	98.94	98.88	100.06	98.33	98.61

	AUL 046.2	AUL 051.2	AUL 062.2	AUL 066.4	AUL 068.1	AUL 071.3	AUL 082.1	AUL 087.2	AUL 094.1	AUL 096.1
Q	2.93	0.00	0.00	0.00	0.00	.64	4.37	0.00	.34	0.00
OR	11.72	5.55	3.61	7.08	5.96	5.34	12.72	5.74	10.01	9.62
AB	22.62	20.97	16.46	14.98	15.39	16.50	20.99	19.37	23.34	21.70
AN	25.94	25.82	30.26	23.51	22.55	28.55	24.82	28.30	22.16	24.96
NE	0.00	0.00	0.00	.31	0.00	0.00	0.00	0.00	0.00	0.00
DI	4.14	23.21	15.17	25.73	28.60	13.03	13.65	14.93	9.15	14.44
HY	15.88	11.24	13.78	0.00	2.56	20.64	13.77	17.98	21.67	7.80
OL	0.00	2.14	9.12	15.20	12.43	0.00	0.00	0.00	0.00	8.39
MT	2.80	2.46	2.81	2.89	2.55	3.22	2.34	2.86	2.86	2.83
IL	9.73	7.11	7.45	8.27	8.81	10.03	6.11	9.03	8.83	8.85
AP	4.24	1.51	1.34	2.04	1.16	2.05	1.25	1.76	1.62	1.43
TOTAL	100.00	100.00	100.00	100.00	100.00	100.00	100.00	100.00	100.00	100.00

Nb	65	58	45	50	48	51	68	56	54	59
Y	49	32	25	30	30	36	32	36	30	33
Sr	1089	775	632	596	577	783	784	850	739	780
Rb	41	9	11	21	13	24	41	13	34	26
Zr	263	238	171	216	207	210	309	258	244	259
Cr	53	282	414	386	439	234	281	187	273	295
Ni	38	93	138	165	203	77	89	66	62	94

TABLE 9: Cont'd.

	AUL 098.2	AUS 098.5	AUL 099.1	AUL 108.1	AUS 111.2	AUL 112.1	AUL 114.1	AUL 124.1	AUL 134.1	AUL 136.1
SIO2	54.58	52.51	54.54	46.87	52.10	49.43	46.41	49.06	45.40	45.79
TIO2	2.28	2.65	2.26	4.04	2.72	2.96	3.94	3.64	4.49	4.22
AL2O3	17.57	17.24	17.97	12.50	16.36	15.31	13.96	16.64	15.57	15.20
CR2O3	0.00	0.00	0.00	0.00	0.00	0.00	0.00	0.00	0.00	0.00
FE2O3	.93	1.14	.88	1.75	1.19	1.40	1.59	1.50	1.79	1.70
FEO	5.25	6.41	4.91	9.86	6.69	7.92	8.96	8.51	10.08	10.17
MNO	.09	.09	.15	.13	.12	.16	.18	.18	.21	.20
NIO	0.00	0.00	0.00	0.00	0.00	0.00	0.00	0.00	0.00	0.00
MGO	3.03	3.92	2.13	7.24	5.36	4.87	5.59	3.26	4.04	4.37
CAO	5.14	5.03	6.56	8.71	5.31	8.78	11.52	8.75	10.54	10.39
NA2O	3.29	3.09	3.88	3.11	3.16	3.28	2.52	3.07	2.29	2.48
K2O	3.82	3.75	3.49	1.22	3.85	2.61	1.80	2.44	2.04	1.96
P2O5	.89	.66	.91	.56	.55	.70	.56	.77	.65	.59
CO2	0.00	0.00	0.00	0.00	0.00	0.00	0.00	0.00	0.00	0.00
H2O	1.48	2.50	1.43	2.77	1.84	1.25	1.59	1.55	2.30	1.43
S	0.00	0.00	0.00	0.00	0.00	0.00	0.00	0.00	0.00	0.00
TOTAL	98.35	98.99	99.11	98.76	99.25	98.67	98.62	99.37	99.40	98.50

	AUL 098.2	AUS 098.5	AUL 099.1	AUL 108.1	AUS 111.2	AUL 112.1	AUL 114.1	AUL 124.1	AUL 134.1	AUL 136.1
Q	5.57	2.49	2.95	0.00	0.00	0.00	0.00	0.00	0.00	0.00
OR	23.33	22.99	21.13	7.52	23.38	15.85	10.97	14.75	12.43	11.94
AB	28.74	27.09	33.61	27.41	27.45	28.49	19.73	26.55	19.95	21.62
AN	20.31	21.38	21.81	17.23	19.58	19.85	22.12	24.96	26.96	25.29
NE	0.00	0.00	0.00	0.00	0.00	0.00	1.21	0.00	0.00	0.00
DI	0.00	0.00	4.46	19.47	3.05	16.51	26.92	11.83	18.62	19.71
HY	13.24	16.98	8.18	6.80	14.76	.02	0.00	9.26	2.29	.27
OL	0.00	0.00	0.00	9.57	3.40	9.77	7.61	1.53	6.74	8.97
MT	1.39	1.71	1.31	2.64	1.77	2.08	2.38	2.22	2.67	2.54
IL	4.47	5.22	4.39	7.99	5.30	5.77	7.71	7.07	8.78	8.26
AP	2.13	1.59	2.16	1.35	1.31	1.67	1.34	1.83	1.55	1.41
C	.84	.55	0.00	0.00	0.00	0.00	0.00	0.00	0.00	0.00
TOTAL	100.00	100.00	100.00	100.00	100.00	100.00	100.00	100.00	100.00	100.00

	AUL 098.2	AUS 098.5	AUL 099.1	AUL 108.1	AUS 111.2	AUL 112.1	AUL 114.1	AUL 124.1	AUL 134.1	AUL 136.1
Nb	94	75	95	54	59	71	60	87	69	70
Y	56	44	54	31	36	39	35	42	42	41
Sr	1226	880	1315	565	609	665	660	892	792	834
Rb	67	64	63	20	57	60	39	41	109	115
Zr	419	358	405	226	309	365	295	374	321	307
Cr	12	71	12	327	90	194	227	-	64	55
Ni	18	22	17	74	27	73	70	-	23	24

	AUL 138.1	AUL 143.1
SIO2	46.58	47.16
TIO2	4.43	3.71
AL2O3	15.85	16.00
CR2O3	0.00	0.00
FE2O3	1.78	1.77
FEO	10.03	9.91
MNO	.17	.19
NIO	0.00	0.00
MGO	4.28	3.20
CAO	8.49	8.94
NA2O	2.82	2.92
K2O	2.09	2.47
P2O5	.69	.77
CO2	0.00	0.00
H2O	1.81	1.65
S	0.00	0.00
TOTAL	99.02	98.69

	AUL 138.1	AUL 143.1
OR	12.72	15.06
AB	24.54	25.46
AN	25.11	23.96
DI	11.20	13.84
HY	7.37	2.34
OL	6.10	7.60
MT	2.66	2.65
IL	8.66	7.26
AP	1.65	1.84
TOTAL	100.00	100.00

	AUL 138.1	AUL 143.1
Nb	77	82
Y	42	46
Sr	711	880
Rb	50	52
Zr	321	355
Cr	49	-
Ni	24	-
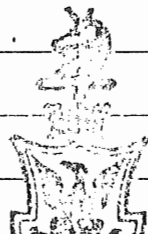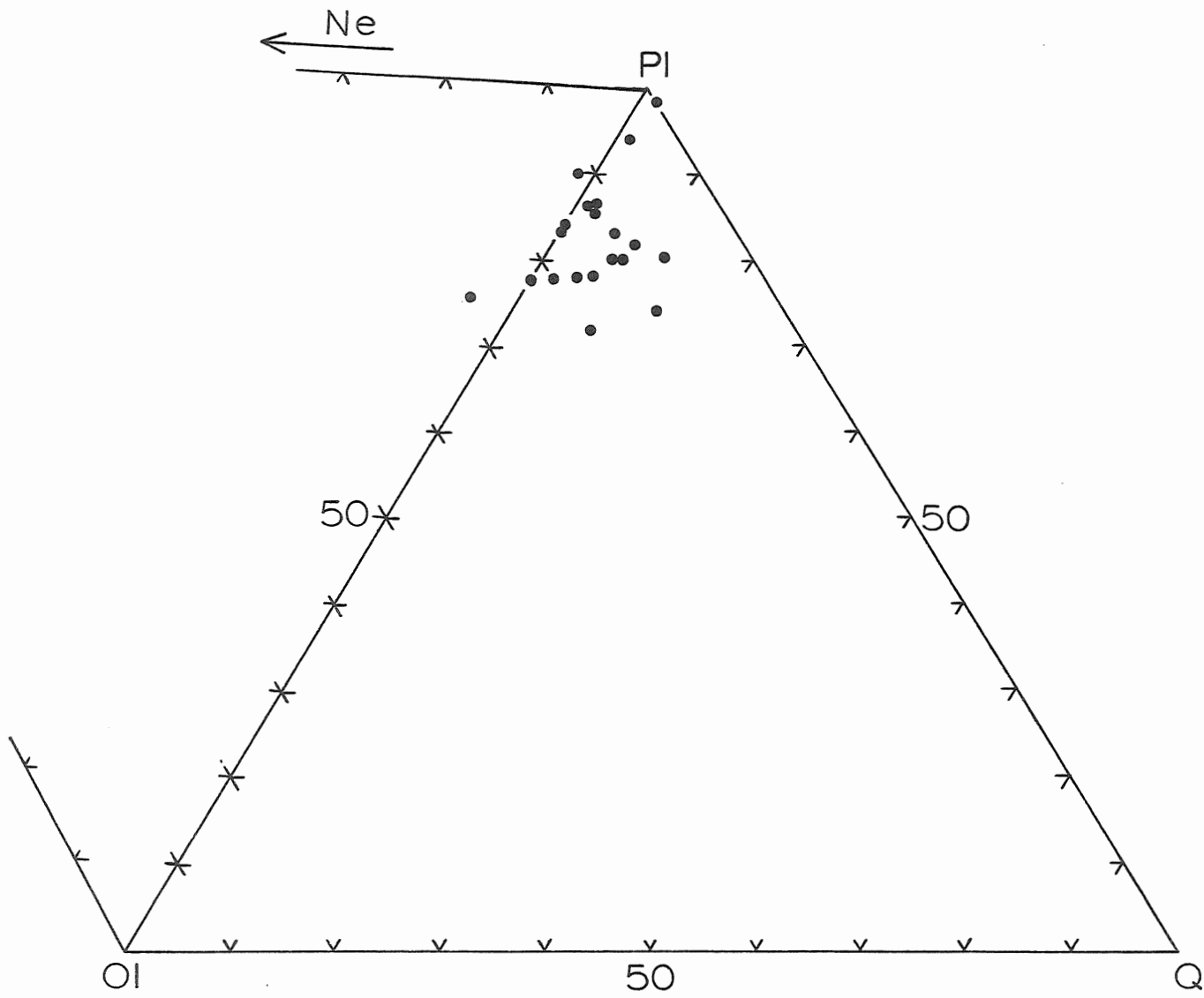
FIGURE 6: Ol-Pl-Q projection in normative basalt tetrahedron. Samples CO_2-free.
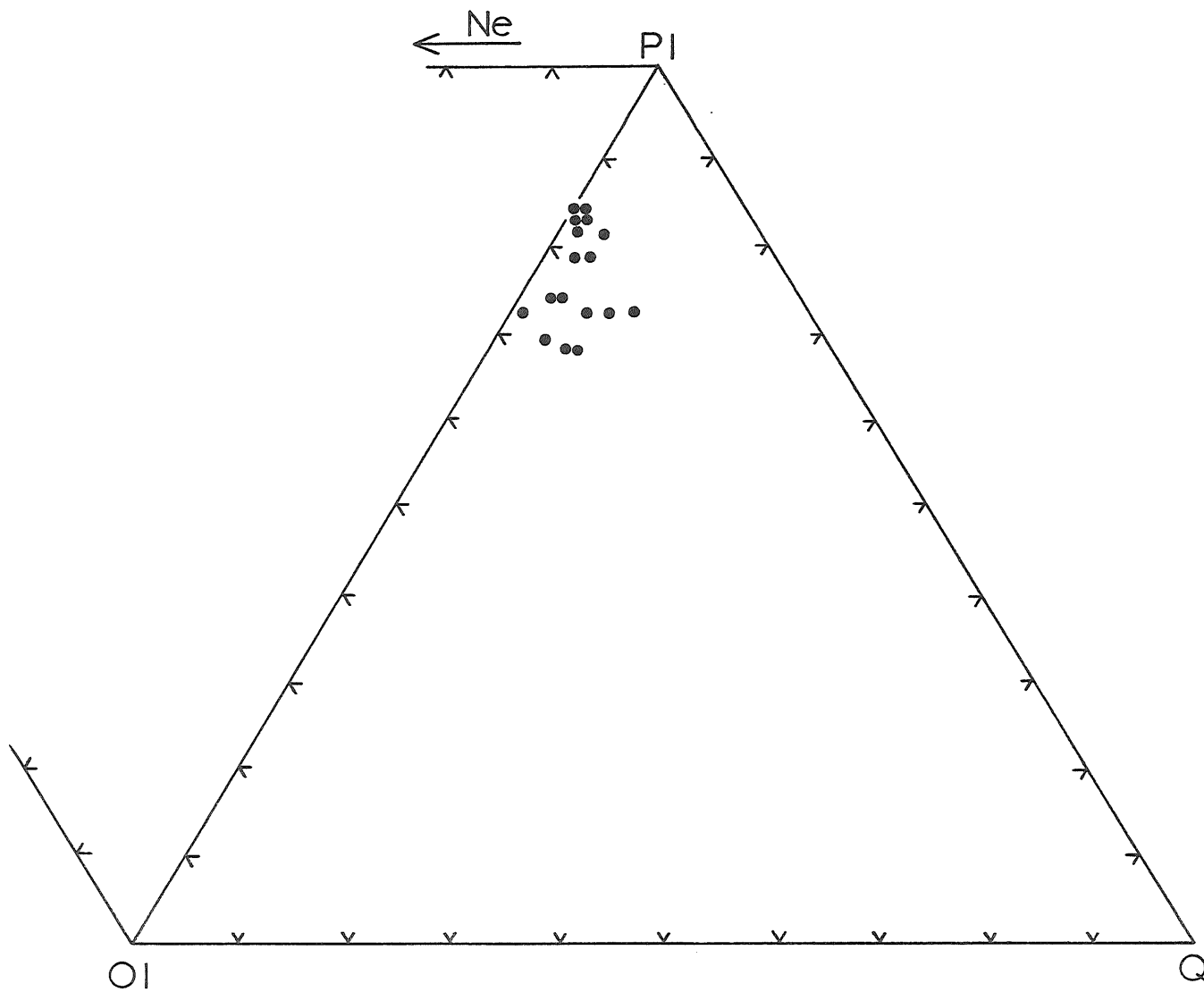
FIGURE 7: Ol-Pl-Q projection in normative basalt tetrahedron.

Samples CO_2-free, $Fe_2O_3/(FeO + Fe_2O_3) = 0.15$.
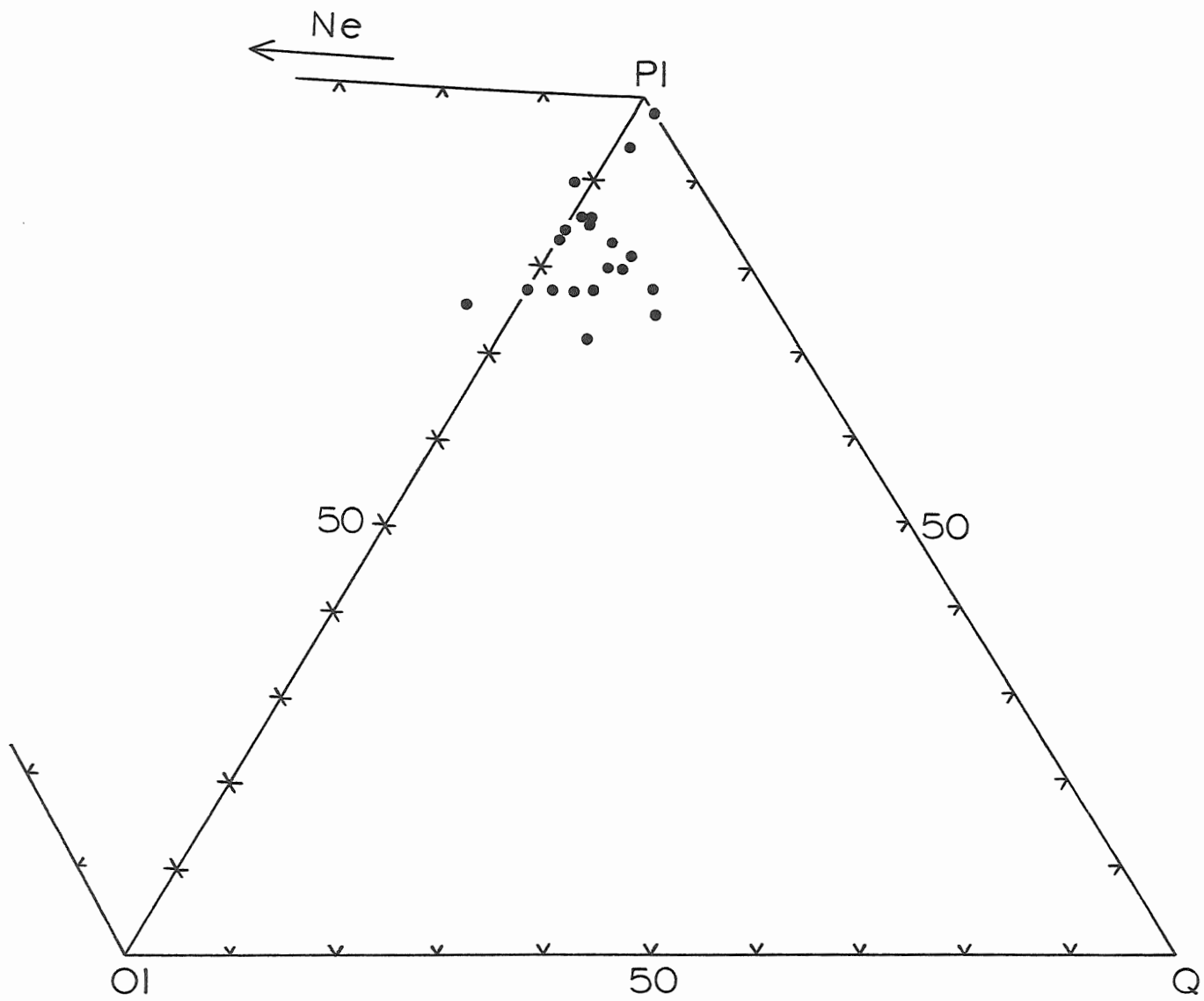
FIGURE 8: Ol-Pl-Q projection in normative basalt tetrahedron.

Samples CO_2-free, $Fe_2O_3 = TiO_2 + 1.5$ wt.%
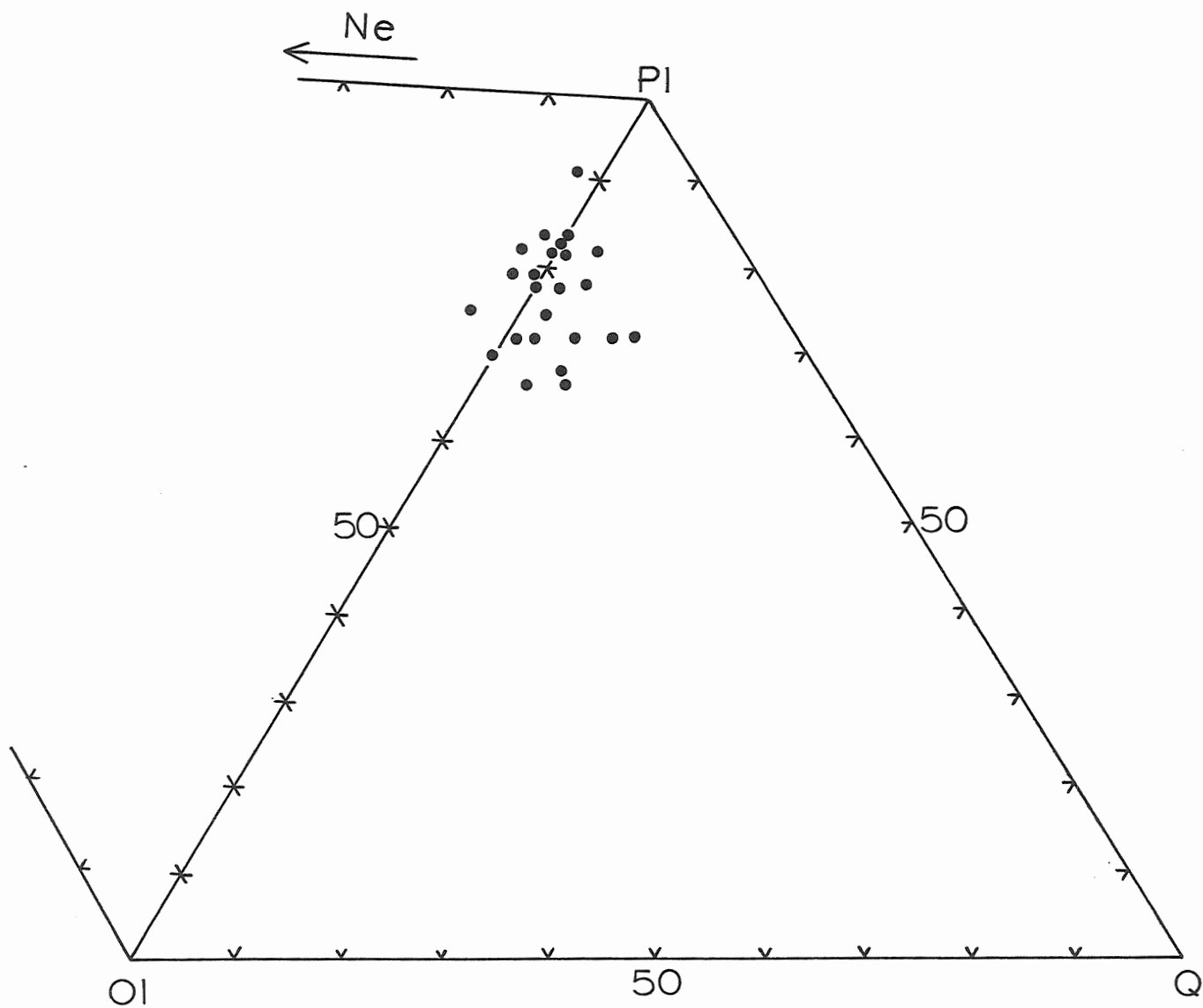
FIGURE 9: Ol-Pl-Q projection in normative basalt tetrahedron.

Samples CO_2-free, $Fe_2O_3 = 0.15$.

is to change the norms of the rocks from tholeiitic to alkalic by changing the concentrations of the normative minerals. This effect is illustrated by Figure 10. Here, the ratio, Fe_2O_3 /(FeO + Fe_2O_3) of AUL 006.1 (CO_2-free) has been varied from the original value of 0.25 to a maximum of 0.80 and to a minimum of 0.15. As is apparent on the diagram, decreasing this ratio causes the sample to move into the field of alkali basalts (Ne-normative) on this projection in the basalt tetra-hedron. Increasing Fe_2O_3 /(FeO + Fe_2O_3) causes the sample to become Q-normative, or tholeiitic. In this case, AUL 006.1 reaches a maximum of 0.21 normative quartz and then changes occur in the normative amounts of magnetite, hematite, rutile, and ilmenite (Table 10).

The adjustment for iron used by Irvine and Baragar (1971) has been shown (Table 7) to have little effect on the norms of the analyses. After the adjustment, Fe_2O_3 = (TiO_2 + 1.5) weight per cent has been applied, some samples still appear to have been oxidized. Thus, it appears that, because of the high TiO_2, the relationship used by Irvine and Baragar is not valid for these rocks. Setting Fe_2O_3 = (maximum) 1.5 weight per cent is a some-what arbitrary relationship, whereas, using Fe_2O_3 / (FeO + Fe_2O_3) = 0.15 does have some validity since it is frequently observed in fresh basalts.
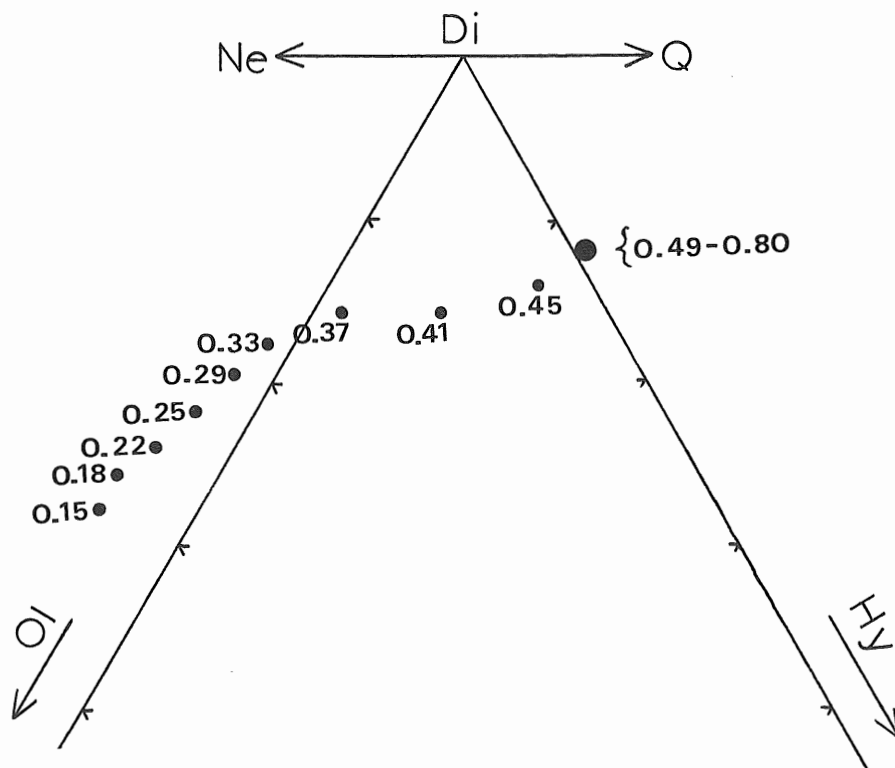
FIGURE 10: Change in norms of AUL 006.1 as Fe_2O_3 /(FeO + Fe_2O_3)
is varied.

TABLE 10: Change in norms with change in $Fe_2O_3/(FeO + Fe_2O_3)$ for sample AUL 006.1.

	1	2	3	4	5	6	7	8	9	10
SIO2	43.89	43.89	43.89	43.89	43.89	43.89	43.89	43.89	43.89	43.89
TIO2	5.00	5.00	5.00	5.00	5.00	5.00	5.00	5.00	5.00	5.00
AL2O3	13.65	13.65	13.65	13.65	13.65	13.65	13.65	13.65	13.65	13.65
CR2O3	0.00	0.00	0.00	0.00	0.00	0.00	0.00	0.00	0.00	0.00
FE2O3	3.48	4.04	4.60	5.16	5.72	6.28	6.84	7.40	7.96	8.52
FEO	10.18	9.68	9.18	8.68	8.18	7.68	7.18	6.68	6.18	5.68
MNO	.26	.26	.26	.26	.26	.26	.26	.26	.26	.26
NIO	0.00	0.00	0.00	0.00	0.00	0.00	0.00	0.00	0.00	0.00
MGO	5.37	5.37	5.37	5.37	5.37	5.37	5.37	5.37	5.37	5.37
CAO	11.47	11.47	11.47	11.47	11.47	11.47	11.47	11.47	11.47	11.47
NA2O	2.39	2.39	2.39	2.39	2.39	2.39	2.39	2.39	2.39	2.39
K2O	1.59	1.59	1.59	1.59	1.59	1.59	1.59	1.59	1.59	1.59
P2O5	.93	.93	.93	.93	.93	.93	.93	.93	.93	.93
CO2	0.00	0.00	0.00	0.00	0.00	0.00	0.00	0.00	0.00	0.00
H2O	.89	.89	.89	.89	.89	.89	.89	.89	.89	.89
S	0.00	0.00	0.00	0.00	0.00	0.00	0.00	0.00	0.00	0.00
TOTAL	99.10	99.16	99.22	99.28	99.34	99.40	99.46	99.52	99.58	99.64

	1	2	3	4	5	6	7	8	9	10
Q	0.00	0.00	0.00	0.00	0.00	0.00	.21	.21	.21	.21
OR	9.58	9.57	9.56	9.56	9.55	9.55	9.54	9.54	9.53	9.52
AB	18.91	19.60	20.28	20.55	20.54	20.53	20.51	20.50	20.49	20.48
AN	22.22	22.20	22.19	22.18	22.16	22.15	22.14	22.12	22.11	22.10
NE	.91	.53	.15	0.00	0.00	0.00	0.00	0.00	0.00	0.00
DI	24.04	23.89	23.73	23.55	23.35	23.12	22.90	22.89	22.87	22.86
HY	0.00	0.00	0.00	.68	1.77	2.82	2.95	2.95	2.95	2.95
OL	7.35	6.39	5.45	4.04	2.37	.77	0.00	0.00	0.00	0.00
MT	5.14	5.96	6.78	7.60	8.42	9.24	9.64	8.00	6.36	4.72
HM	0.00	0.00	0.00	0.00	0.00	0.00	.29	1.99	3.68	5.37
IL	9.67	9.66	9.66	9.65	9.65	9.64	9.63	9.63	9.62	9.62
AP	2.20	2.20	2.19	2.19	2.19	2.19	2.19	2.19	2.19	2.19
TOTAL	100.00	100.00	100.00	100.00	100.00	100.00	100.00	100.00	100.00	100.00

1 AUL 006.1-1
2 AUL 006.1-2
3 AUL 006.1-3
4 AUL 006.1-4
5 AUL 006.1-5
6 AUL 006.1-6
7 AUL 006.1-7
8 AUL 006.1-8
9 AUL 006.1-9
10 AUL 006.1-10

	1	2	3	4	5	6	7	8	9
SIO2	43.89	43.89	43.89	43.89	43.89	43.89	43.89	43.89	43.89
TIO2	5.00	5.00	5.00	5.00	5.00	5.00	5.00	5.00	5.00
AL2O3	13.65	13.65	13.65	13.65	13.65	13.65	13.65	13.65	13.65
CR2O3	0.00	0.00	0.00	0.00	0.00	0.00	0.00	0.00	0.00
FE2O3	9.08	9.64	10.20	10.76	10.32	10.88	2.98	2.48	1.98
FEO	5.18	4.68	4.18	3.68	3.18	2.68	10.63	11.08	11.53
MNO	.26	.26	.26	.26	.26	.26	.26	.26	.26
NIO	0.00	0.00	0.00	0.00	0.00	0.00	0.00	0.00	0.00
MGO	5.37	5.37	5.37	5.37	5.37	5.37	5.37	5.37	5.37
CAO	11.47	11.47	11.47	11.47	11.47	11.47	11.47	11.47	11.47
NA2O	2.39	2.39	2.39	2.39	2.39	2.39	2.39	2.39	2.39
K2O	1.59	1.59	1.59	1.59	1.59	1.59	1.59	1.59	1.59
P2O5	.93	.93	.93	.93	.93	.93	.93	.93	.93
CO2	0.00	0.00	0.00	0.00	0.00	0.00	0.00	0.00	0.00
H2O	.89	.89	.89	.89	.89	.89	.89	.89	.89
S	0.00	0.00	0.00	0.00	0.00	0.00	0.00	0.00	0.00
TOTAL	99.70	99.76	99.82	99.88	98.94	99.00	99.05	99.00	98.95

	1	2	3	4	5	6	7	8	9
Q	.21	.21	.21	.21	.21	.21	0.00	0.00	0.00
OR	9.52	9.51	9.51	9.50	9.59	9.59	9.58	9.59	9.59
AB	20.46	20.45	20.44	20.43	20.62	20.61	18.29	17.68	17.06
AN	22.08	22.07	22.06	22.04	22.25	22.24	22.23	22.24	22.25
NE	0.00	0.00	0.00	0.00	0.00	0.00	1.25	1.59	1.93
DI	22.84	22.83	22.82	22.80	23.02	23.01	24.15	24.26	24.36
HY	2.94	2.94	2.94	2.94	2.97	2.96	0.00	0.00	0.00
OL	0.00	0.00	0.00	0.00	0.00	0.00	8.22	9.11	10.00
MT	3.09	1.46	0.00	0.00	0.00	0.00	4.40	3.67	2.93
HM	7.06	8.75	10.31	10.87	10.53	11.09	0.00	0.00	0.00
IL	9.61	9.60	9.49	8.41	7.42	6.34	9.67	9.68	9.68
RU	0.00	0.00	.06	.62	1.19	1.76	0.00	0.00	0.00
AP	2.18	2.18	2.18	2.18	2.20	2.20	2.20	2.20	2.20
TOTAL	100.00	100.00	100.00	100.00	100.00	100.00	100.00	100.00	100.00

1 AUL 006.1-11
2 AUL 006.1-12
3 AUL 006.1-13
4 AUL 006.1-14
5 AUL 006.1-15
6 AUL 006.1-16
7 AUL 006.1-17
8 AUL 006.1-18
9 AUL 006.1-19

Therefore, since it appears to come closest to the unaltered state of these rocks, Table 9, with Fe_2O_3 adjusted so that $Fe_2O_3/(FeO + Fe_2O_3) = 0.15$, has been used for the values plotted in subsequent chapters. The difference in using Table 9 rather than the other iron corrections means small changes in the value of the Thornton-Tuttle Differentiation Index (norm $Q + Ab + Or + Ne + Lc + Ks$), but these changes do not alter the basic relationships between the different samples on plots of elements versus differentiation index. Also, choosing Table 9 rather than Tables 6 or 7 means that, generally, the samples are less Q-normative, i.e. are more undersaturated.

Part of the problem in determining which adjustments to use lies in the inadequacy of the norm programme, and also with limits to the analytical methods. Stice (1968) found that for intermediate basalts, a change in Na_2O from 2.00 to 1.82 weight per cent changed the sample from alkalic picrite basalt (Ne-normative) to tholeiitic picrite basalt (Hy-normative). He also found that laboratories could differ as much as 0.4% Na_2O, 0.3% K_2O, and 0.7% Fe_2O_3 in their analyses. These three elements are all important in determining whether a rock is Ne- or Hy- normative, i.e. whether a rock is alkalic or tholeiitic. MacDonald and Katsura (1964) note that the presence or absence of hypersthene in the norm depends not only on the degree of alkali richness and silica poorness, but also on the oxidation state of iron, as has

been demonstrated above in Figure 10.

Thus, one must consider many factors in deciding whether these rocks are originally alkalic and have been altered to tholeiites, or whether both alkalic and tholeiitic basalts were originally present in the core and have not been affected by the alteration. The effects of alteration on these rocks will be considered in a later chapter as a discussion of the nature of the magmatism on Sao Miguel. The analyses which were used for chemical plots in subsequent chapters are, as noted above, those of Table 9: CO_2-free, $Fe_2O_3/(FeO + Fe_2O_3) = 0.15$.

b) Trace Elements

The trace element analyses were performed by Dr. Ian Gibson, Bedford College, London, and have been presented with the major element oxides in Table 9. All values are in ppm. A discussion of errors has been included in Appendix II along with the method of analysis.

c) Pyroclastic Units

Table 11 contains the analyses of four pyroclastic units: AUA 026.4, AUA 048.1, AUA 058.9, and AUA 080.1. These results are presented here to illustrate that the pyroclastic units are chemically closer to the trachytes than to the basalts. These pyroclastics have SiO_2, TiO_2, MgO, CaO, and P_2O_5 concentrations intermediate to the values for the trachytes and trachybasalts. A notable feature of these units is the high Al_2O_3 content, to a maximum of 22.00

TABLE 11: Analyses for the pyroclastic units.

Trace element data included.

	AUA 026.4	AUA 048.1	AUA 058.9	AUA 080.1
SIO2	60.40	57.13	64.22	63.03
TIO2	.71	1.05	.96	.93
AL2O3	20.07	22.00	17.97	17.10
CR2O3	0.00	0.00	0.00	0.00
FE2O3	3.13	5.95	3.16	2.40
FEO	.46	.74	.82	1.09
MNO	.02	.03	.06	.14
NIO	0.00	0.00	0.00	0.00
MGO	.72	1.72	1.70	1.95
CAO	.78	1.28	1.85	2.16
NA2O	5.29	2.52	2.04	2.34
K2O	4.41	3.18	2.53	3.69
P2O5	.11	.19	.15	.13
CO2	.14	0.00	.23	1.21
H2O	2.63	4.14	3.39	3.33
S	0.00	0.00	0.00	0.00
TOTAL	98.87	99.93	99.08	99.50

	AUA 026.4	AUA 048.1	AUA 058.9	AUA 080.1
Q	11.10	26.64	38.89	32.67
OR	27.10	19.64	15.64	22.70
AB	46.51	22.26	18.04	20.59
AN	2.35	5.33	7.05	2.30
HY	1.86	4.47	4.42	5.05
MT	0.00	0.00	.06	1.33
HM	3.25	6.21	3.26	1.58
IL	1.05	1.70	1.91	1.84
RU	.18	.20	0.00	0.00
AP	.27	.46	.36	.31
C	5.99	13.09	9.83	8.78
CC	.33	0.00	.55	2.86
TOTAL	100.00	100.00	100.00	100.00

	AUA 026.4	AUA 048.1	AUA 058.9	AUA 080.1
Nb	206	269	189	196
Y	76	77	71	76
Sr	100	309	230	358
Rb	109	115	96	122
Zr	1227	1143	945	968
Cr	N.D.	–	N.D.	N.D.
Ni	10	–	8	2

weight per cent, a value 5 weight per cent higher than any of the basalts or the trachytes.

CHAPTER 5: PLOTS OF RESULTS

The data contained in Chapter 4 can be overwhelming
and not particularly meaningful unless summarized carefully
and presented in a graphical manner. Therefore, the follow-
ing pages contain a series of plots which attempt to illus-
trade trends and variations inherent in the chemical data.
A summary of the salient points regarding the variations is
also included.

i) Elements Versus Depth

Chemical changes in the eruptive products with time
are common features of volcanoes. Therefore, to demonstrate
these changes, plots of the major oxides (as weight percent-
ages) versus depth (in metres) in the drillcore have been
made and presented as Figures 11, 12, and 13. The data have
been taken from Table 9.

Two areas of major chemical differences are present:
the three trachytic flow units in Subaerial Sequence II
between approximately 300 and 350 m, and a series of trachy-
basalt units between 650 and 700 m in Subaerial Sequence I.
The flow unit at the top of the volcanic pile (AUL 001.2) is
also trachytic.

The presence of the three trachyte units in Subaerial
Sequence II is evident on the plots as distinct minima of
MnO, MgO, P_2O_5, CaO, TiO_2, and FeO_T (all Fe expressed as FeO)
on Figures 11d, 12a, 12c, 13a, 13b, and 13c, respectively,
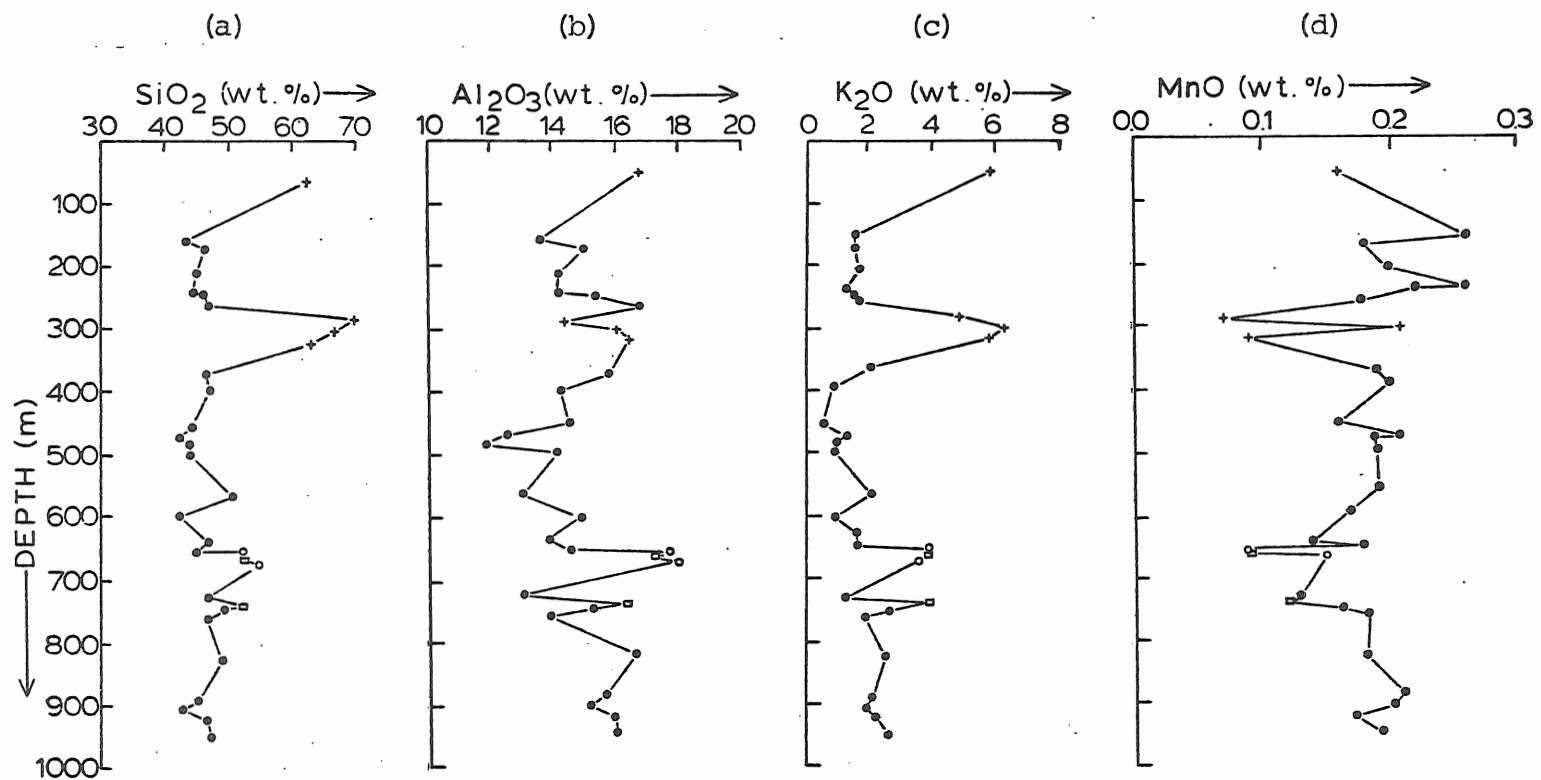
FIGURE 11:   (a) SiO_2, (b) Al_2O_3, (c) K_2O, and (d) MnO as weight per cent plotted versus depth(m).

Symbols: basalts (•), trachybasalts (○), trachytes (+), and intrusives (□).

Correlation coefficients of +0.35, +0.21, +0.47, and −0.45 for (a), (b), (c), and (d),

respectively.
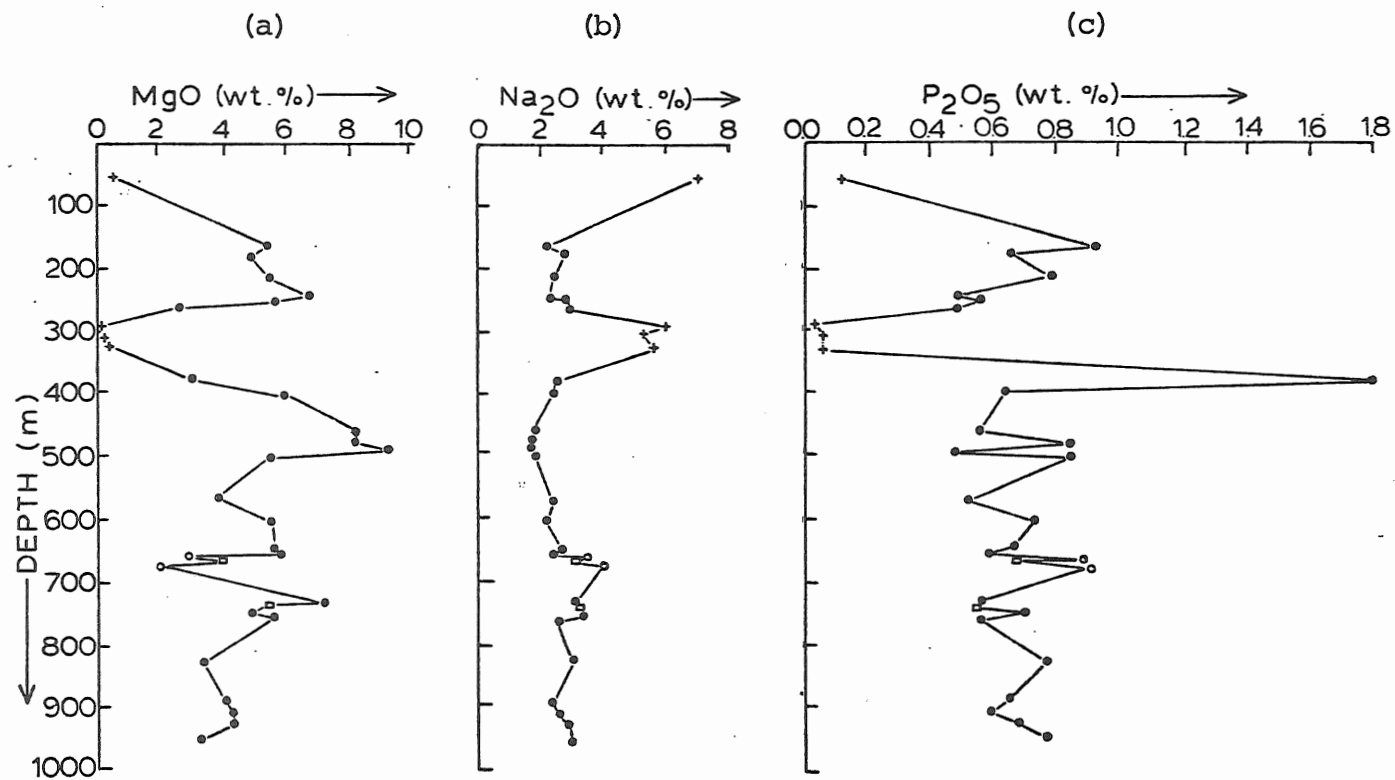
FIGURE 12: (a) MgO, (b) Na$_2$O, and (c) P$_2$O$_2$ as weight per cent plotted versus depth (m).
Correlation coefficients of −0.21, + 0.25, and −0.12 for (a), (b), and (c),
respectively.
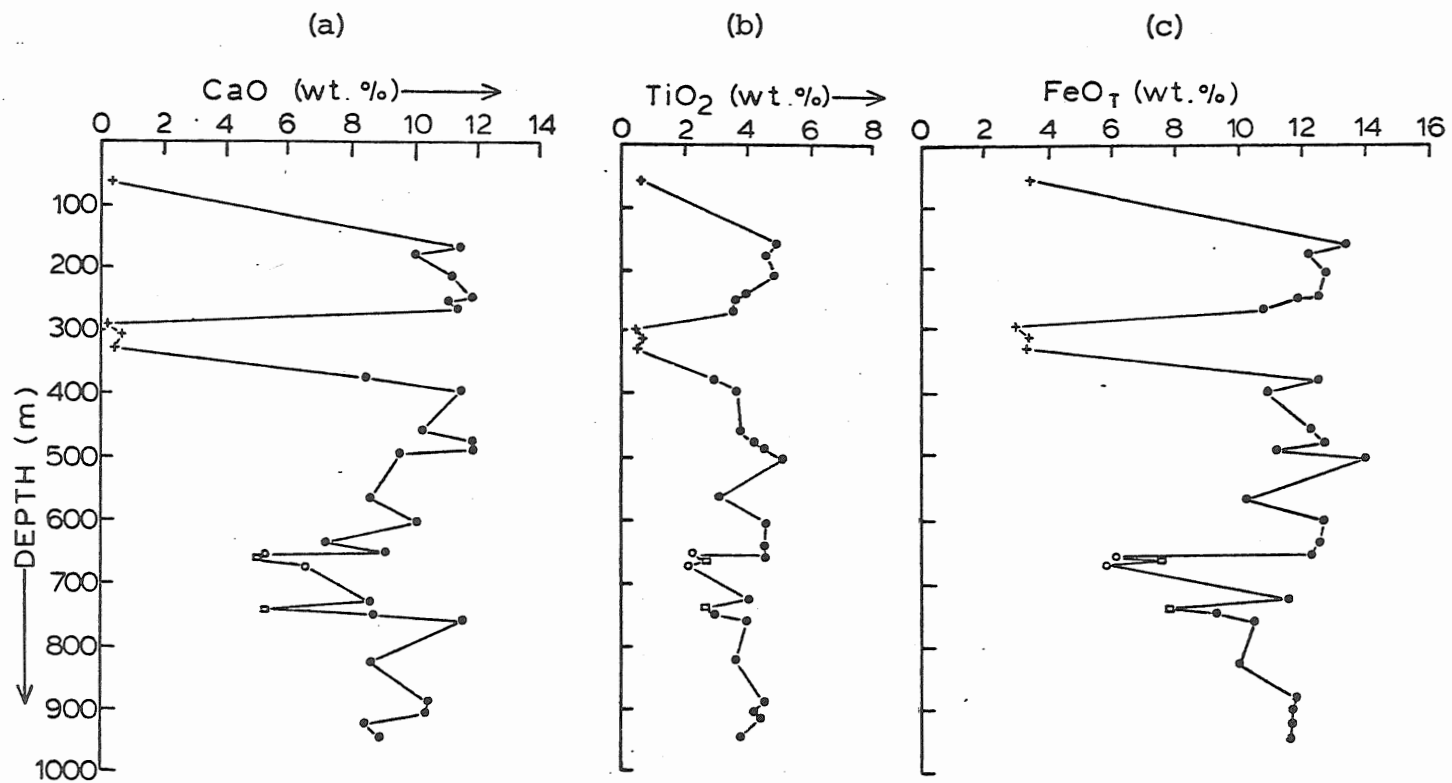
FIGURE 13: (a) CaO, (b) TiO$_2$, and (c) FeO$_T$ as weight per cent plotted versus depth (m).
Correlation coefficients of -0.51, -0.23, and -0.37 for (a), (b), and (c),
respectively.

and as distinct maxima of SiO_2, K_2O, and Na_2O (Figures 11a, 11c, and 12b, respectively).

The samples AUL 094.1, 096.1, 098.2, 099.1, and AUS 098.5 in the section of the core between 650 and 700 m have the chemical characteristics of trachybasalts. These rocks exhibit the same maxima and minima shown by the trachytes described above, but the trachytic features are not as pronounced, and the maxima and minima are intermediate to the values of the trachytes and the basalts. This is particularly noticeable in the intermediate potassium, sodium, and silicon values of the trachybasalts.

There appears to be no systematic variation of K_2O, Na_2O, or SiO_2 in the basalts from top to bottom of the core. CaO, TiO_2, and MgO appear to decrease slightly with depth in the core. FeO_T and Al_2O_3 appear to vary randomly, although alumina appears to undergo a slight increase overall with depth (Figure 11b).

Figure 14a is a plot of $Fe_2O_3/(FeO + Fe_2O_3)$ versus depth using the Fe_2O_3 and FeO values without adjustment. The diagram appears to show an increase in $Fe_2O_3/(FeO + Fe_2O_3)$ in the basalts with depth to approximately 730 m (sample AUL 108.1). Below this depth, the value of the ratio for the basalts decreases as the depth increases.

Figure 14b is a plot of the analysed value of $Fe_2O_3/(FeO + Fe_2O_3)$ versus $(CO_2 + H_2O^+)$ in weight per cent. There appears to be a rough positive correlation between the two
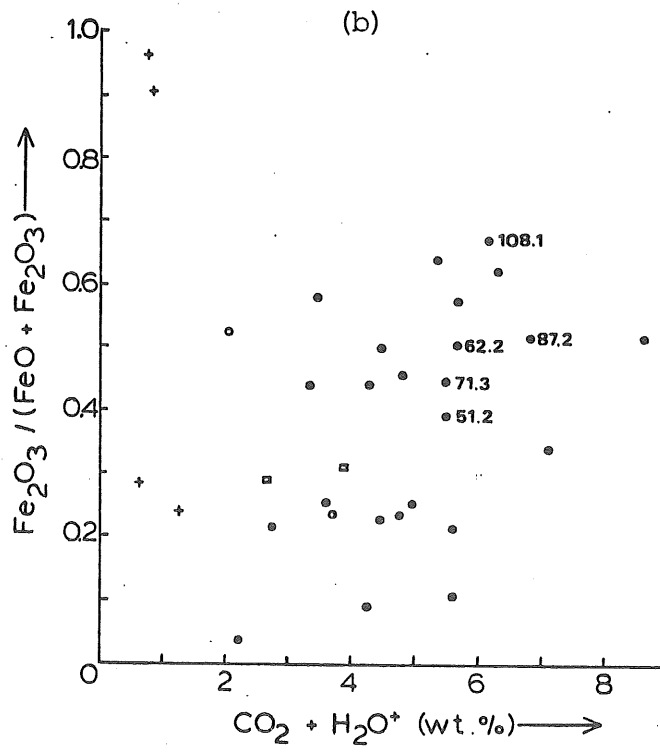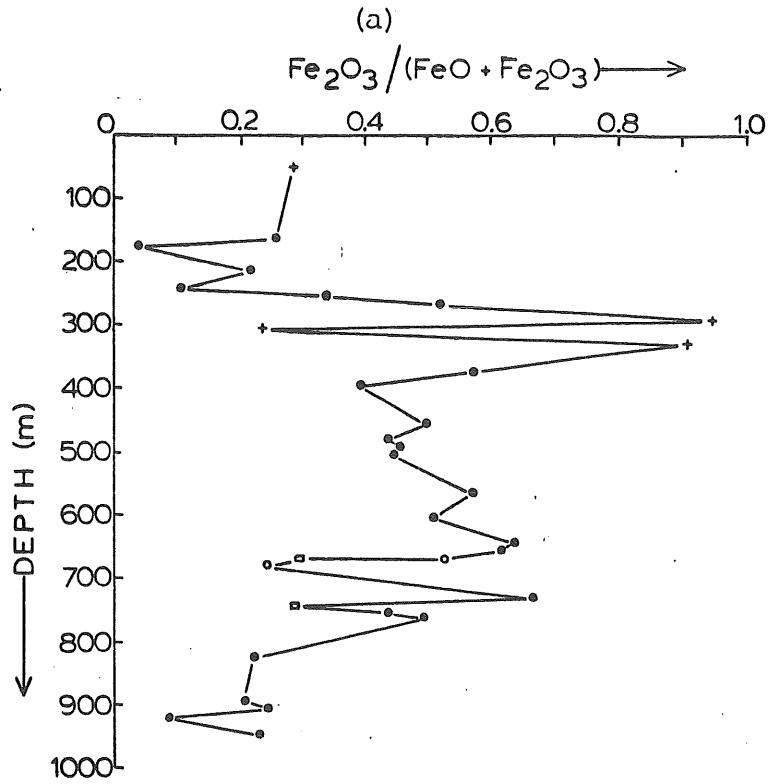
FIGURE 14: Analysed $Fe_2O_3/(FeO + Fe_2O_3)$ plotted versus

(a) depth (m) and (b) $CO_2 + H_2O^+$ (wt.%)

quantities, but in general, the scatter of the points is too great to make any definite statement. This scatter appears to indicate that the oxidation of Fe^{2+} to Fe^{3+} is not associated with an increase in CO_2 and H_2O^+ in all cases.

The concentrations of the trace elements (in ppm) have also been plotted against depth (in metres) in the core. These diagrams are included as Figures 15, 16 and 17.

The trachytic flow units between 300 and 350 m and, to a less noticeable extent, the trachybasalts between 650 and 700 m define maxima and minima on these diagrams. The trachytes show maxima for Nb, Rb, Y, and Zr (Figures 15a, 16a, 16c, and 17b, respectively), and distinct minima for Sr, Cr, and Ni (Figures 15b, 16b, and 17a, respectively). The trachybasalts show slight maxima for Nb, Zr, Sr, Rb, and Y, and slight minima for Cr and Ni.

Nb and Zr (Figures 15a and 17b, respectively) show irregular increases in concentration with increasing depth in the core. These possible trends are dealt with in Chapter 8. The Cr and Ni values (Figures 16b and 17a, respectively) show extremely random variations, possibly reflecting the fact that these two elements are concentrated in olivine, which is the most easily altered mineral in these samples. The other trace elements (Sr, Rb, and Y, Figures 15b, 16a, and 16c, respectively) show no marked trends with increasing depth.

ii) Elements Versus Differentiation Index

Thornton and Tuttle (1960) proposed a concept which

(a)

(b)

Nb (ppm)⟶

Sr (ppm)⟶

⟶ + 163 ppm

⟶ + 202 ppm
⟶ + 216 ppm
⟶ + 198 ppm
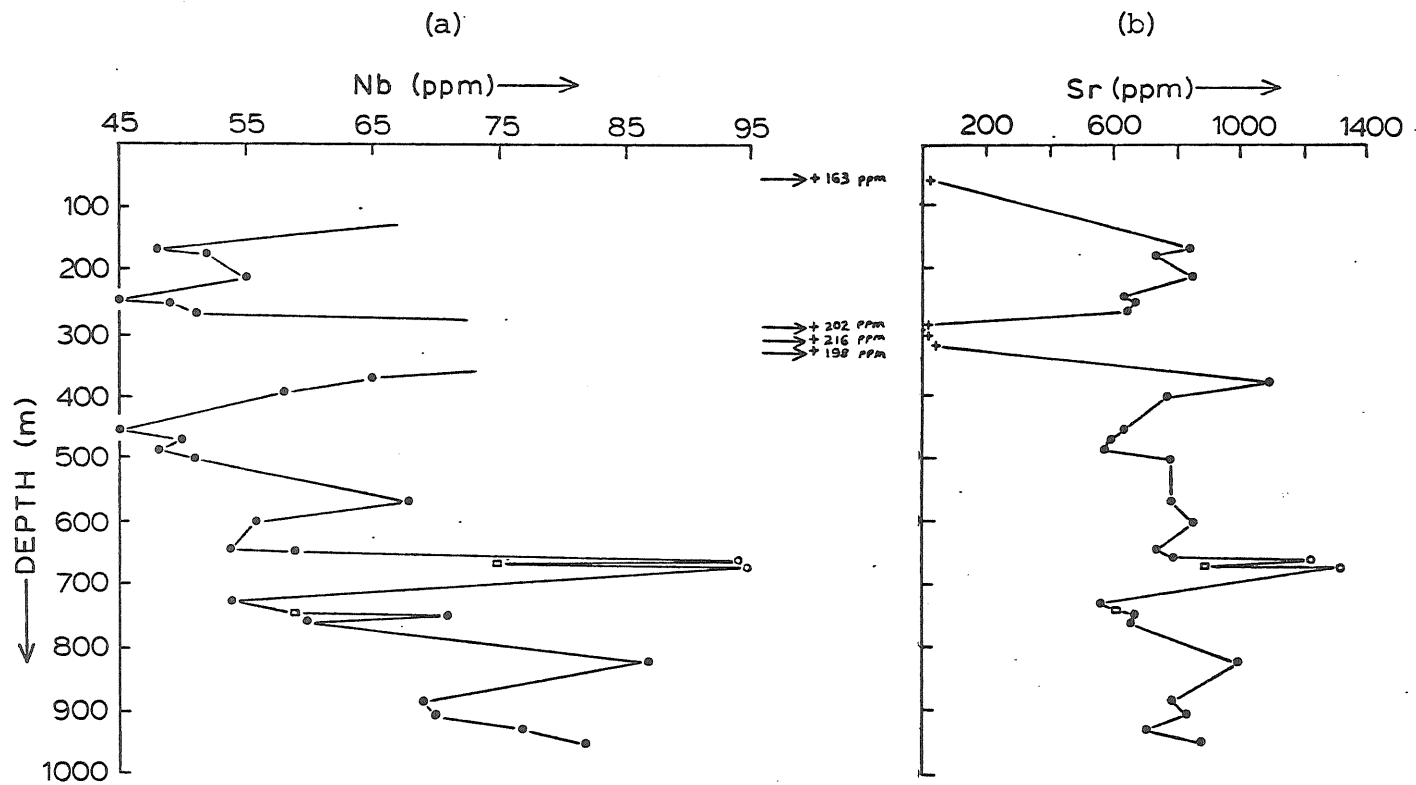
FIGURE 15: (a) Nb and (b) Sr as ppm plotted versus depth (m). Correlation coefficients

of +0.76 and + 0.09 for (a) and (b), respectively.
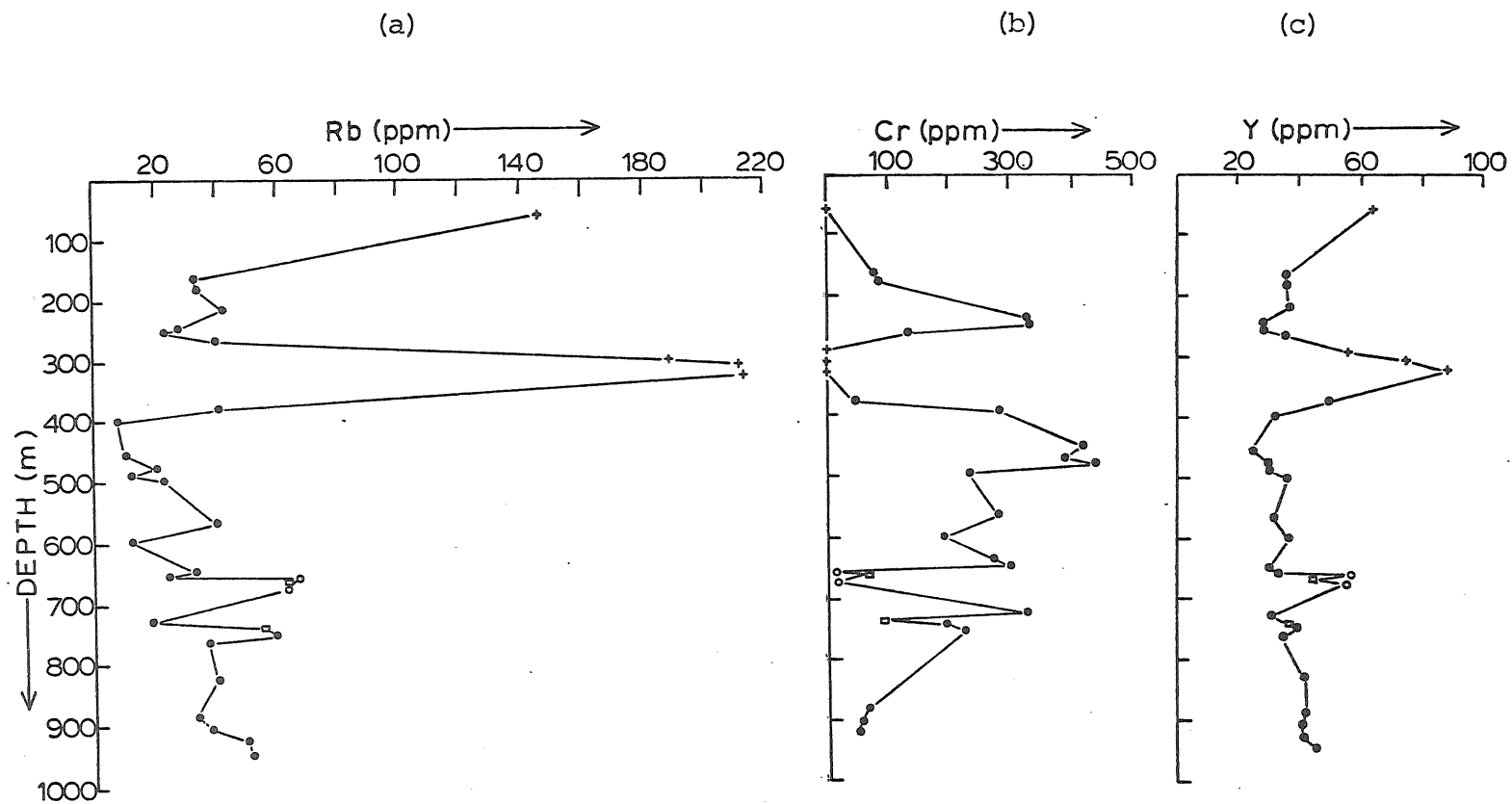
FIGURE 16: (a) Rb, (b) Cr, and (c) Y as ppm plotted versus depth (m). Correlation coefficients of +0.39, -0.18, and +0.43 for (a), (b), and (c), respectively.
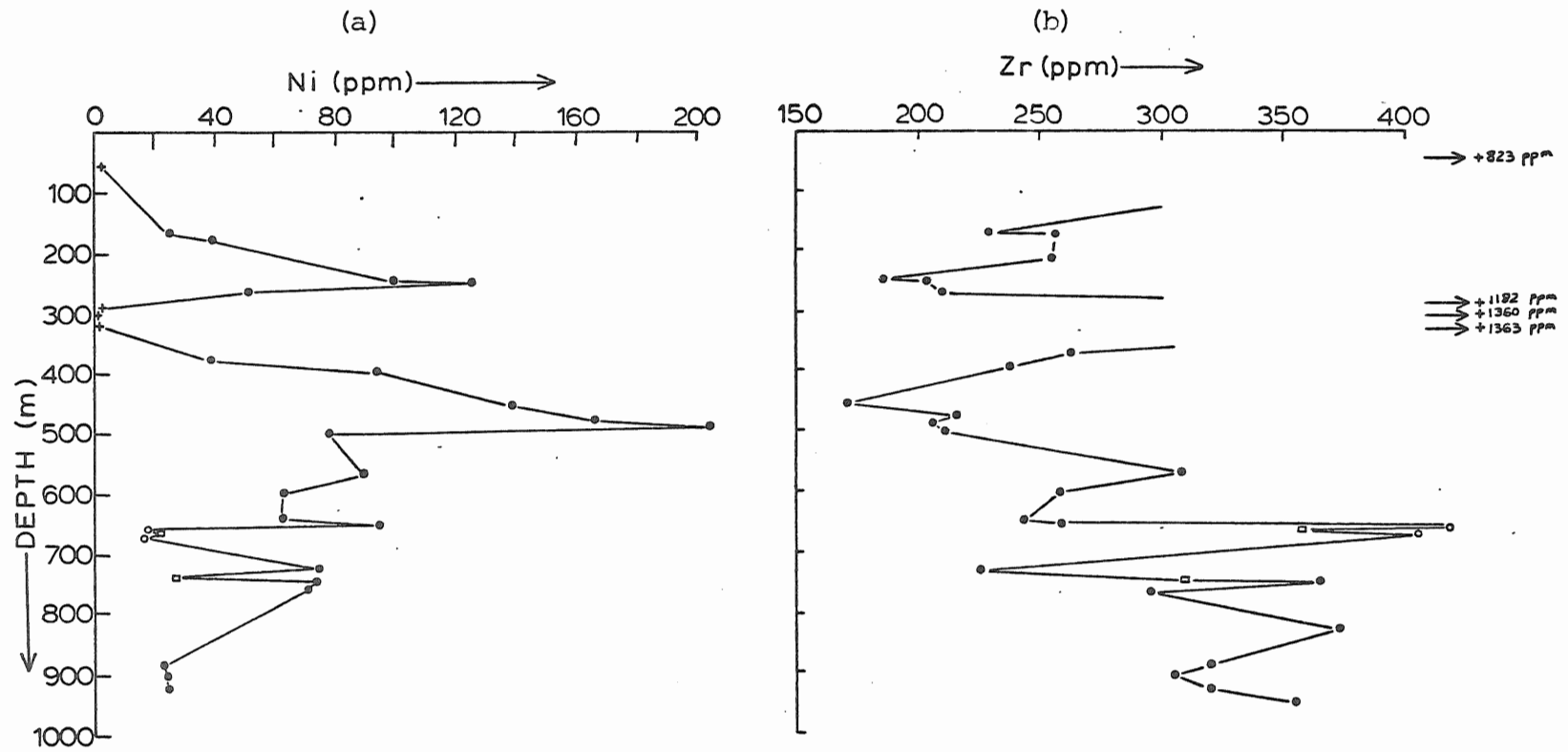
FIGURE 17: (a) Ni and (b) Zr as ppm plotted versus depth (m). Correlation coefficients of −0.24 and +0.71 for (a) and (b), respectively.

has been termed the Thornton-Tuttle Differentiation Index
and is defined as D.I. = (Norm Q + Or + Ab + Ne + Lc + Ks).
It is based on the observation that in both natural and
experimental systems, most magmas tend to crystallize toward
the system of silica-nepheline-kalsilite (SiO_2-$NaAlSiO_4$-$KAlSiO_4$)
or, as it is commonly known, petrogeny's residua system.

Thornton and Tuttle (1960) plotted oxides versus D.I.
and outlined limits to chemically define the nature of the
rocks. Borley (1974) has used similar limits to those pro-
posed by Thornton and Tuttle. Rocks of alkaline affinity
are those with SiO_2 values which plot below the an-or line
on the plot of SiO_2 versus D.I. Figure 18). Of the rocks
which plot in this region of SiO_2 undersaturation, alkali
basalts tend to have a D.I. less than 40, trachybasalts a
D.I. between 40 and 65, trachyandesites a D.I. between 65
and 75, and trachytes a D.I. greater than 75.

The D.I. for a rock changes in value as the ratio
Fe_2O_3/(FeO + Fe_2O_3) changes. This is shown by Table 12, which
lists the value of the D.I. as the Fe_2O_3/(FeO + Fe_2O_3) ratio
changes for sample AUL 006.1. As Fe_2O_3/(FeO + Fe_2O_3) changes
from 0.15 to 0.80, the value of the D.I. changes from 28.577
to a maximum of 30.425 at Fe_2O_3/(FeO + Fe_2O_3) = 0.76, a diff-
erence of 1.848 in the value of the D.I. Thus, changing the
Fe_2O_3/(FeO + Fe_2O_3) ratio will produce a significant change
in the evaluation of a sample only if it is on the border
between two rock types, or if it plots close to the an-or line.

TABLE 12: Change in Thornton-Tuttle D.I. with changing
$Fe_2O_3/(FeO + Fe_2O_3)$ for sample AUL 006.1

$Fe_2O_3/(FeO + Fe_2O_3)$	D.I.
0.15	28.577
0.18	28.850
0.22	29.123
0.25	29.396
0.29	29.689
0.33	29.999
0.37	30.110
0.41	30.091
0.45	30.073
0.49	30.267
0.53	30.246
0.56	30.228
0.60	30.209
0.64	30.191
0.67	30.173
0.71	30.154
0.74	30.136
0.76	30.425
0.80	30.406

In the latter case a change of ± 2 in the D.I. could move the sample into or out of the undersaturated region of the plot.

Thus, on a plot of SiO_2 versus D.I. such as Figure 18 changes in D.I. resulting from adjustments of the $Fe_2O_3/$ $(FeO + Fe_2O_3)$ ratio will not change the basic trend of the graph. In Figure 25, the values for D.I. used are for $Fe_2O_3/$ $(FeO + Fe_2O_3) = 0.15$. The silica-saturation line (an-or) of Thornton and Tuttle (1960) has been included. Rocks which plot above this line are considered to be saturated. Those which plot below it are undersaturated.

As is evident in Figure 18a, all but seven of the Azores rocks plot below the an-or line in the region of silica undersaturation, i.e., as rocks of alkaline affinity. What is also evident in Figure 18a is that there are no rock units represented which possess a D.I. between 60 and 85. The apparent absence of rocks with the compositions of trachyandesites will be discussed later in more detail.

Based on Borley's (1974) definitions, one can chemically classify 17 of these rocks as alkali basalts, 7 of them as trachybasalts, and 2 as trachytes. Six of the samples plot above the an-or line as saturated rocks. Not one of the analysed rocks falls within the range of composition of trachyandesites.

The oxides of the major elements (in weight per cent, CO_2-free) and the concentrations of the trace elements (in ppm) have also been plotted against the Thornton-Tuttle
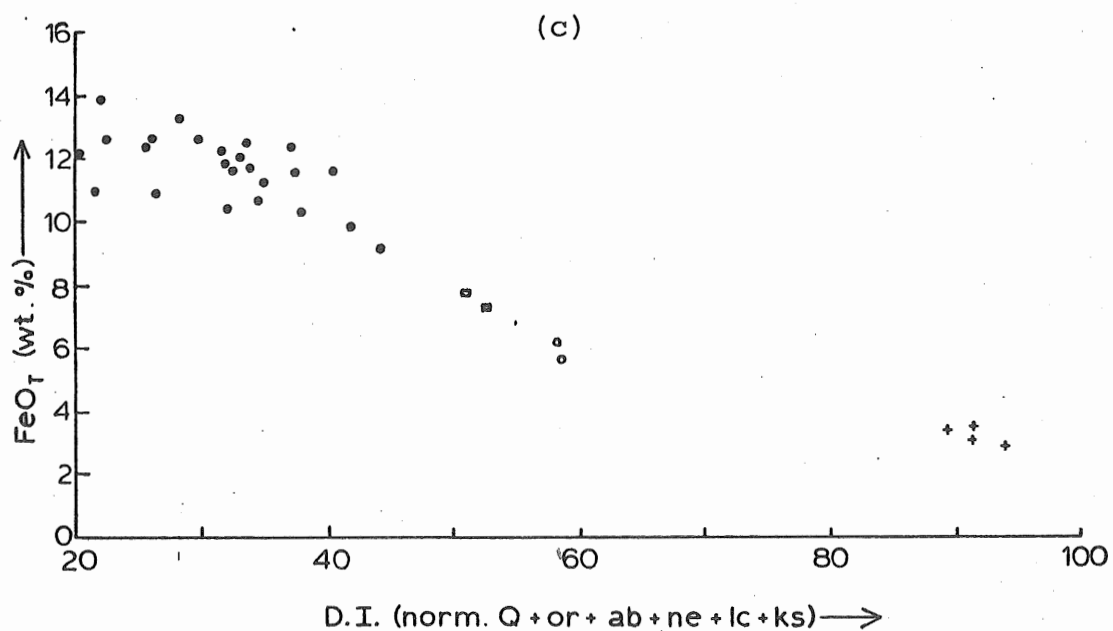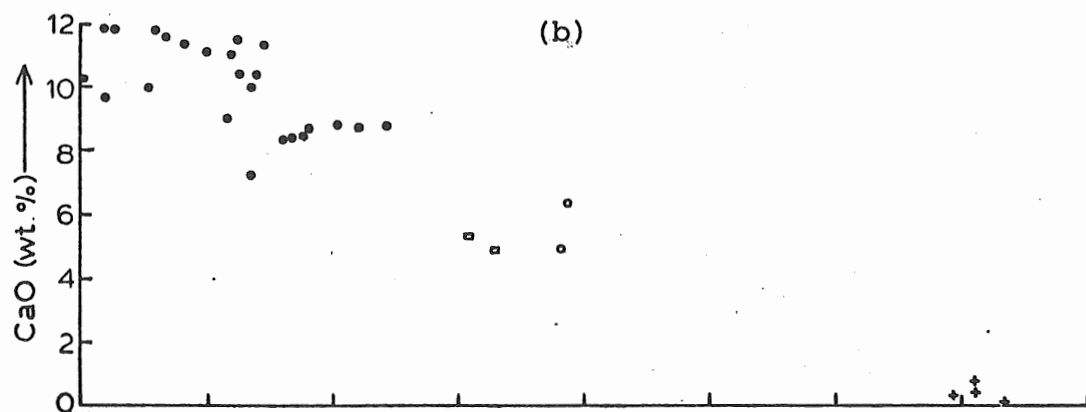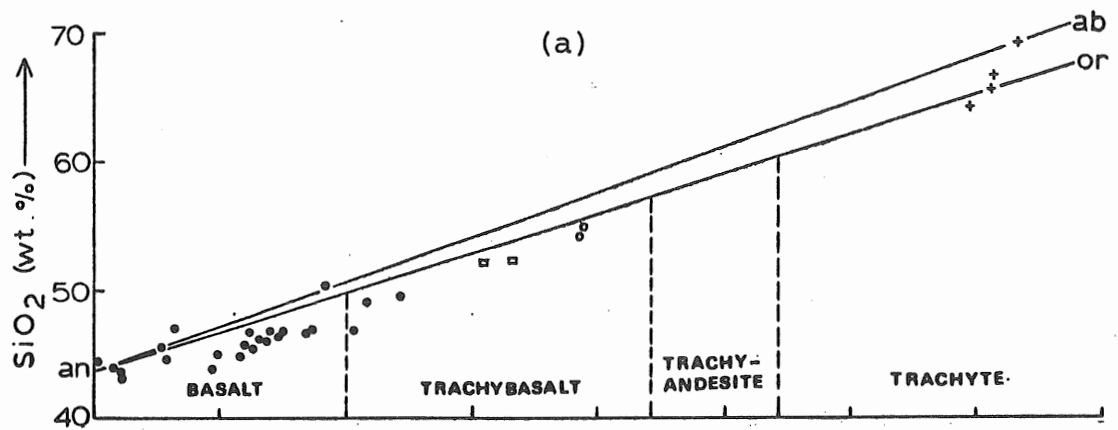
FIGURE 18: (a) SiO$_2$, (b) CaO, and (c) FeO$_T$ as weight per cent plotted versus Thornton-Tuttle differentiation index.
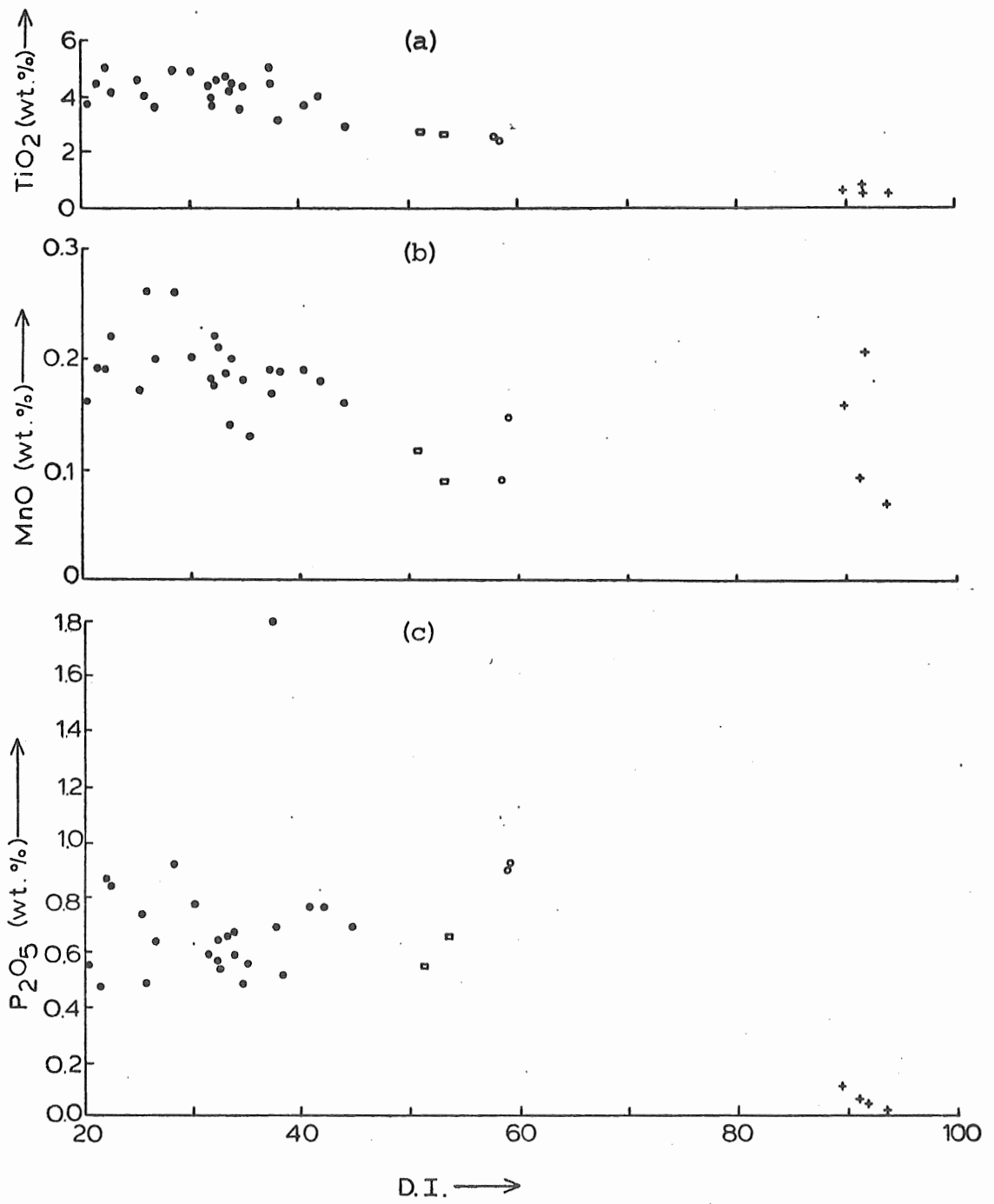
FIGURE 19: (a) TiO_2, (b) MnO, and (c) P_2O_5 as weight per cent
plotted versus D.I.
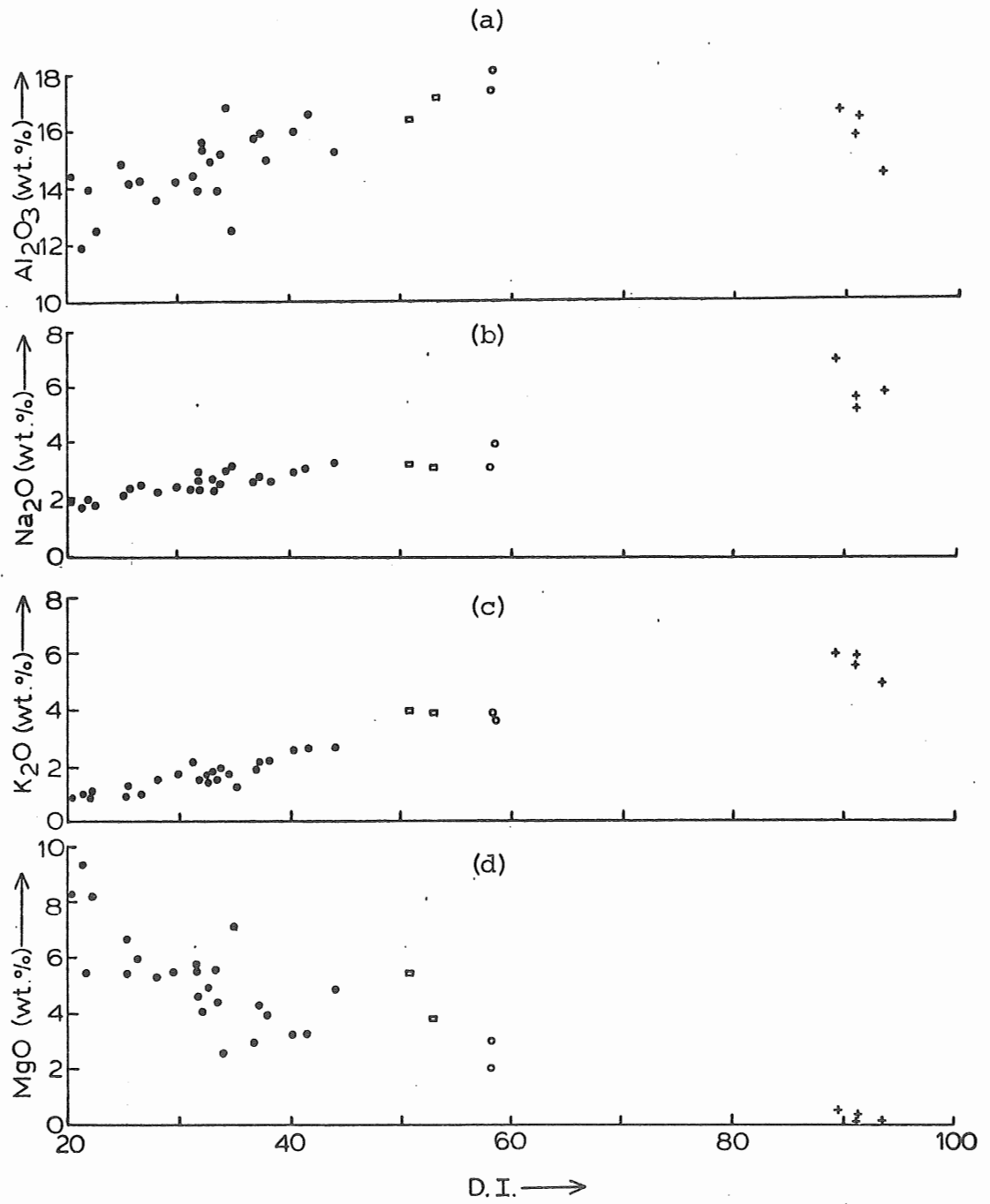
FIGURE 20: (a) Al_2O_3, (b) Na_2O, (c) K_2O, and (d) MgO as weight per cent plotted versus D.I.

differentiation index for each analysed unit (Figures 18 to 23). This series of plots illustrate how each element reacts to increasing differentiation.

Of the major elements, CaO, FeO_T, TiO_2, P_2O_5, and MgO (Figures 18b, 18c, 19a, 19c, and 20d, respectively) show distinct decreases in concentration with an increase in the value of the D.I. MnO (Figure 19b) shows a very slight decrease at higher differentiation indices. Na_2O and K_2O (Figures 20b and 20c) both show marked increases in value as the D.I. increases. The samples with higher D.I. also have slightly higher Al_2O_3 contents (Figure 20a).

The trace elements also show variations with changes in the differentiation index. Zr, Nb, Rb, and Y (Figures 21a, 21b, 22b, and 23c, respectively) are all distinctly higher in those samples with higher differentiation indices. Sr, Ni, and Cr (Figures 22a, 23a, and 23b) show decreases in concentration with increases in the D.I.

The plot of Sr versus D.I. shows that Sr is slightly enriched in the trachybasalts but is depleted in the trachytes relative to the basalts. Hughes and Brown (1972) noted two trends for alkali olivine basalts from Madeira and attributed them to two different trends in fractionation. However, the presence of this trend on one plot does not necessarily imply that two types of fractionation have occurred.

Thus, patterns of variation for the major and the trace elements can be seen in these plots of elements versus
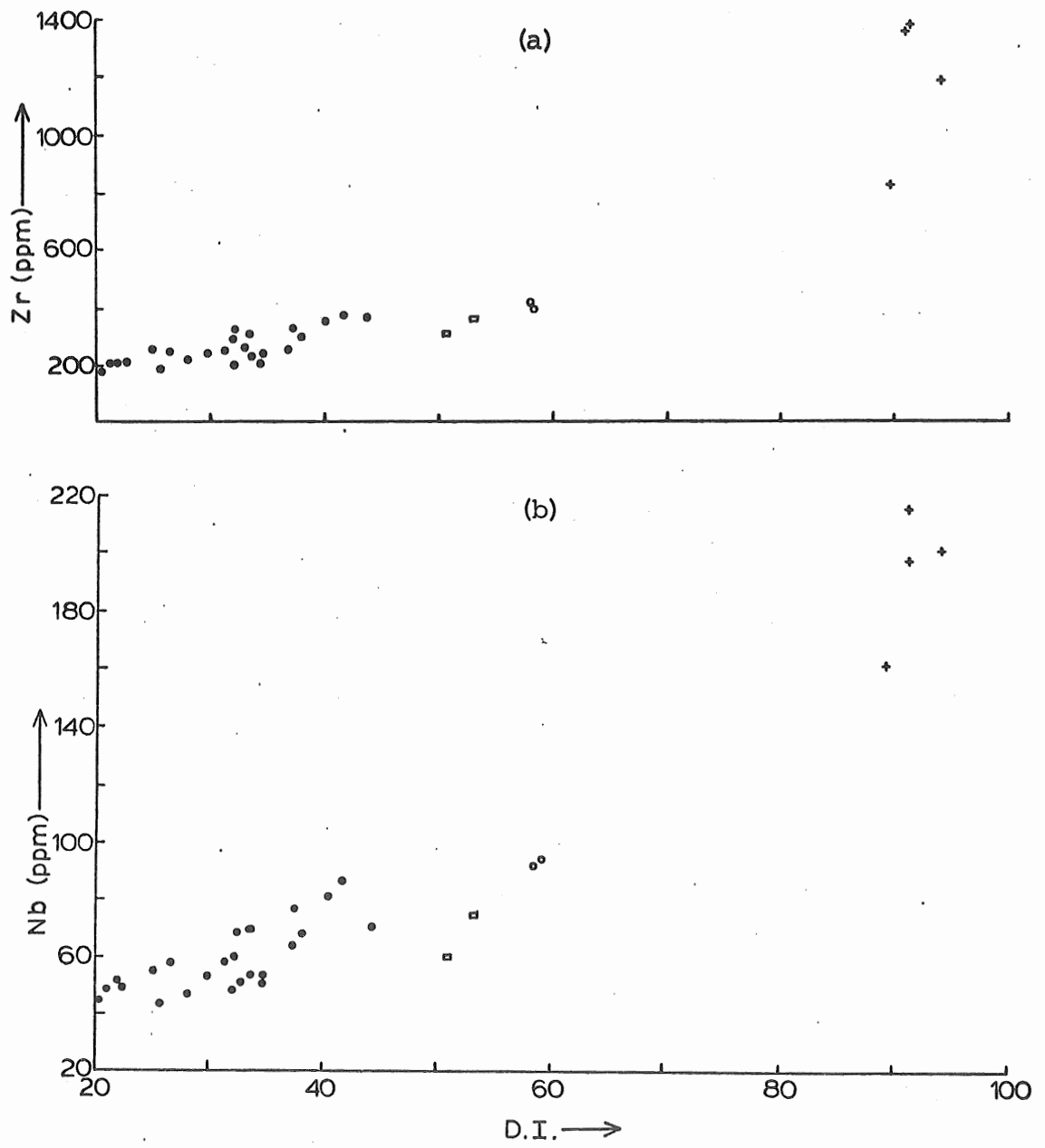
FIGURE 21:   (a) Zr and (b) Nb as ppm plotted versus D.I.
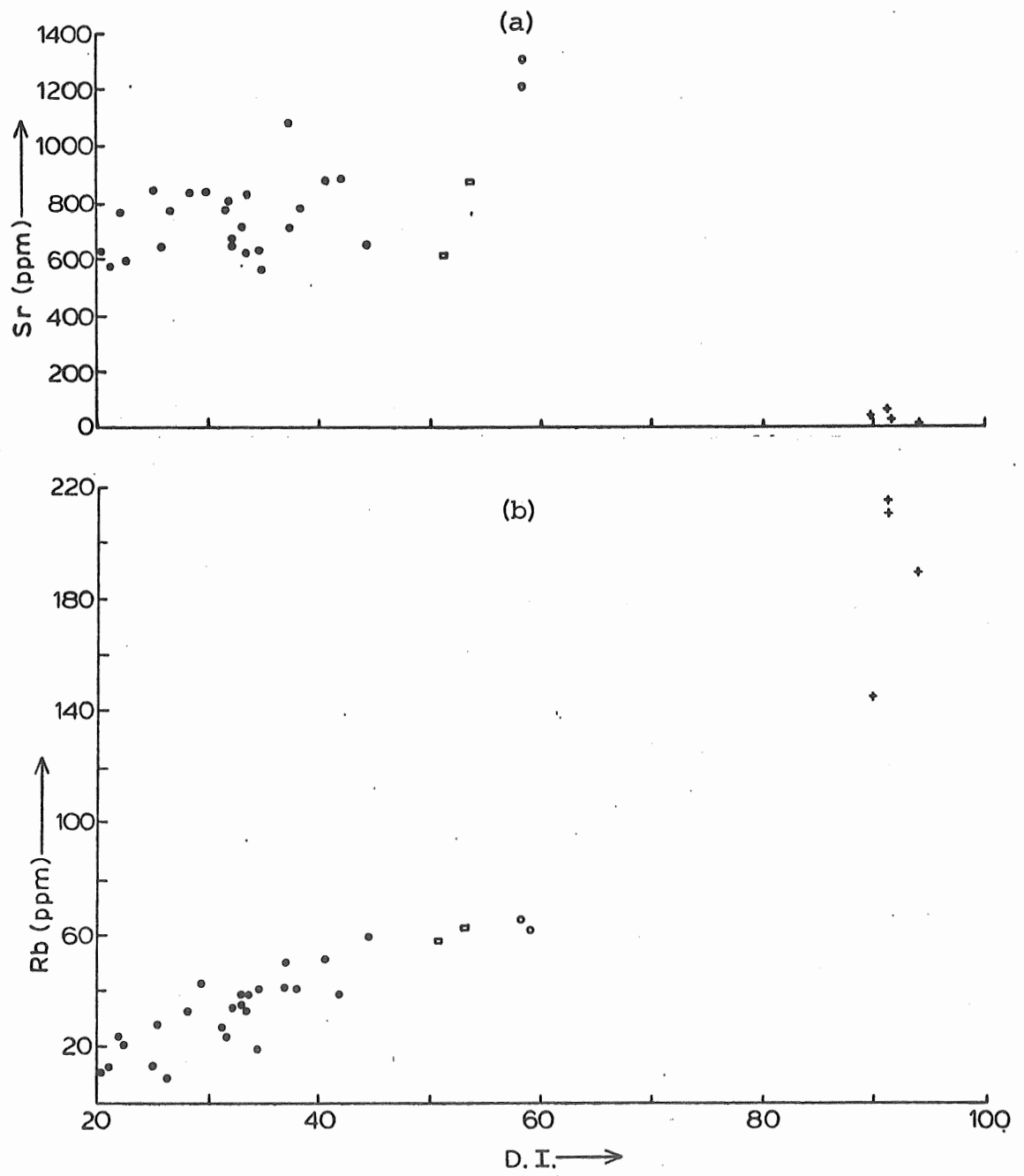
FIGURE 22: (a) Sr and (b) Rb as ppm plotted versus D.I.
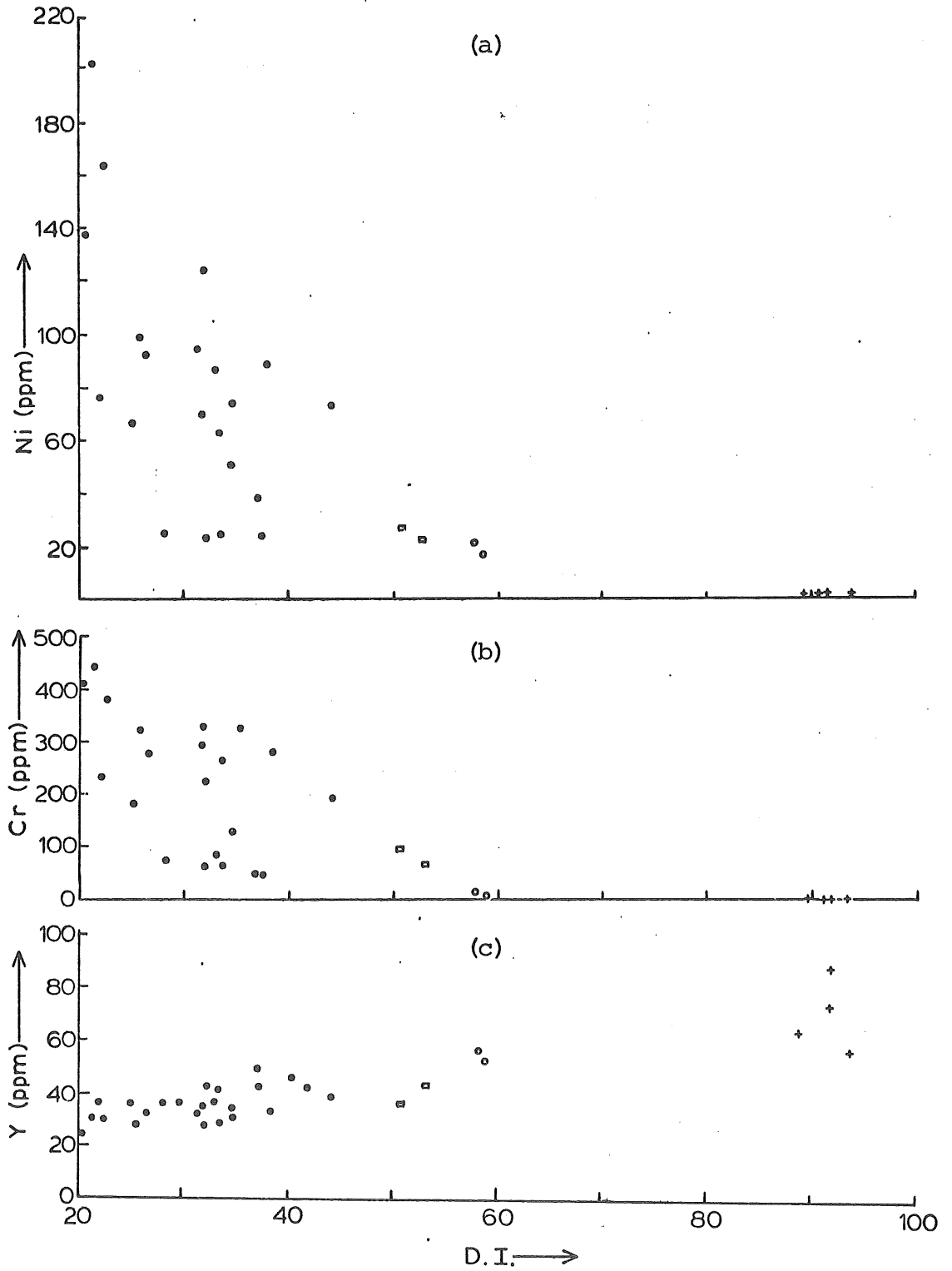
FIGURE 23:   (a) Ni, (b) Cr, and (c) Y as ppm plotted versus D.I.

differentiation index. Similar trends have been shown by
Baker (1969) for the island of St. Helena, and Borley (1974)
has amply demonstrated the SiO_2 variation pattern for many
of the oceanic islands which have alkaline rocks. It thus
appears that alteration effects have not obscured the major
differentiation trends for these Azores rocks.

iii) <u>Variations in the Alkali Elements</u>
a) $Na_2O + K_2O$ Versus SiO_2 Diagram

  A common method used to chemically distinguish between
alkalic and tholeiitic rocks is to construct a plot of total
alkalis ($Na_2O + K_2O$) versus SiO_2. Such a diagram has been
presented for the Azores data as Figure 24.

  In order to separate tholeiitic and alkalic rocks,
the dividing line proposed by MacDonald (1968) has been
included. Alkaline rocks from Hawaii plot above this line;
tholeiitic rocks plot below.

  This type of division was first made by MacDonald and
Katsura (1964) to separate the alkaline and tholeiitic rocks
of Hawaii. Since that time, there have been several pro-
posals as to where to plot this line: MacDonald, 1968;
Kuno, 1968; Irvine and Baragar, 1971; Hyndman, 1972; and
Schwarzer and Rogers, 1974. What is evident from all these
proposals is that it appears to be valid to divide basalts
into alkaline and tholeiitic on the basis of their total
alkalis content. The position of the separating line is
dependent on the bulk composition of the individual magmatic
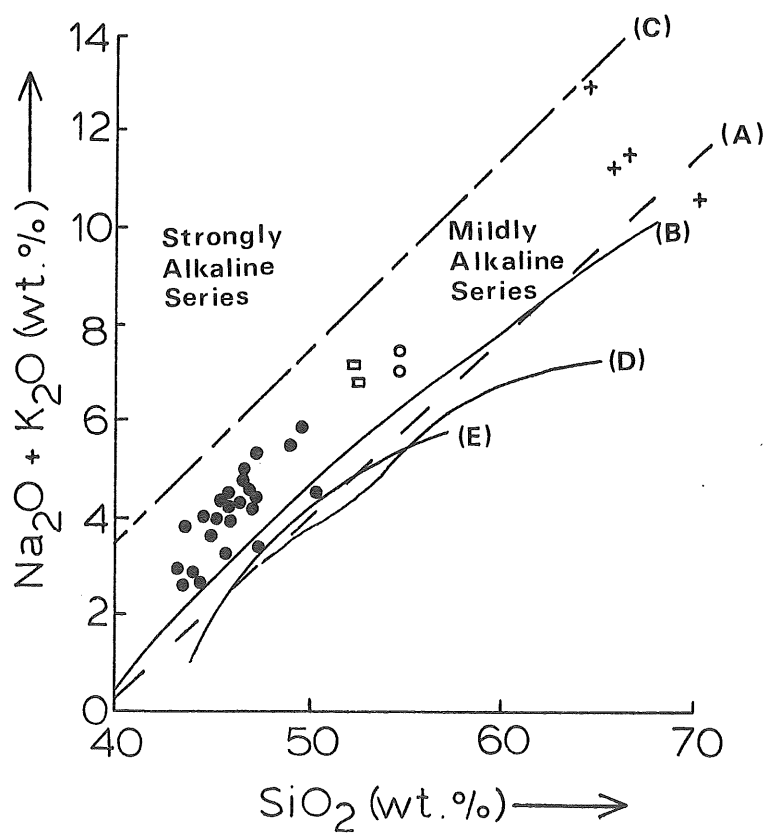
FIGURE 24: Total alkalis (wt.%) plotted versus SiO_2 (wt.%).

(A) MacDonald [1968], (B) Irvine and Baragar [1971],

(C) Saggerson and Williams [1964], (D) Kuno [1968],

(E) Hyndman [1972].

province.

The presentation of such a plot for these Azores analyses is useful in indicating the alkaline affinities of these rocks. All but one of the Azores rocks plots above MacDonald's (1968) dividing line. They plot within what Schwarzer and Rogers (1974) classify as a mildly alkaline series.

b) Na_2O/K_2O Versus SiO_2 Diagram

A plot of Na_2O/K_2O versus SiO_2 is useful in distinguishing sodic volcanic rock suites from those which are more potassic. It is also useful in determining the behaviour of Na_2O and K_2O relative to each other.

Figure 25a is a plot of Na_2O/K_2O versus SiO_2 for the Azores analyses. There appears to be a wide variation of the ratio for basalts with SiO_2 between 45 and 50 weight per cent. However, of the 24 basalts with that range of SiO_2, 19 plot between Na_2O/K_2O = 1.0-2.0. Other oceanic islands have Na_2O/K_2O for basalts ranging from 1.8-2.5 (Cape Verde Islands), 1.3-1.5 (Tristan da Cunha), and 2.5-3.4 (Terceira) (Schmincke, 1973). Therefore, it appears that these Azores samples have alkali chemistry consistent with fresh rocks from other oceanic islands. The remaining five units (AUL 051.2, 062.2, 071.3, 087.2, and 108.1) have widely varying ratios from 2.0 to 3.25. In these five samples, this may be a manifestation of alkali movement during or after magma emplacement.
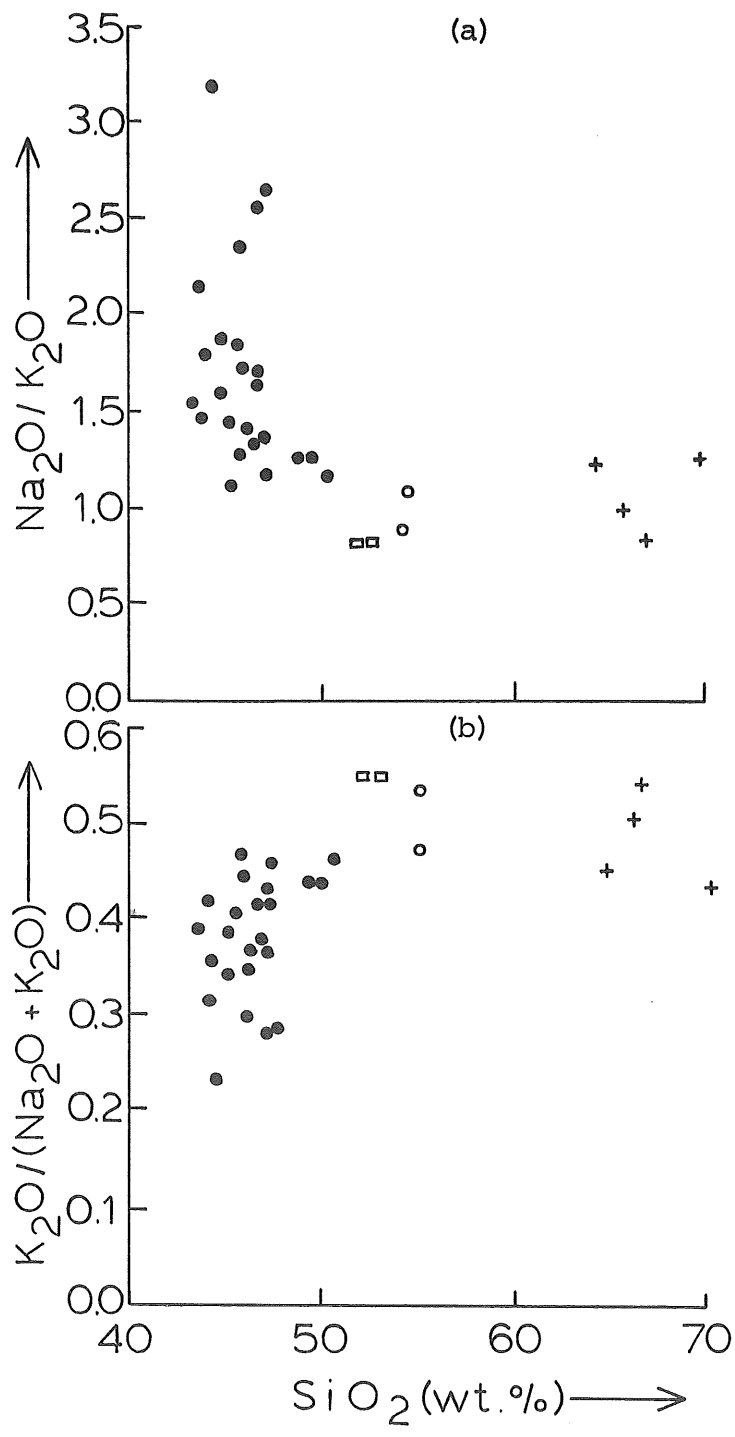
FIGURE 25: (a) Na$_2$O / K$_2$O and (b) K$_2$O /(Na$_2$O + K$_2$O) plotted

versus SiO$_2$ (wt.%).

On Figure 25a, the main trend appears to be for the trachytes to decrease slightly in the Na_2O/K_2O ratio. This indicates that K_2O has not been greatly enriched relative to Na_2O during the evolution of the magma.

c) $K_2O/Na_2O + K_2O$ Versus SiO_2 Diagram

Figure 25b is a plot of $K_2O/Na_2O + K_2O$ versus SiO_2. This is a different presentation of the data used above for Figure 25a. In this diagram, the variation of K_2O is judged relative to the total alkali content of the rock.

A similar trend to Figure 25a is shown: K_2O is slightly higher relative to total alkalis in the trachytes and the trachybasalts than in the basalts. A range of $K_2O/Na_2O + K_2O$ between 0.3 and 0.5 is notable for the basalts, with the five basalt samples mentioned above (AUL 051.2, 062.2, 071.3, 087.2, and 108.1) having this ratio less than 0.316. This appears to indicate that in these samples, K_2O has been mobile during or after extrusion. The variation in $K_2O/Na_2O + K_2O$ for these four samples could be a reflection of the mobility of the alkalis, and also incorporates an analytical error. However, on the plots of Na_2O and K_2O versus D.I. (Figures 20b, 20c), there are no anomalous values. Thus, it is a possibility that these five rocks represent a continuation of the differentiation trend, and not movement of the alkalis.

d) K/Rb Versus K Diagram

Figure 26 is a plot of K/Rb versus K (ppm) on a log-
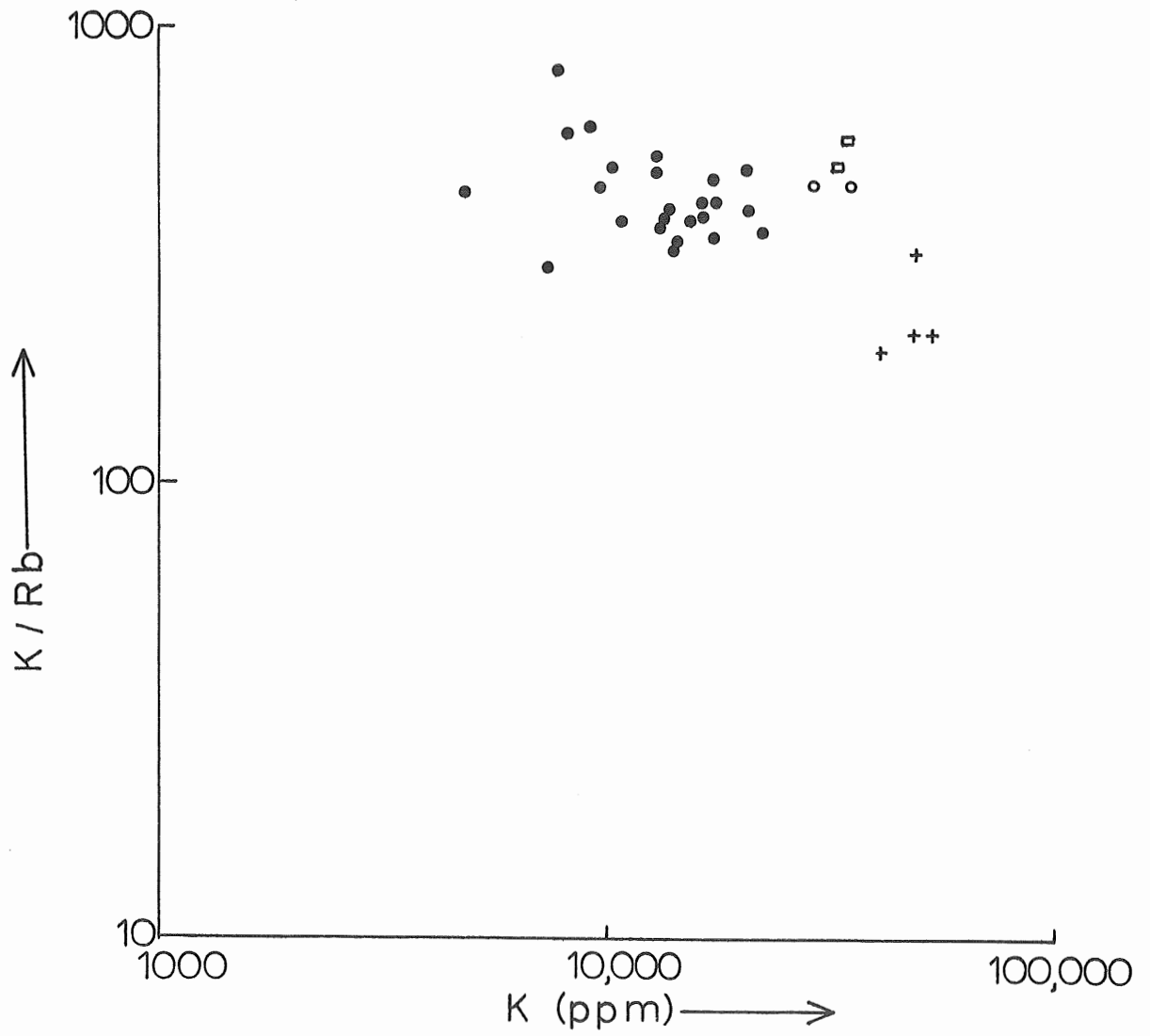
FIGURE 26: Plot of K / Rb versus K(ppm) on a log-log scale.

log scale. The ratio K/Rb varies from 300 to 849 for basalts, with an average value of approximately 400. The K/Rb ratio is slightly less for the trachytes and varies from 210 to 328. AUL 051.2, 062.2, 071.3, 087.2, and 108.1, which have anomalous Na_2O/K_2O and $K_2O/Na_2O + K_2O$, have K/Rb ratios of 849, 445, 301, 607, and 506. Removing these as possibly being altered samples reduces the range of K/Rb for basalts from 324-619. However, if, as noted above, these five samples were a continuation of the differentiation trend, they would be expected to have the highest values for K/Rb, and they thus may not have suffered alkali depletion.

An important feature of this plot is the decrease in the K/Rb ratio in the trachytes, while the K content has increased. This type of variation was noted by Lessing et al. (1963) for potassium and rubidium distributions in Hawaiian lavas. Lessing et al. suggested that a contamination of the Hawaiian magma with Rb-rich material had occurred, or that there had been a differential gaseous transfer of the alkali elements. The average K/Rb recorded for Hawaiian rocks was 512 ± 11 for low-K tholeiites to a low of 260 for the high-K trachytes. In the study of Lessing et al., the basalts varied from 428 to 612 K/Rb ratio and the trachytes from K/Rb = 260 to 312. The Azores lavas of this study have a similar high value, ignoring the possible altered samples, and a much lower value for the basalts and a slightly higher and slightly lower value for the high-K trachytes.

Hughes and Brown (1972) report low K/Rb ratios of 325 (average) for Madeiran alkali basalts with a range of values from 247 to 454. This is considerably lower than the recorded average for the Azores rocks. The suites are not directly comparable since Madeiran lavas have high Na_2O/K_2O values ranging from 3 to 4, contrasting with the Azores average value of $Na_2O/K_2O = 1.25$.

e) Na_2O - K_2O - CaO Diagram

A triangular plot of Na_2O - K_2O - CaO (all oxides as weight per cent) is presented as Figure 27. A distinct trend from calcium-poor to calcium-rich rocks can be seen, with the trachytes at the calcium-poor side of the diagram, and the basalts at the calcium-rich corner. The trachybasalts plot at intermediate points. On this diagram, too, there is a gap between the trachytes and the trachybasalts. Of interest is the relatively constant Na_2O/K_2O value. This illustrates again that these rocks do not become more sodic or more potassic with increasing evolution.

A triangular plot of Na_2O - K_2O - CaO was presented by Le Maitre (1962) for all of the Azores islands. Le Maitre's diagram shows a similar trend to that shown by Figure 27, but his plot does not show the outstanding gap between CaO = 20 to 50 weight per cent that is exhibited by these rocks from Sao Miguel.

It should be kept in mind that CaO values for these rocks can be expected to be in error on the high side, due to
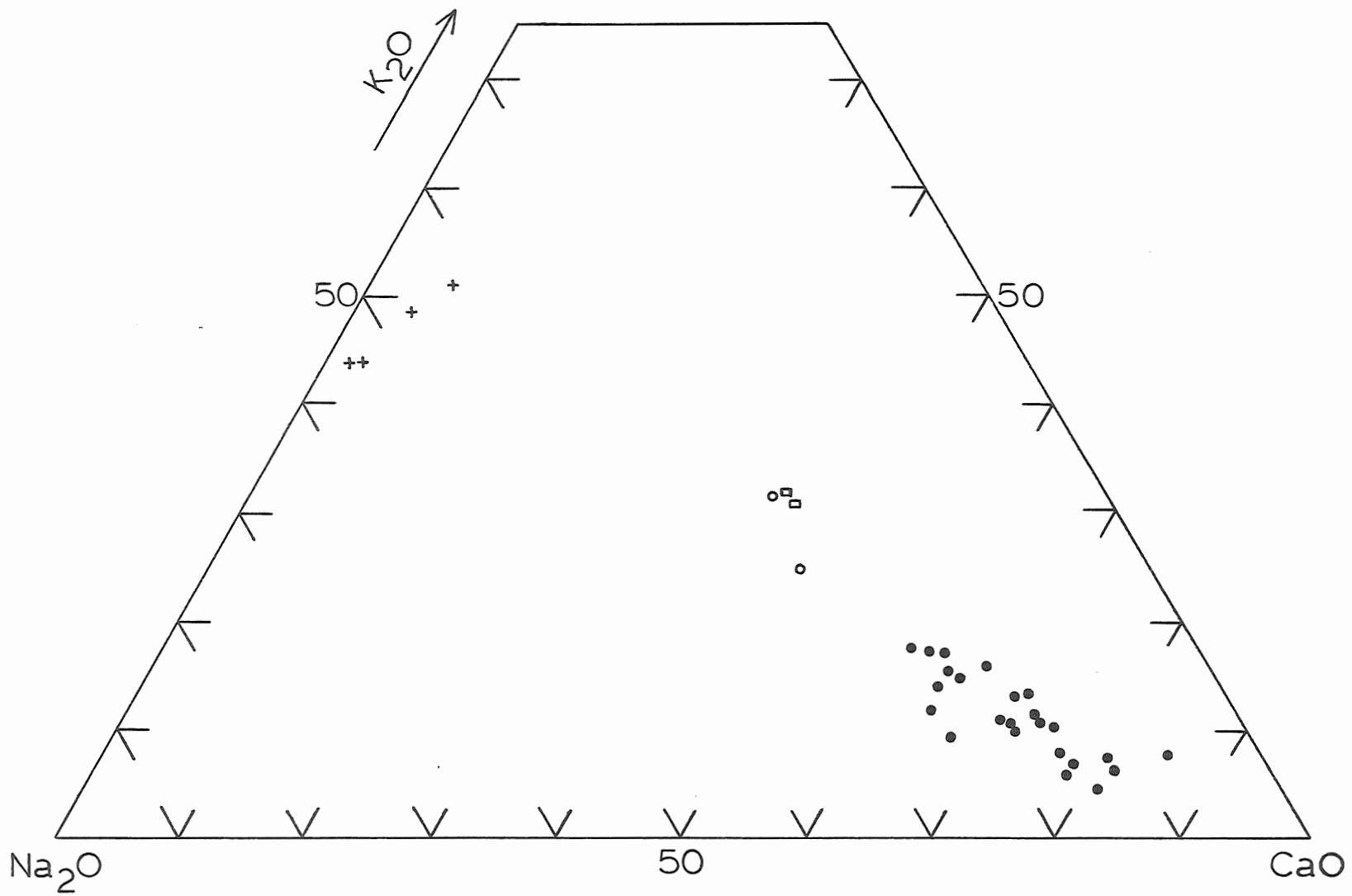
FIGURE 27: Na$_2$O-K$_2$O-CaO diagram. All oxides as weight per cent.

the addition of CaO from vesicle filling. Assuming that this affects all of the analyses equally, the general trend of this plot can still be considered realistic.

f) Movement of the Alkali Elements

What appears to be happening is that in these rocks, with the exception of the five samples mentioned above, the Na_2O/K_2O, $K_2O/Na_2O + K_2O$ do not vary greatly, although K/Rb ratios have a broader range than that recorded by other studies (Lessing et al., 1963; Hughes and Brown, 1972). Na_2O and K_2O are not changing greatly relative to each other. There is only a slight difference between the value of $K_2O/Na_2O + K_2O$ for basalts and trachytes, and also, K/Rb for the basalts is only slightly higher than that value for the trachytes. This appears to indicate that total alkalis are being increased with increasing differentiation and K_2O is increasing only slightly relative to Na_2O, which has been shown by Figure 27.

The samples which have high Na_2O/K_2O, low $K_2O/Na_2O + K_2O$, and anomalous K/Rb ratios for a given SiO_2 weight per cent (AUL 051.2, 062.2, 071.3, 087.2, and 108.1) could be the most highly altered samples in this suite, and could have suffered loss of the alkali elements as a result of this. Figure 28 plots $K_2O/Na_2O + K_2O$ versus (a) $Fe_2O_3/(FeO + Fe_2O_2)$, (b) H_2O^+ (weight per cent), and (c) CO_2 (weight per cent). The five samples show evidence of their alteration in having $Fe_2O_3/(FeO + Fe_2O_3)$ between 0.39 and 0.67, H_2O^+
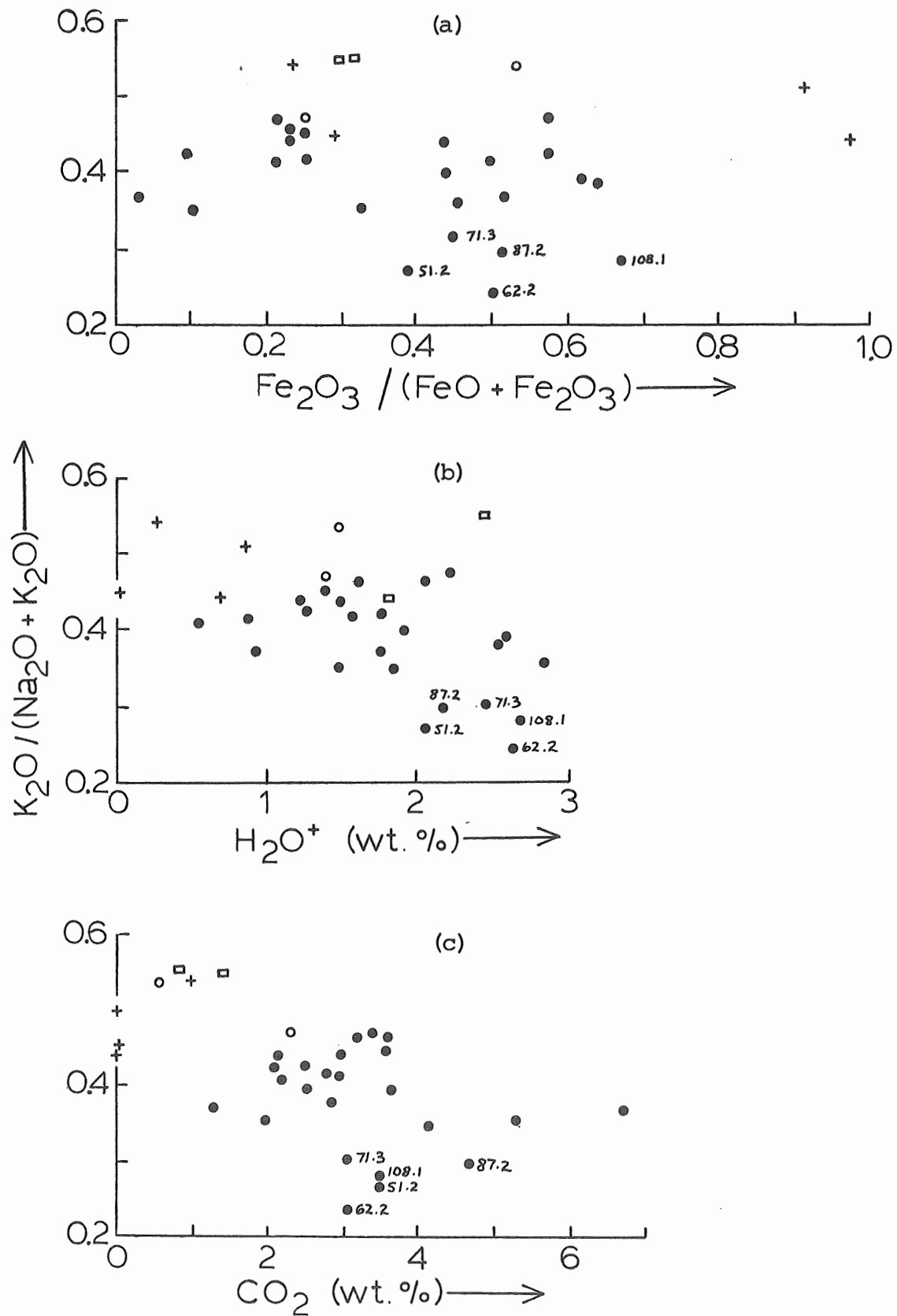
FIGURE 28: $K_2O/(Na_2O + K_2O)$ plotted versus (a) $Fe_2O_3/(FeO + Fe_2O_3)$, (b) H_2O^+ (wt.%), and (c) CO_2 (wt.%).

between 2.05 and 2.67 weight per cent, and CO_2 between 3.05
and 4.67 weight per cent, values which appear to be higher
than most of the other basalts. Some of the other basalts
have CO_2, H_2O^+ or $Fe_2O_3/(FeO + Fe_2O_3)$ values higher than these
altered rocks, but they are different in that all three values
are not consistently higher. These five samples are at the
higher values of $Fe_2O_3/(FeO + Fe_2O_3)$ and $(CO_2 + H_2O^+)$ in
Figure 14b, and therefore could have suffered the most alkali
movement.

iv) Other Plots

a) AFM Diagram

Figure 29 shows a triangular plot of total alkalis
$(A = Na_2O + K_2O)$, FeO_T (F), and MgO (M). The samples plot
in the central region of the graph, characteristic of many
other basaltic rocks. The trachytes (AUL 001.1, 030.4, 031.1,
036.1) plot towards the alkali-rich corner of the diagram,
with the trachybasalts plotting between the basalts and the
trachytes. In general, the trend of the analyses is towards
the alkali corner, away from both the FeO_T and MgO corners.

A plot made by Le Maitre (1962) including all of the
analyses then available for all of the Azores islands shows
a similar diagram to that presented in Figure 29. However,
the rocks of this study exhibit the distinct lack of analyses
with total alkalis intermediate between the trachybasalts and
the trachytes.
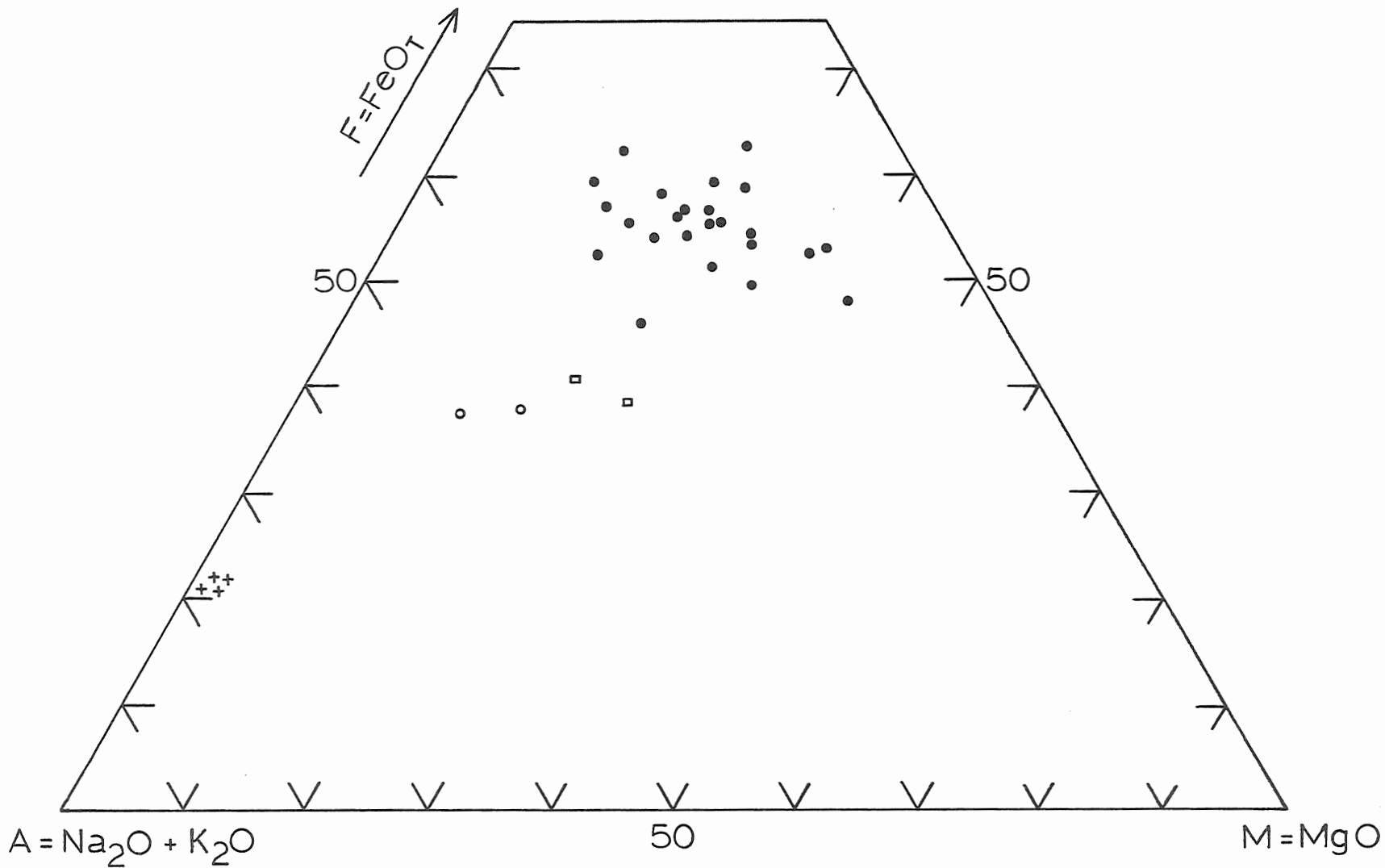
FIGURE 29: AFM diagram. All oxides as weight per cent.

b) Ni Versus Cr Diagram

Figure 30a is a plot of Ni (ppm) versus Cr (ppm).
A direct, simple correlation between Ni and Cr is illustrated:
Ni appears to increase linearly with an increase in Cr. The
low Ni and Cr values in the trachytes are an indication of
the lack of olivine and poikilitically included spinel in
these rocks. The fact that there is a linear trend, even
though much of the olivine is altered, indicates that these
two elements behave similarly under conditions of alteration.

c) Ni Versus NgO Diagram

Figure 30b is a plot of Ni (ppm) versus MgO (weight
per cent). An increase in Ni appears generally to be accom-
panied by an increase in MgO, probably reflecting the assoc-
iation of these two elements in the mineral olivine.

d) Pearce and Cann Diagram

Pearce and Cann (1973) have proposed a method of
characterising the tectonic setting of basic volcanic rocks.
Samples of basalts are analysed for Ti, Zr, Y, and Nb, which
are less mobile trace elements and thus can be used with
altered samples. Comparisons of concentrations of these
elements are used to separate "within-plate" basalts (oceanic
island or continental basalts) from ocean-floor basalts,
low-K tholeiites, and calc-alkali basalts. Once boundaries
have been established using rocks of known tectonic regime,
the plots can be used to characterise the tectonic setting
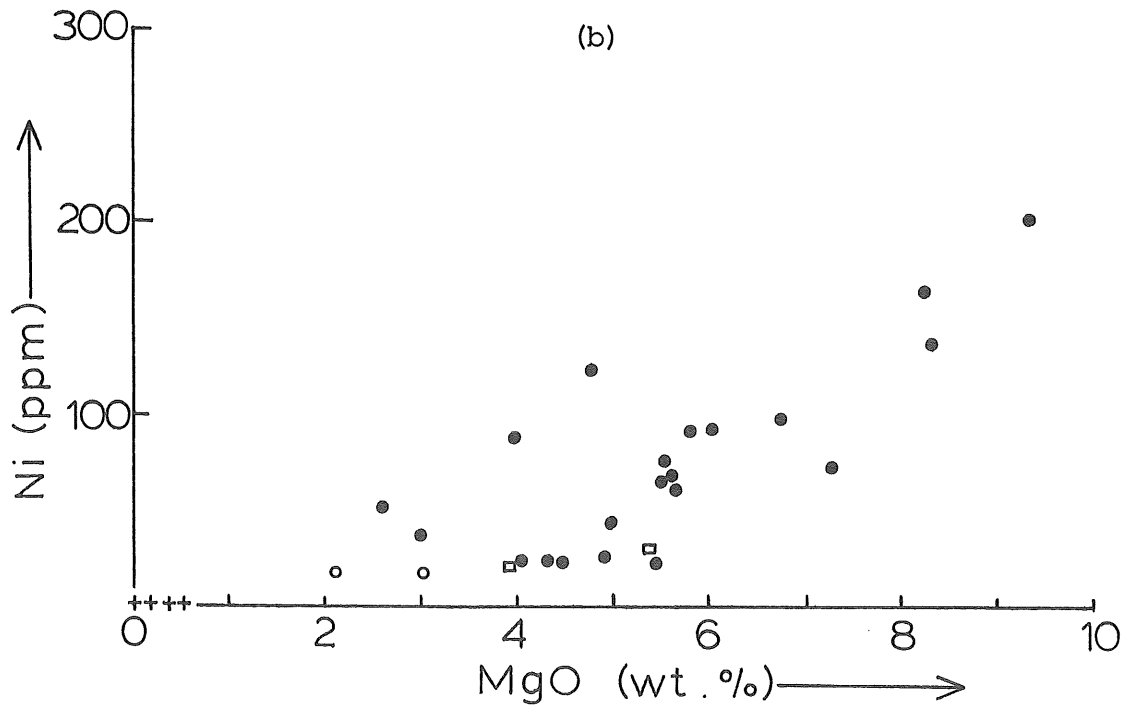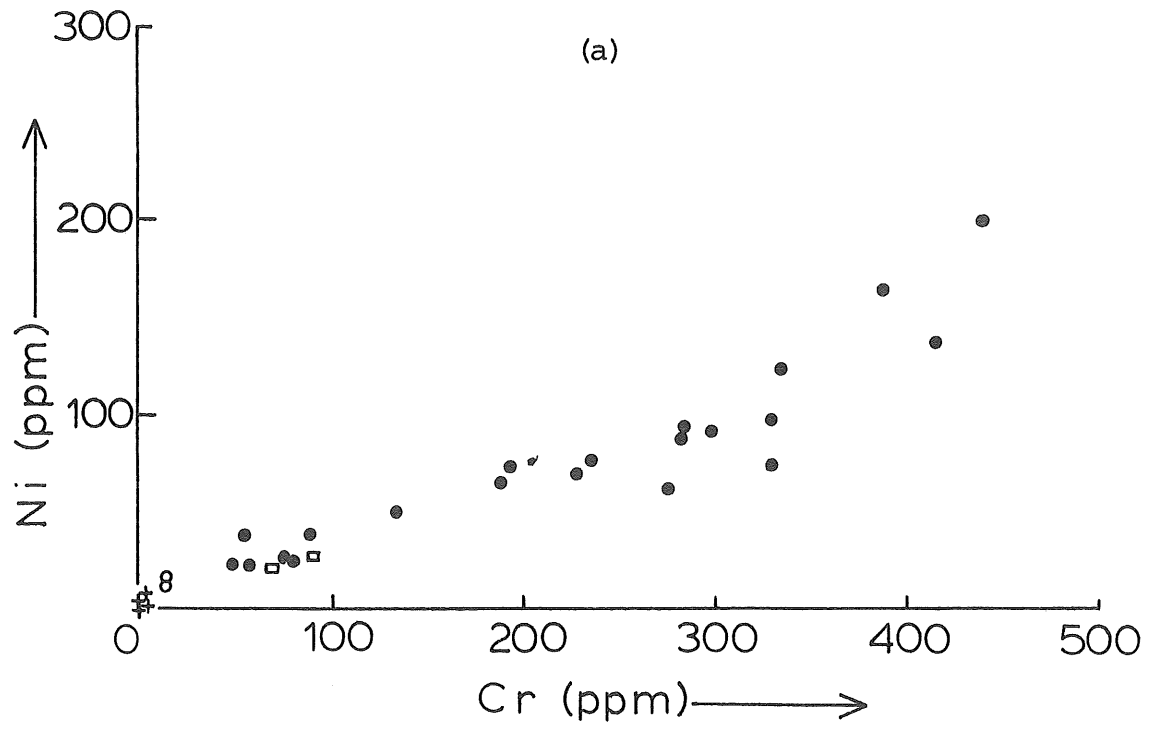
FIGURE 30: Ni (ppm) plotted versus (a) Cr (ppm) and (b) MgO (wt.%).
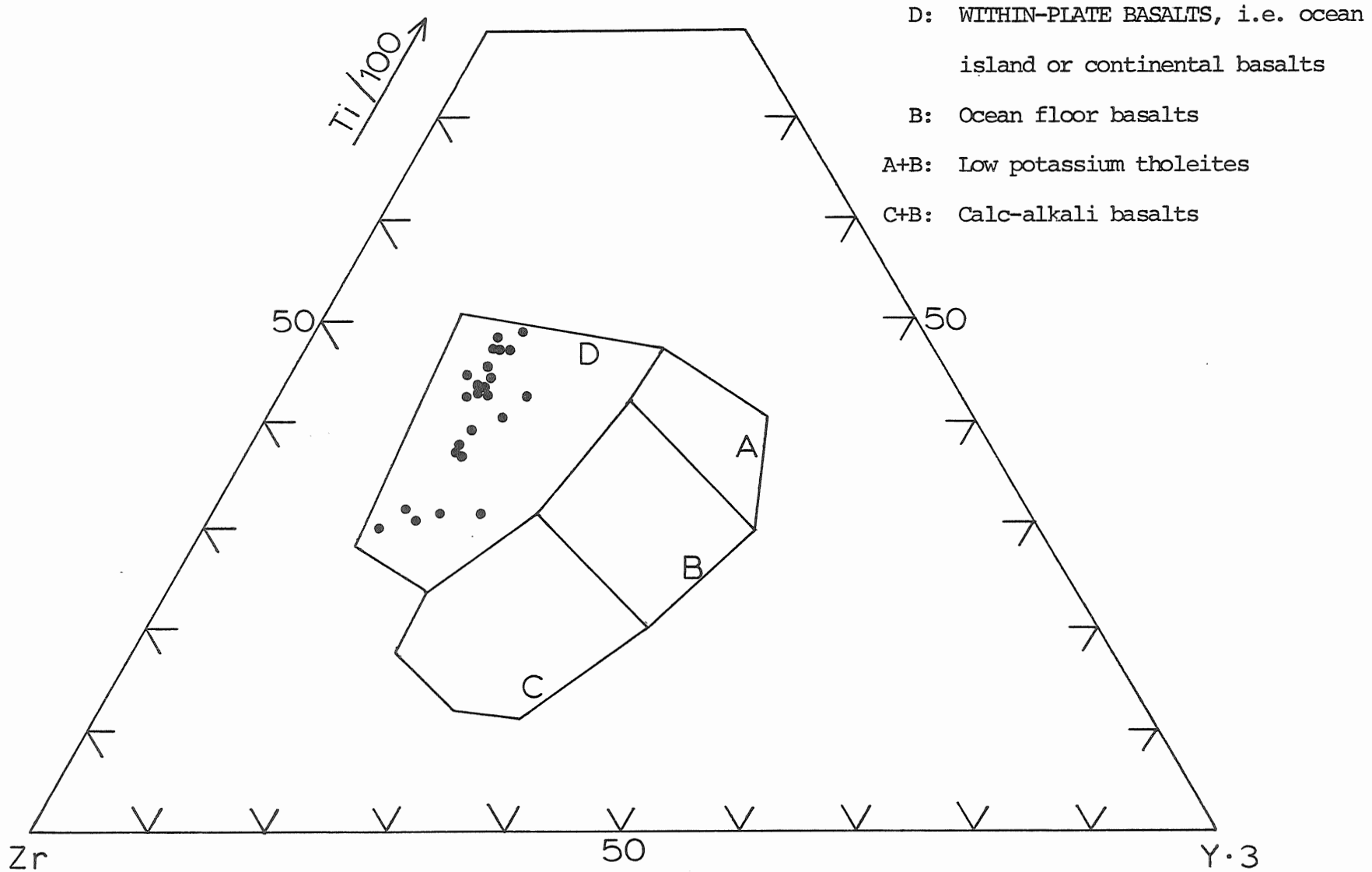
FIGURE 31: Discrimination diagram using Ti, Zr, and Y.

Boundaries after Pearce and Cann (1973).

for older rocks.

Initially, Y/Nb is determined and compared with the limits of Pearce and Cann (1973, p. 297). For alkali basalts, Y/Nb is less than 1 for "within-plate basalts and is less than 2 for ocean-floor basalts. Tholeiitic rocks have Y/Nb greater than 2 for "within-plate" basalts, and greater than 3 for ocean-floor basalts. Y/Nb for the basalts of this suite range from 0.47 to 0.75, establishing them as alkalic in nature, according to the above criteria.

Once the petrologic nature of the basic rocks has been determined from the Y/Nb ratio, Pearce and Cann plot Zr, Ti/100, and y·3 on a triangular diagram such as Figure 31. The boundaries suggested by Pearce and Cann (1973, Figure 3, p. 295) have been added. Within-plate basalts plot in area D; ocean-floor basalts plot in field B; low potassium tholeiites plot in fields A and B, and calc-alkali basalts plot within C and B. The Azores basalts on this plot are within field D, i.e., according to the classification of Pearce and Cann, these are within-plate basalts in either oceanic or continental setting. The usefulness of this dis- crimination scheme for these Azores rocks is discussed in more detail in Chapter 7.

e) CaO Versus Y Diagram

Lambert and Holland (1974) have demonstrated various trends from plots of CaO (weight per cent) versus Y (ppm)

which depend on the type of crystal fractionation which has occurred. Figure 32 is a plot of CaO versus Y of the averages of the basalts (CaO = 10.09, Y = 39), trachybasalts (CaO = 5.85, Y = 55), and trachytes (CaO = 0.45, Y = 71) for this suite. It is evident that with increasing crystal fractionation, CaO concentration decreases and Y increases, resulting in trachytes with lower CaO, and higher Y than the associated basalts. This trend corresponds with the L-type "pyroxenic" trends presented by Lambert and Holland (1974, Figure 4, p. 1402). According to Lambert and Holland, all of the L-type trends occur in alkaline or peralkaline rocks.

L-type trends would be expected to result from kaersutite or plagioclase + clinopyroxene fractionation in high-Ca melts, or K-silicate fractionation at low calcium concentrations. Since there is an increase of potassium content with increasing evolution of these Azores rocks, it is likely that, if Lambert and Holland are correct, a fractionation of plagioclase + clinopyroxene could be a mechanism for the evolution of these Azores rocks.

v) Discussion of Chemical Study

a) Nature of the Volcanism

The TiO_2 values for these Azores rocks varies from 0.50 to 0.74 weight per cent for the trachytes and from 2.26 to 5.09 weight per cent for the basalts and trachybasalts. According to Chayes (1965), oceanic island basalts can be distinguished from other basalts by TiO_2 values greater than
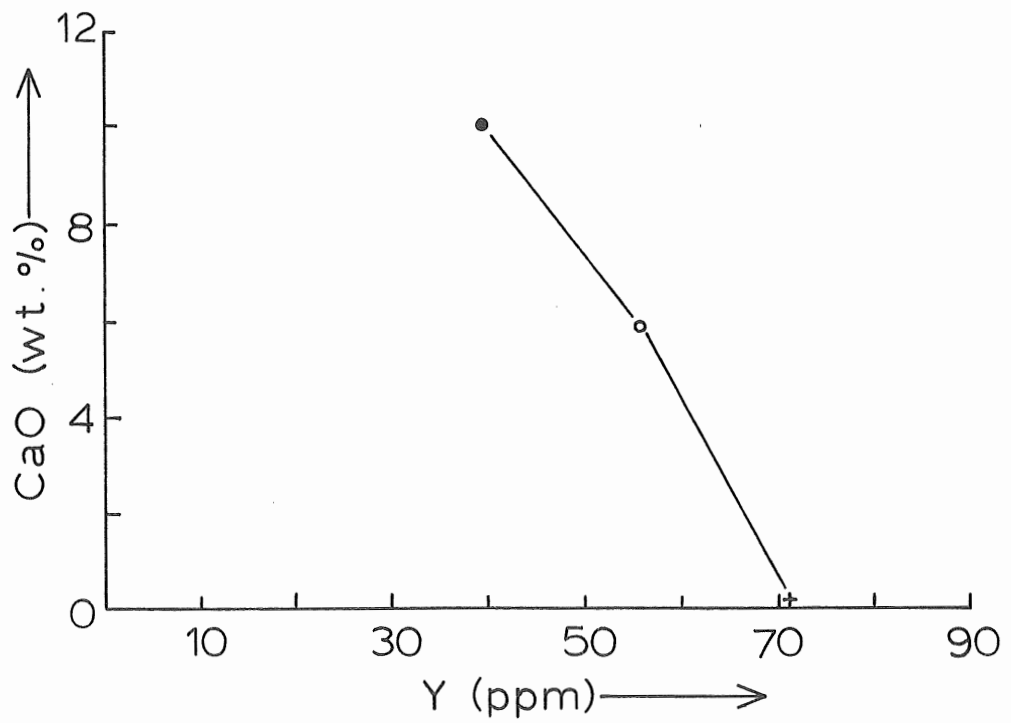
FIGURE 32: CaO (wt.%) versus Y (ppm). Average basalt, trachybasalt, and trachyte plotted.

1.75 weight per cent. All of the basalts and trachybasalts of this study satisfy Chayes' criterion.

From the analyses published in the literature, it appears to be quite common for oceanic island alkali basalts to have a TiO_2 value greater than 2.00 weight per cent, and values up to 5.00 weight per cent TiO_2 do occur. In terms of other oceanic islands, the high values for TiO_2 in these rocks are not unusual. For example, the basalts studied by Le Maitre (1962) from Gough Island have TiO_2 values ranging from 1.85 to 3.40 weight per cent.

The K_2O values for these Azores rocks vary from 4.79 to 6.29 weight per cent for the trachytes and from 0.59 to 3.85 weight per cent for the basalts and trachybasalts. This contrasts with other non-potassic oceanic islands in which K_2O is usually less than 1.00 weight per cent in the basalts. These high K_2O values will be discussed further in comparing Sao Miguel with other oceanic islands.

b) The Trachytic Sequence

It has been previously noted, and is visible on the plots of the elements versus depth, that there is a series of trachytic lavas between 290.8 m and 327.9 m, and also a trachyte as the topmost flow of the volcanic pile. A gradation from basalt to trachybasalt to trachyte is indicated, but the rocks intermediate between trachybasalts and trachytes are absent.

Baker (1973) has noted that on the island of Ascension

both basalts and trachytes were erupted at various stages, with trachytes pre-dating basalts in some cases. He also noted that there was no visible sign of a gradation in chemistry between basalts and trachytes. Similarly, in this Azores core, there is no visible, gradual chemical evolution from basaltic to trachytic lavas.

One feature which is notable is the trachytic nature of the pyroclastics. Even when the lavas are basaltic in character, the pyroclastics are trachytic, and in general are more aluminous than the basalts. The pyroclastics comprise 22% of the volume of material of the core (Muecke et al., 1974), so that, together with the 6% volume of the trachytic flows, trachytic material makes up approximately 28% of the material of drillcore.

Thus, within this volcanic pile on São Miguel, it can be said that there are two sequences which are terminated by the eruption of trachytic flows. However, there exists little chemical variation between the sequences, and certainly no good evidence of a gradational change within the lava succession.

vi) SUMMARY

The following points can be summarized from this chapter:

1) The plots of the elements versus depth show maxima and minima for the trachytes and trachybasalts. For the basalts, there appears to be increasing Al_2O_3, Nb, and Zr, decreasing CaO, TiO_2, and MgO random variations of FeO_T, Cr, and Ni and no significant variations of K_2O, Na_2O, SiO_2, Sr, Rb, and Y with depth in the core.

2) Plots of the elements versus the Thornton-Tuttle Differentiation Index show a continued variation of the elements with increasing D.I., but with an absence of rocks with D.I. between 60 and 85.

3) A plot of total alkalis versus SiO_2 shows that these rocks are of a mildly alkaline affinity.

4) Plots of Na_2O/K_2O versus SiO_2, $K_2O/Na_2O + K_2O$ versus SiO_2, and K/Rb versus K indicate that K_2O has increased slightly in the trachytes and trachybasalts relative to Na_2O. Five samples show depletion of K_2O which could be attributed to movement of alkalis.

5) Plots of Ni versus Cr and Ni versus MgO show similar behaviour of Ni and Cr and a correlation of Ni with MgO.

6) On discrimination diagrams used by Pearce and Cann (1973) the Azores rocks plot with other oceanic

islands and continental basalts in the field of "within-plate" basalts; the Y/Nb ratios for these rocks show them to be of alkaline affinity.

7) A plot of Ca0 versus Y shows an L-type trend which involves Y-enrichment which could be attributed to clinopyroxene-plagioclase fractionation (Lambert and Holland, 1974) and is an indication of alkaline affinity.

CHAPTER 6: MICROPROBE STUDIES

i) Nature of the Phenocrysts

Electron microprobe studies of the mineral phases in the Azores lavas were undertaken to determine the chemistry of the phenocrysts. A knowledge of the nature of the phenocrysts is useful in deciding whether these rocks have alkaline or tholeiitic affinities.

Five samples were taken from the core: AUL 020.3, AUL 022.1, AUL 051.2, AUL 062.2, and AUL 108.1. Polished thin sections were made and coated with carbon in preparation for analysis. The analyses were done on a Cambridge wavelength dispersive, 2 channel, Microscan V electron microprobe.

The olivine phenocrysts were analysed for SiO_2, FeO, MgO, and CaO. The clinopyroxene grains were analysed for SiO_2, TiO_2, Al_2O_3, FeO, MnO, CaO, and Na_2O. In the plagioclase phenocrysts, SiO_2, TiO_2, Al_2O_3, MnO, CaO, and Na_2O were determined.

ii) Olivine Phenocrysts

Sample AUL 020.3 is the only sample in which fresh olivine grains were present for analysis. Table 13 shows the analyses for olivines from AUL 020.3. The samples are seen to be forsteritic in composition, with $Fo_{77.6}$ and $Fo_{74.2}$ recorded as compositions for two separate grains. Boone and Fernandez (1971) reported phenocrysts of olivine

TABLE 13: Microprobe analyses of olivine
phenocrysts from AUL 020.3.

	1	2
SiO_2	38.95	38.22
TiO_2	0.00	0.00
Al_2O_3	0.00	0.00
Fe_2O_3	0.00	0.00
FeO	20.60	23.37
MnO	0.00	0.00
MgO	39.95	37.76
NiO	0.00	0.00
CaO	0.22	0.22
TOTAL	99.72	99.57

Si	1.006	1.006	1.002	1.002
Ti	0.000	*	0.000	*
Al	0.000	*	0.000	*
Fe^{3+}	0.000	*	0.000	*
Fe^{2+}	0.445	*	0.513	*
Mn	0.000	*	0.000	*
Mg	1.538	*	1.476	*
Ni	0.000	*	0.000	*
Ca	0.006	1.988	0.006	1.995
O	4.000	*	4.000	*

Fo	77.323	73.995
Fa	22.371	25.695
Larn	0.306	0.310
Fo	77.561	74.225
Fa	22.439	25.695
Niol	0.000	0.000
F/M	0.289	0.347
F/FM	0.224	0.258

from alkaline basalts of the Nordeste Complex on the east
end of Sao Miguel as having compositions ranging from Fo_{87}
to Fo_{69}, both more and less magnesium-rich than the pheno-
crysts analysed here.

iii) <u>Clinopyroxene Phenocrysts</u>

Table 14 presents the analyses of the clinopyroxenes
from samples AUL 020.3, AUL 051.2, AUL 062.2, and AUL 180.1.

In sample AUL 062.2, the core and the rim of a
zoned clinopyroxene grain were analysed. The core was
green while the rim was purple in colour in plane
polarised light. The zoning was subtle and more easily
observed as a difference in interference colours under
crossed nicols. The microprobe analyses indicate that
there is a definite chemical difference between the
core and the rim of the zoned grain. The core of the
grain is higher in SiO_2, FeO, MnO, and Na_2O than the rim.
The rim is enriched in TiO_2, Al_2O_3, MgO, and CaO
relative to the core.

With depth in the core, and within the limit of the
small number of samples analysed, the clinopyroxenes appear
to become less rich in TiO_2, Al_2O_3, FeO, MnO, and Na_2O,
and slightly richer in SiO_2, MgO, and CaO. In thin
section, there is no visible change in the pyroxenes
with depth to indicate that these chemical changes are
taking place. However, the changes are subtle, and thus

TABLE 14: Microprobe analyses of clinopyroxene phenocrysts
from AUL's 020.3, 022.1, and 051.2.

	AUL 020.3		AUL 022.1		AUL 051.2	
SiO_2	47.81		46.84		48.34	
TiO_2	2.43		1.92		2.11	
Al_2O_3	6.36		7.08		5.20	
FeO	8.10		8.19		6.13	
MnO	0.19		0.19		0.15	
MgO	13.43		14.28		14.78	
CaO	21.45		20.12		22.36	
Na_2O	0.50		0.57		0.33	
TOTAL	100.27		99.19		99.40	
Si	1.782	*	1.762	*	1.806	*
Al	0.218	2.000	0.238	2.000	0.194	2.000
Al	0.062	*	0.076	*	0.035	*
Ti	0.068	*	0.054	*	0.059	*
Fe^{2+}	0.253	*	0.258	*	0.192	*
Mn	0.006	*	0.006	*	0.005	*
Mg	0.746	1.135	0.801	1.195	0.823	1.113
Ca	0.857	*	0.811	*	0.895	*
Na	0.036	0.893	0.042	0.853	0.024	0.919
O	6.000	*	6.000	*	6.000	*

		AUL 020.3	AUL 022.1	AUL 051.2
	Wo	46.173	43.382	46.870
	En	40.217	42.834	43.100
	Fs	13.610	13.784	10.030
	Wo	45.148	42.304	46.178
	Hyp	52.948	55.527	52.589
	Jd	1.904	2.169	1.233
	F/M	0.346	0.329	0.238
	F/FM	0.257	0.248	0.193

TABLE 14: Cont'd. Microprobe analyses of clinopyroxene phenocrysts from AUL's 062.2 and 108.1.

	AUL 062.2 (core)		AUL 062.2 (rim)		AUL 108.1	
SiO_2	52.11		45.74		51.17	
TiO_2	0.39		2.69		0.97	
Al_2O_3	0.77		7.53		2.10	
FeO	12.57		6.95		5.71	
MnO	1.23		0.14		0.13	
MgO	12.40		13.22		16.09	
CaO	20.79		22.59		22.56	
Na_2O	0.64		0.42		0.30	
TOTAL	100.90		99.28		99.03	
Si	1.965	*	1.725	*	1.909	*
Al	0.034	1.999	0.275	2.000	0.091	2.000
Al	0.000	*	0.060	*	0.001	*
Ti	0.011	*	0.076	*	0.027	*
Fe^{2+}	0.396	*	0.219	*	0.178	*
Mn	0.039	*	0.004	*	0.004	*
Mg	0.697	1.144	0.743	1.103	0.895	1.105
Ca	0.840	*	0.913	*	0.912	*
Na	0.047	0.877	0.031	0.944	0.022	0.923
O	6.000	*	6.000	*	6.000	*

Wo	43.447	48.679	45.667
En	36.050	39.613	45.311
Fs	20.504	11.690	9.022
Wo	41.595	47.783	45.078
Hyp	56.088	50.610	53.837
Jd	2.317	1.608	1.085
F/M	0.625	0.301	0.204
F/FM	0.385	0.231	0.169

a visible change is not always to be expected. The chemical changes are evident in the molecular compositions as a decrease in jadeite content with depth, but by little change in the other molecular proportions.

Gibb (1973) published analyses for zoned clinopyroxenes from the Shiant Isles Sill, Scotland, which showed similar trends between core and rim to the trends observed in this study; Ca0, TiO_2 and Al_2O_3 are enriched in the rims relative to the cores. These Azores clinopyroxenes show the characteristics of being of alkaline affinity in being more Ca- and Ti-rich than tholeiitic pyroxenes, as noted by Barberi et al., (1971). Thus these analyses of clinopyroxene grains are additional indications of the alkaline affinities of these rocks.

iv) Plagioclase Phenocrysts

Table 15 presents the plagioclase phenocrysts analysed from samples AUL 020.3 and AUL 022.1. The plagioclase in AUL 020.3 is of the composition $An_{83.6}Ab_{16.4}$. The plagioclase in AUL 022.1 is of the composition $An_{71.4}Ab_{28.6}$. This is reflected in the chemical compositions as lower Al_2O_3 and Ca0, and higher SiO_2 and Na_2O in AUL 022.1.

Thus the plagioclase grains examined here are calcic in nature, ranging between labradorite-bytownite in composition.

TABLE 15: Microprobe analyses of plagioclase
phenocrysts from AUL's 020.3 and 022.1.

	AUL 020.3	AUL 022.1
SiO_2	47.50	50.64
TiO_2	0.10	0.09
Al_2O_3	32.62	30.61
MnO	0.02	0.01
CaO	16.99	14.56
Na_2O	1.84	3.23
K_2O	0.00	0.00
TOTAL	99.07	99.14

Si	8.795	*	9.298	*
Ti	0.014	*	0.012	*
Al	7.117	*	6.623	*
Mn	0.003	15.929	0.002	15.935
Ca	3.370	*	2.864	*
Na	0.661	*	1.150	*
K	0.000	4.031	0.000	4.014
O	32.000	*	32.000	*

Or	0.000	0.000
Ab	16.386	28.645
An	83.614	71.355
Qz	93.014	88.995
Ne	6.986	11.005
Ks	0.000	0.000
F/M	0.000	0.000
F/FM	0.000	0.000

v) <u>Co-Existing Phenocrysts</u>

Figure 33 is a triangular plot of Wo-En-Fs $(CaSiO_3-MgSiO_3-FeSiO_3)$ with Fo-Fa $(Mg_2SiO_4-Fe_2SiO_4)$ included on the En-Fs line, and An-Ab $(CaAl_2Si_2O_8-NaAlSi_3O_8)$ added in order to represent the compositions of the phenocrysts co-existing in these lavas. This diagram shows the greater difference in the composition of plagioclase than there is in clinopyroxene grains in AUL 020.3 and AUL 022.1. With the exception of the core of the clinopyroxene analysed in AUL 062.2, the clinopyroxenes appear to be uniform in composition. Also, the decrease in the jadeite content of the clinopyroxene between the core and the rim of the zoned grains in AUL 062.2 is evident as a move away from the Fs corner towards the Wo-En side of the diagram. The position of the clinopyroxenes is similar to that illustrated by Barberi <u>et</u> <u>al</u>., (1971) for alkali basalts from Gough Island and from Japan. The core of the zoned pyroxene from AUL 062.2 shows a different chemistry from the remaining clinopyroxenes, which could indicate that the core represents a xenocryst rather than a phenocryst, and was rimmed with a different pyroxene <u>in situ</u>. However, the absence of such clinopyroxene in the most highly evolved rocks suggests that these are not xenocrysts, but they could be a higher pressure phase.
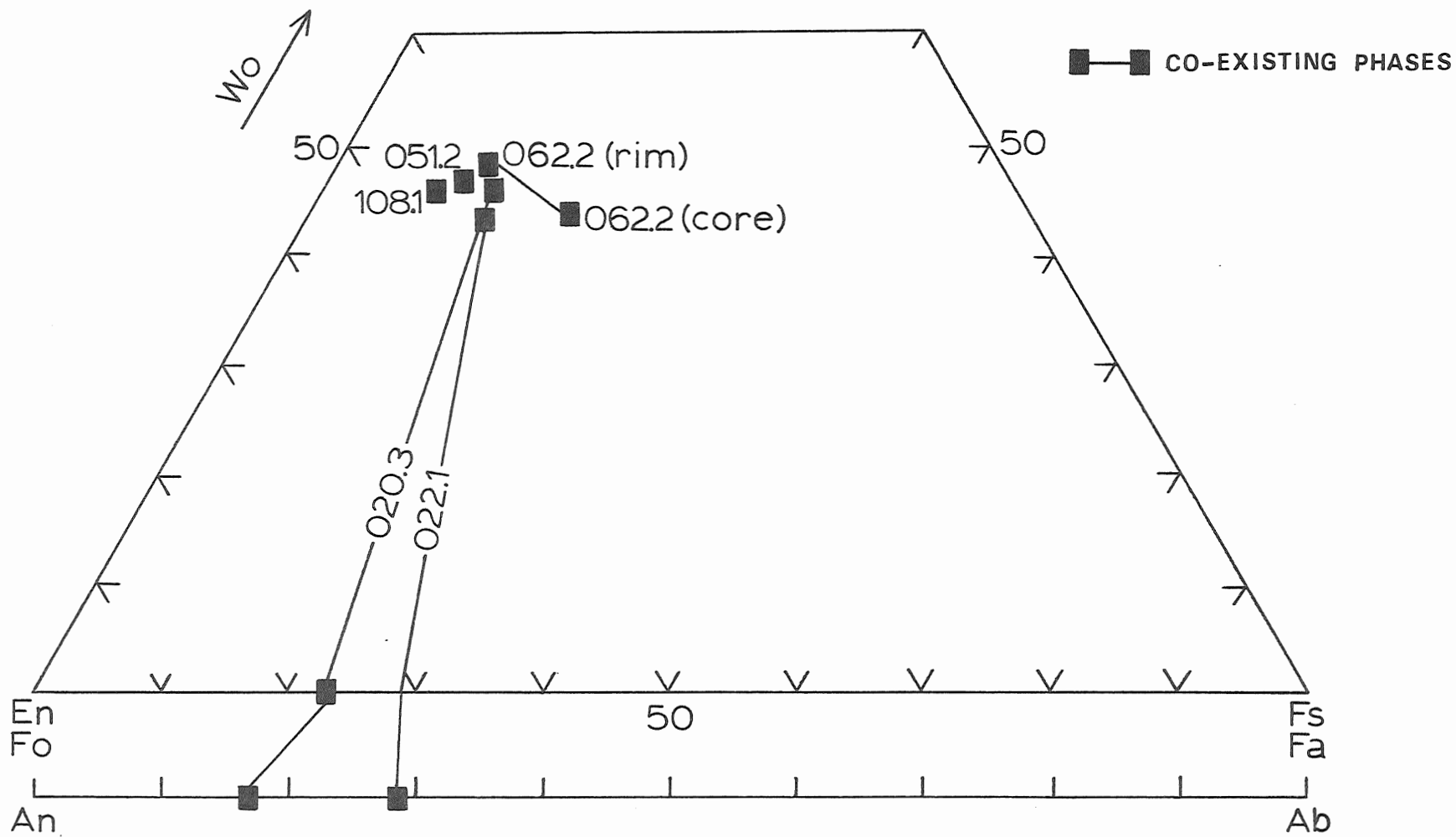
FIGURE 33: Wo-En-Fs diagram showing compositions of phenocrysts and co-existing phases.

CHAPTER 7: DISCUSSION

i) Alkaline Versus Tholeiitic Nature of the Magmatism

The problem has arisen in the course of this study
as to whether these rocks from Sao Miguel were originally
of alkaline or tholeiitic affinity. In some respects,
the rocks appear alkalic, in others, tholeiitic.

The features which indicate an alkaline affinity
are as follows:

1) Petrography: The electron microprobe study has
shown that the clinopyroxenes, which have TiO_2 varying
from 0.39 to 2.69 per cent, and CaO ranging from 20.12 to
22.59 per cent, are Ti- and Ca-rich augites. According
to Wilkinson (1974), augites with CaO greater than 20
per cent and TiO_2 between 2 and 3% are the characteristic
clinopyroxenes found in alkali basalts, whereas tholeiitic
basalts tend to have Ca-poor augites.

According to Poldervaart (1964), orthopyroxene is a
common, but not universal mineral found in tholeiitic basalts,
and is not found in alkaline rocks. The rocks of this study
do not contain orthopyroxene.

2) Total Alkalis: The plot of total alkalis (Na_2O +
K_2O) versus SiO_2 (Figure 24) indicates that, with the
exception of AUL 030.4, which is a trachyte, all of the
rocks of this study lie within the "mildly alkaline

series" delineated by Schwarzer and Rogers (1974) after Saggerson and Williams (1964). This conclusion is based on the assumption that the alkali elements have not been mobile as a result of alteration. As presented in Chapter 5, only 5 samples appear to have anomalous values of K_2O, which could be the result of alkali depletion or could be part of the differentiation trend and not an indication of the movement of the alkali elements.

3) <u>Thornton-Tuttle Index</u>: On the plot of SiO_2 versus Thornton-Tuttle Differentiation Index (Figure 18a) all but 7 of the rocks of this study plot as alkaline rocks in the undersaturated region below the an-or line used by Thornton and Tuttle (1960) and Borley (1974).

4) <u>Trace Elements</u>: According to Pearce and Cann (1973) Y/Nb for "within-plate" alkali basalts is less than 1. The Y/Nb ratios for the basalts of this suite range from 0.47 to 0.75.

The plot of CaO versus Y (Figure 32) corresponds to an L-type "pyroxenic" trend presented by Lambert and Holland (1974) which is found in alkaline or peralkaline rocks.

5) <u>C.I.P.W. Norms</u>: When the chemical analyses are presented as CO_2-free, and a correction applied to the iron so that $Fe_2O_3/(FeO + Fe_2O_3) = 0.15$ as an approximation

to the original condition of the rocks, 7 of the basalts appear as Ne-normative, a characteristic of alkali basalts.

The features which favour a tholeiitic affinity for the rocks of this study are as follows:

1) C.I.P.W. Norms: On a CO_2-free basis and with $Fe_2O_3/$ $(FeO + Fe_2O_3)$ adjusted to equal 0.15, all but seven of the norms of the basalts contain Hy and/or Q, indicators of a tholeiitic nature.

2) Differentiates: The trachytes of this study all have Q in the norms, a feature consistent with a tholeiitic nature.

The evidence for a tholeiitic nature for these rocks lies in the appearance of Q and/or Hy in the norms of some of the basalts, and in the norms of all of the trachy-basalts and trachytes. However, alteration is known to have occurred, and thus it is possible that the presence of normative hypersthene could be an indication of alteration rather than a tholeiitic characteristic.

A study of the secondary minerals carried out by P. Sarkar (personal communication) has indicated that silica has been added to the material of the drillhole as an effect of the alteration. If this has occurred, then the appearance of Q in the norms of some of these rocks is a reflection of the hydrothermal conditions and not an indication of tholeiitic affinities.

In addition, it has been demonstrated by Stice
(1968) that inherent analytical errors in the determination
of Na_2O, K_2O, and Fe_2O_3 can produce a Hy-normative rock
from one that previously appeared to be Ne-normative and
vice versa. MacDonald and Katsura (1964) concluded that
the presence or absence of hypersthene in the norm could not
be used alone to adequately decide the alkaline or tholeiitic
nature of a rock since rocks with clearly alkaline mineralogy
were found to produce norms containing Hy. Baker (1969) has
also demonstrated that alteration of the groundmass of
basalts from St. Helena produced hypersthene in the norms
of alkali basalts.

Thus, the evidence which implies a tholeiitic affinity
appears to be unreliable. The most reliable criteria, the
trace element data and the mineralogy, indicate an alkaline
affinity. It can therefore be concluded that these are
alkaline rocks which, having been subjected to hydrothermal
conditions, show hypersthene and quartz in their norms.
There appears to be no evidence that the primary volcanic
material changes from alkaline to tholeiitic affinity as
seen during the eruption of Surtsey to the depth represented
by the drillcore.

ii) Comparison of S. Miguel with other Oceanic Islands

The oceanic islands vary widely in their chemistry and mineralogy but a comparison of the different islands is useful. In the correlation of various islands and island groups, several points must be considered. The age of the volcanics and the state of magmatic evolution of the islands are important points to be compared, although these data are not readily available for many of the islands. Also, the tectonic setting, i.e., rifts, ridges, etc. which could conceivably influence the magma type present, must be taken into consideration.

While these are necessary points of comparison, the most important comparison is made on the basis of chemistry. According to Borley (1974), with the exception of Hawaii, there are no undisputed associations of alkaline rocks and tholeiites on any oceanic island. She considers Iceland to have continental associations. However, this claim can be questioned since Upton and Wadsworth (1966) have found the "primitive" basalts on Réunion to be transitional between tholeiitic and alkaline. Ascension, Easter Island, and Mauritius all contain olivine tholeiite or transitional lavas (Gunn et al., 1970).

However, most work on oceanic islands has involved the study of alkaline rocks. Two types of diagrams are commonly used for a chemical comparison of these volcanics:

1) $Na_2O + K_2O$ versus SiO_2 and 2) Na_2O/K_2O versus SiO_2.
The former type of plot delineates the alkaline nature
of the rocks and the latter indicates whether the
volcanism is potassic or sodic.

The norms of the rocks are also important indicators
of the degree of alkalinity. However, since alkaline
rocks can have their norms readily changed by alteration,
particularly, as previously illustrated, by the oxidation
of iron (Figure 10), the usefulness of the norms of
oceanic basalts is thus limited.

In the following sections, comparisons of the
island of São Miguel with other islands are made in order
to place it in perspective in terms of its type and nature
of volcanism.

a) The Azores Group

As previously mentioned, the Azores forms a group
of nine islands which stretch from west to east across
the Mid-Atlantic Ridge. Flores and Corvo are on the
west flank of the Ridge, and both are considered
volcanically inactive (Machado, 1967). Of the islands
on the east flank of the Ridge, the volcanoes of Santa
Maria are also considered extinct.

The ages of some of the volcanic rocks from the
Azores have been determined. Muecke et al., (1974) have
dated a sanidine grain from 57 m depth in the drillhole

at 117 $\pm$ 24 x 10^3 years, and a submarine lava from 950 m

at 280 $\pm$ 140 x 10^3 years. Abdel Monem et al. have found

K-Ar ages of the rocks of the Nordeste Complex to range

from 4.01 m.y. to 0.95 m.y. They have also found the

basaltic series below the Coquina unit of Santa Maria to

range from 6 to 8 m.y. in age, and to probably be much

older at greater depths.

Table 16 compares the islands of the Azores group

in terms of location, structure, rock types, and tectonic

setting. The material for this table has come chiefly

from Ridley et al. (1974), Schmincke (1973), and Machado

(1967).

The chemical data for the Azores islands is

incomplete. Four recent summaries of data on the Azores

are those of Assunçao and Canilho (1970), Schmincke and

Weibel (1972), Schmincke (1973) and Ridley et al. (1974).

In terms of chemistry, the two westernmost islands

(Corvo and Flores) and the two easternmost islands

(Santa Maria and São Miguel) are alkaline, while

tholeiitic tendencies have been recognized on the

remaining islands, which are generally classified as

transitional. On the island of Pico, one of the

transitional islands, no differentiation to trachytes

has been observed (Machado, 1967).

Figures 34A and 35a are plots of total alkalis

versus silica for other volcanic centres on São Miguel

TABLE 16: Comparison of the islands of the Azores Group.

Name	Location (Approx.)	Rock Types	Tectonic Setting	Structure
Corvo	40°N,31°W	basalts, trachytes	W flank of MAR	composite volcano
Flores	39°N,31°W	olivine basalts, trachytes	W flank of MAR	composite pyroclastic cone
Fayal	38°N,30°W	olivine andesites, feldspar basalts, trachytes, basanitoids	E flank of MAR	central composite volcano
Pico	38°N,20°W	ankaramites, basalts	E flank of MAR	high central cone
São Jorge	38°N,28°W	basalts, andesites, trachytic pumice	E flank of MAR	linear volcano
Graciosa	39°N,28°W	basalts, andesites, trachytes	E flank of MAR	composite volcano with summit caldera
Terceira	39°N,27°W	basalts, trachytes, andesites, rhyolites	E flank of MAR	2 composite volcanoes
São Miguel	38°N,26°W	ankaramites, basalts, trachytes, trachyandesites	E flank of MAR	4 composite volcanoes with summit caldera
Santa Maria	37°N,25°W	ankaramites, basalts	E flank of MAR	2 periods of basaltic volcanism

and for other Azores islands, respectively. The field
of the analyses of this study is included. The analyses
were obtained from Machado (1967),Assunçao and Canilho
(1970), Schmincke and Weibel (1970), but they had pre-
viously been published elsewhere. These plots show that
the high alkali content is a feature of Sao Miguel, and
also of the other islands represented from the group, since
all plot above MacDonald's (1968) dividing line between
alkaline and tholeiitic basalts on Hawaii. It should
be noted that there are trachyandesites of intermediate
silica content, a rock type which is conspicuously absent
from the analyses of the rocks from the drill core.

Figures 34b and 35b are plots of Na_2O/K_2O versus
SiO_2 for the same analyses as presented above in Figures
34a and 35a. Figure 34b illustrates a similar trend
to that seen for the rocks of this study: most of the
points plot between Na_2O/K_2O equal to 1.0 to 2.5, with
a decrease in the ratio seen with an increase in SiO_2
content, i.e., with increasing trachytic character.

The rocks of the other Azores islands in general
appear to have higher Na_2O/K_2O ratios (between 1.75
and 3.0 for basaltic rocks, Figure 35b) than those of
São Miguel. This is particularly noticeable in the
higher ratios seen for rocks of trachytic composition.
Thus, it appears from these analyses, that the rocks of
Sao Miguel are the most potassic of these islands of the
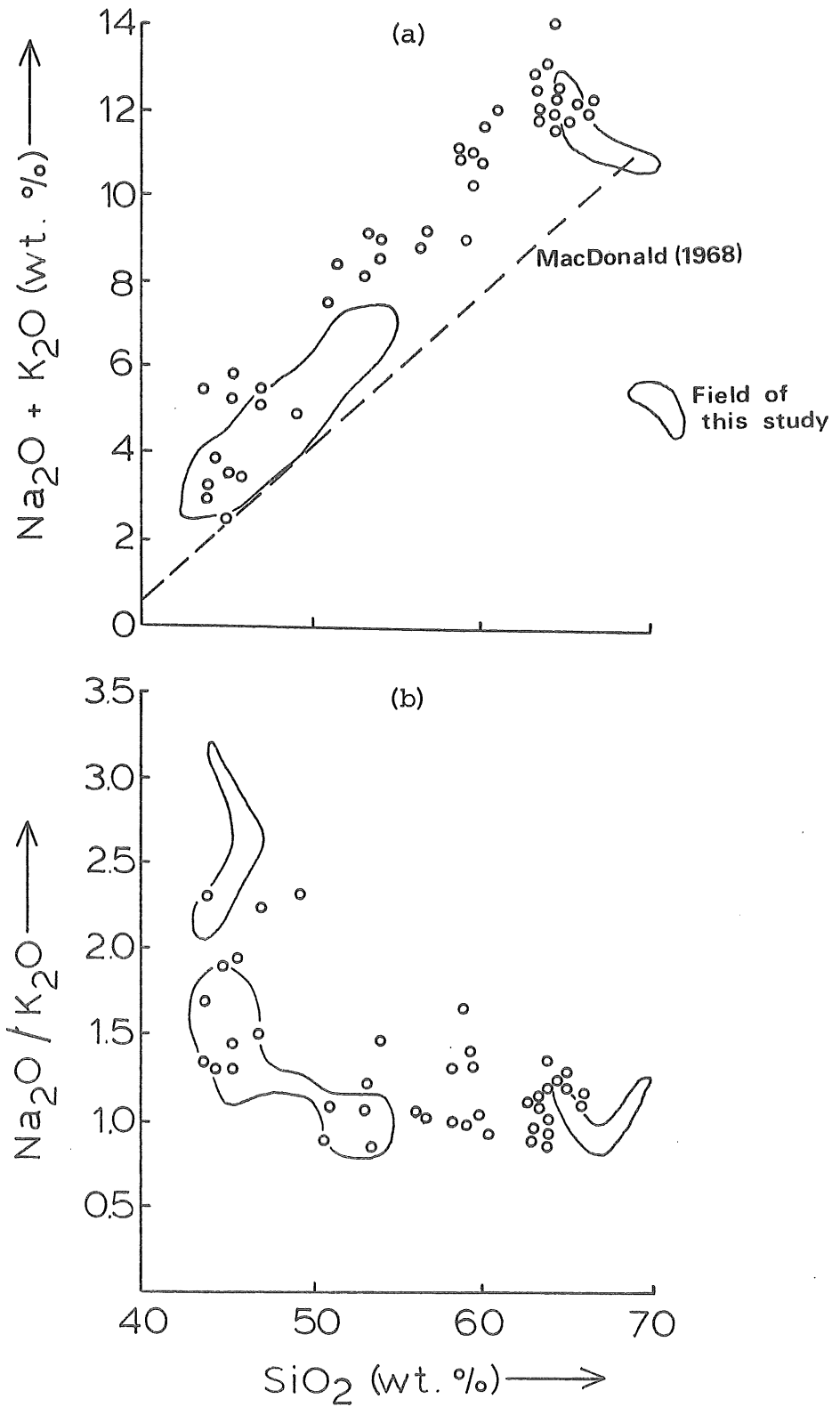
FIGURE 34: (a) (Na$_2$O + K$_2$O) (wt.%) and (b) Na$_2$O/K$_2$O plotted versus

SiO$_2$ (wt.%) for other analyses of São Miguel volcanics.

Analyses from Machado [1967], Assunção and Canilho [1970],

Schmincke and Weibel [1972].
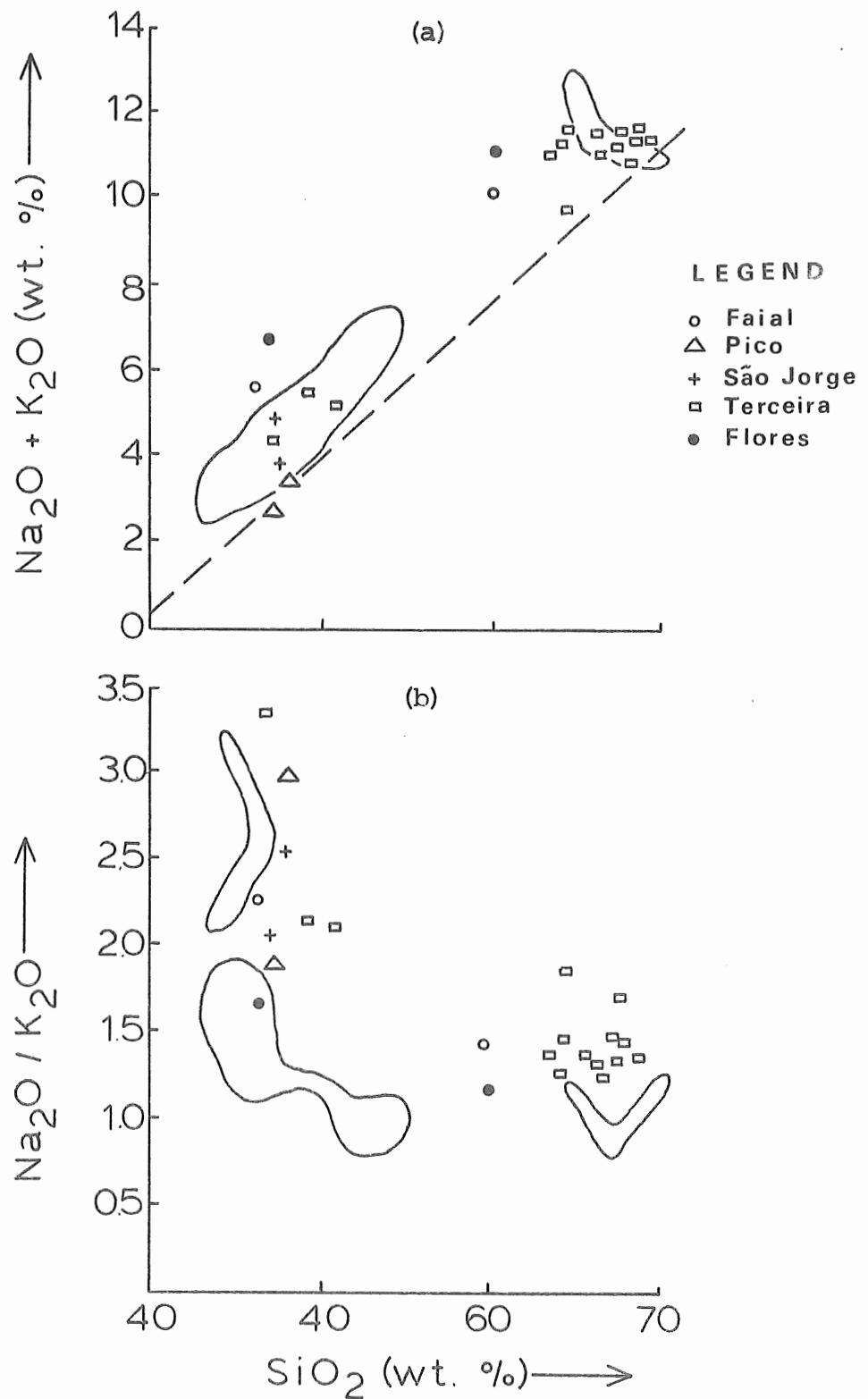
FIGURE 35: (a) $Na_2O + K_2O$ (wt.%) and (b) Na_2O/K_2O plotted versus SiO_2 (wt.%) for other islands of the Azores Group. Analyses from Machado [1967], Assunçao and Canilho [1970], Schmincke and Weibel [1972].

Azores group.

b) Other Atlantic Islands

Figure 36 is a map showing the locations of the
other islands of the Atlantic Ocean. The map also roughly
illustrates the position of each island with respect to
the Mid-Atlantic Ridge.

The occurrence of tholeiites on oceanic islands
is rare. Much of the studies of oceanic islands involve
rock types typical of alkaline associations. Some islands
are potassic in nature, others are sodic. Gough Island
(LeMaitre, 1962), Tristan da Cunha (Baker et al., 1964),
and Jan Mayen (Noe-nygaard, 1974) are notable as potassium-
rich islands. Bouvet (Baker, 1967), the Cape Verde Islands,
and Madeira (McBirney and Gass, 1967) are notably sodic.

Schmincke (1973, Figure 8, p. 639) has published
a plot of Na_2O/K_2O versus weight per cent SiO_2 for
Atlantic islands which presents the alkali ratio as
varying from near 3.8 for Madeira and Bouvet to lows
of Na_2O/K_2O equal to between 1.0 and 1.8 for Jan Mayen,
Gough, Tristan da Cunha, and São Miguel. In all cases,
the ratio of Na_2O to K_2O decreases as the rocks become
more silicic. The Na_2O/K_2O versus SiO_2 plot for the data
of this study (Figure 25a) shows the same decrease in
the ratio as the trachyt nature of the rocks increases.

According to Schmincke (1973), Atlantic oceanic
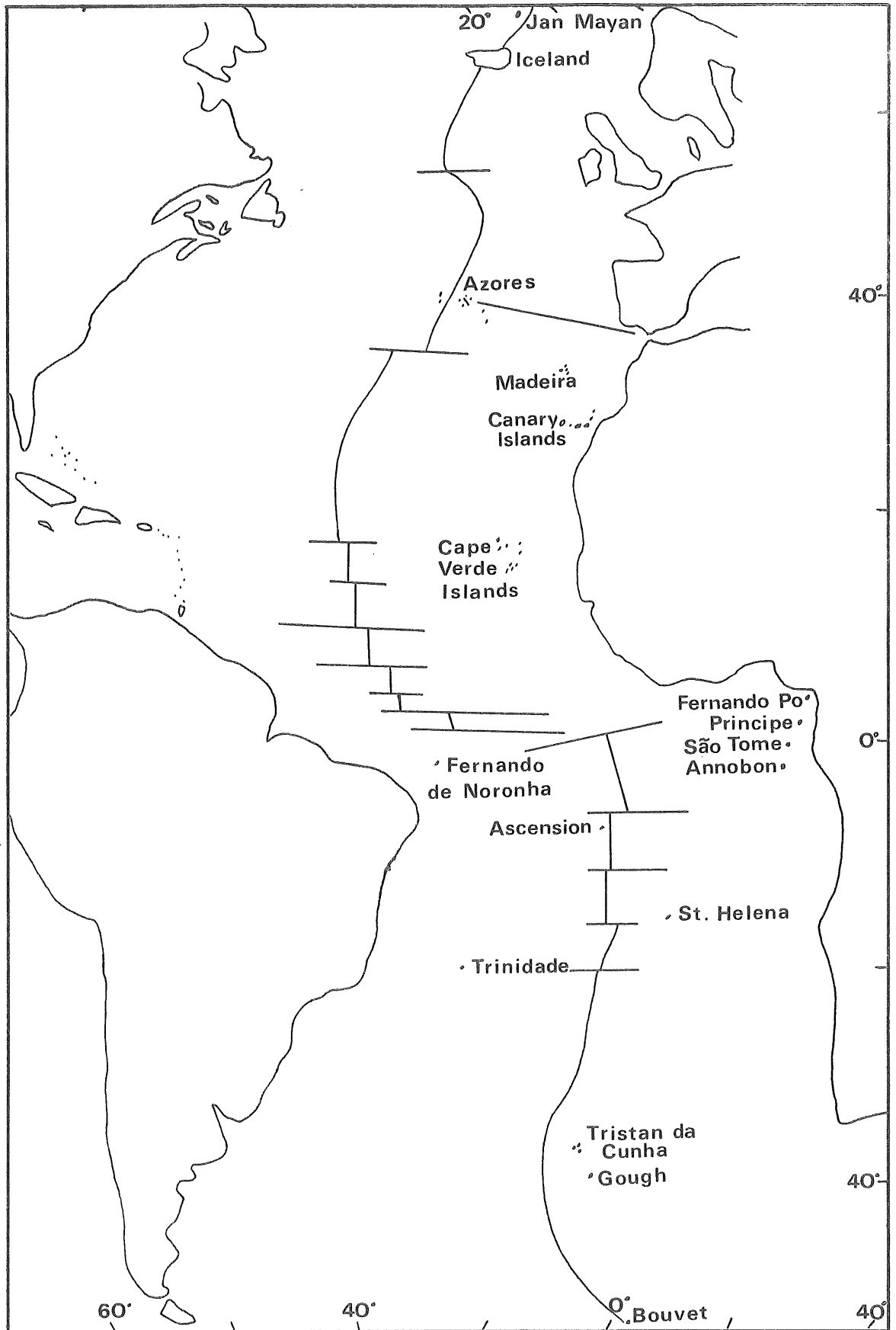
FIGURE 36: Location of islands of the Atlantic Ocean.

island rock suites can be roughly separated on the basis of the total alkali contents of their highly differentiated rocks. In his summary, Tenerife, Gran Canaria (Pliocene) and the Cape Verde Islands have 14 to 16 weight per cent total alkalis; Gough, Tristan da Cunha, São Miguel and St. Helena have 12.5 to 14 weight per cent total alkalis; Terceira, Bouvet, Ascension, Jan Mayen and Gran Canaria (Miocene) have 10 to 12.5 weight per cent total alkalis; Madeira and Iceland have less than 10 weight per cent total alkalis. The trachytic rocks of this study have $(Na_2O + K_2O)$ values of 12.83, 10.73, 11.54 and 11.37 weight per cent, which are, in all but one case, slightly lower than the value presented by Schmincke for Sao Miguel.

Since the common ground for comparison of oceanic island rocks is their alkali content, Figure 37 is a plot of $(Na_2O + K_2O)$, Na_2O/K_2O, and K_2O versus SiO_2 for three of the more potassic of the Atlantic islands. It must be remembered that there is a possibility that the alkali elements have been mobile in some of the analysed samples. Three basalts, two trachybasalts, and four trachytes from Gough Island are included from a report by Le Maitre (1962). An olivine basalt, three trachybasalts, three trachyandesites, and one trachyte from Tristan da Cunha (Baker et al., 1964) are plotted. The rocks from In-accessible Island include a basalt, a trachybasalt, a trachyandesite, and a trachyte obtained from a paper by
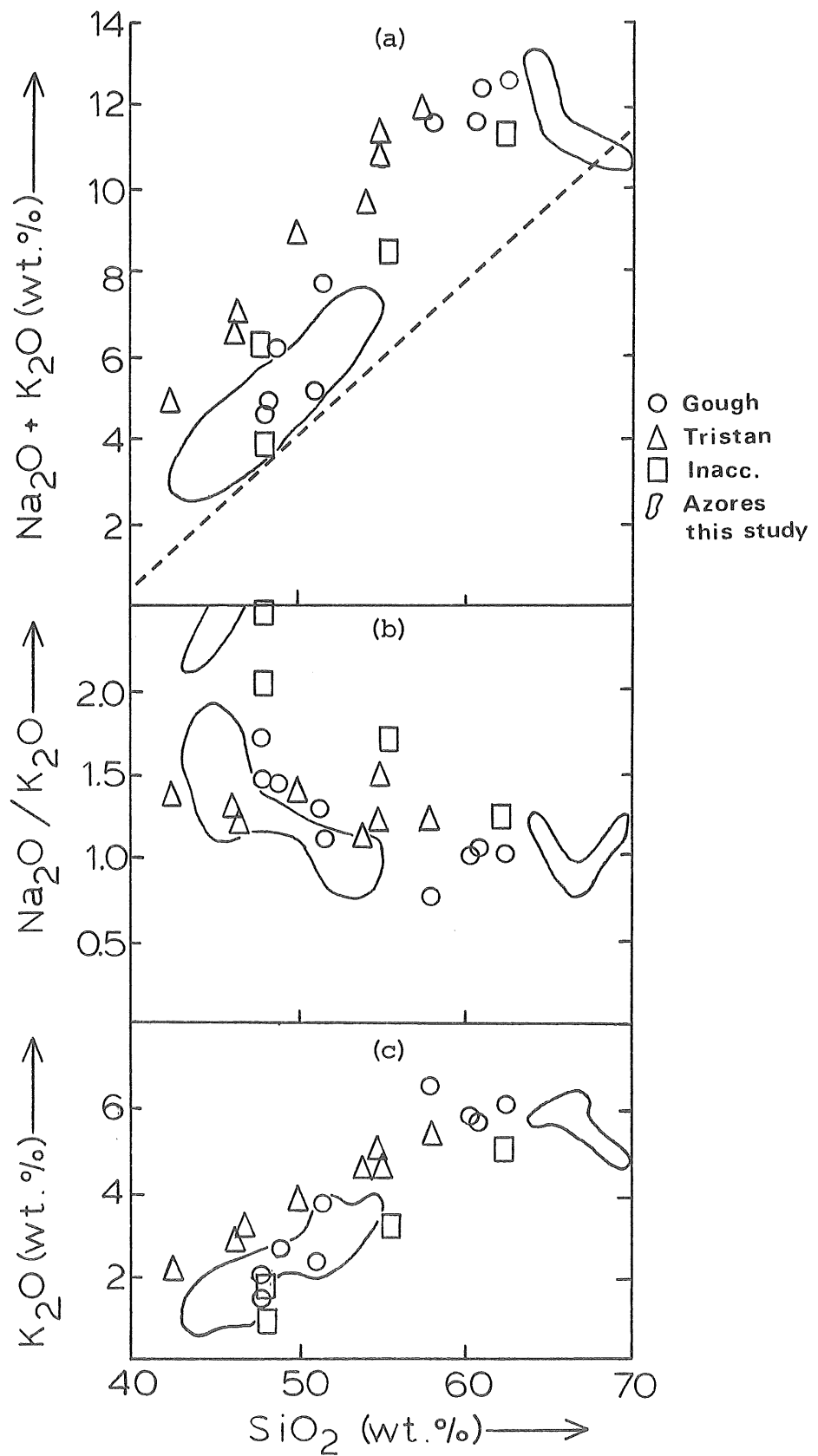
FIGURE 37: (a) $Na_2O + K_2O$ (wt.%), (b) Na_2O/K_2O, and (c) K_2O (wt.%)

plotted versus SiO_2 (wt.%) for potassic islands of the

Atlantic Ocean. Analyses from Le Maitre [1962] and

Baker et al [1964].

Baker et al., (1964). In addition, the field of the analyses
of this study has been outlined.

What is apparent in Figure 37 is that the Sao
Miguel rocks are not the most potassic: Gough Island and
Tristan da Cunha are in general more potassic.
Gough Island and Tristan da Cunha also have total alkalis
greater than those recorded for Sao Miguel.

Thus, while it is obvious that São Miguel is an
alkaline and a potassic island in terms of other Atlantic
Ocean islands, it is not the most alkaline or the most
potassic.

In Figure 38, analyses from four sodic Atlantic
islands have been used to plot ($Na_2O + K_2O$), Na_2O/K_2O,
and K_2O versus SiO_2. For Bouvet, two basalts and a trachyte
taken from Baker (1973) are used. The Canary Islands are
represented by four basalts and two trachybasalts
(Ibarrola, 1969). The analyses for Ascension of two basalts,
one hawaiite, one mugearite, and one trachyte are from
Daly (1925). The rocks from Madeira are represented by
six basalts, nine hawaiites, one mugearite, and one essexite
from Hughes and Brown (1972). The field for the analyses
of this study has been outlined on Figure 38.

In Figure 38, it appears that for the Canary
Islands and for Ascension, the total alkalis are higher
than the values plotted for São Miguel. The ratio of
Na_2O/K_2O is much higher than São Miguel for all three
islands, which is expected since they are sodic and

Sao Miguel is potassic. However, the K_2O values appear similar for the Canary Islands and slightly lower for Bouvet and Ascension than those for Sao Miguel. Thus from these plots, it appears that there is an increase in the Na_2O/K_2O ratio due to an increase in Na_2O and not to a noticeable decrease in K_2O. Therefore, it appears that the sodic nature of these islands is gained not at the expense of K_2O, but by an overall increase in total alkalis by an increase in Na_2O.

It is not the purpose of this thesis to present a detailed comparison of all oceanic islands. Better and more detailed comparisons can be obtained from Borley (1974) and Baker (1973). What is important is that a rough idea of how Sao Miguel compares with other oceanic islands in terms of chemistry and rock types be obtained.

Thus, it is important to see that Sao Miguel plots with the potassic islands of the Atlantic, but is neither the most potassic nor the most alkaline.

iii) The Existence of a Daly Gap

In 1963, Chayes presented distribution diagrams of analyses of rocks of the oceanic basalt-trachyte association which showed a bimodal distribution of SiO_2, CaO, and Thornton-Tuttle Differentiation Index. Chayes' plots illustrated the feature that Daly had originally noted from field observations in 1925: there is a scarcity of rocks of intermediate composition on oceanic islands. The

appearance of this bimodality on frequency plots has been termed the "Daly Gap".

The data used by Chayes (1963), including all analyses, regardless of their water content, have been plotted as Figure 39a. Frequency versus Differentiation Index has been plotted with a class width of D.I. = 5. The bimodality is clearly evident: there are peaks for D.I. between 20 and 40 and for D.I. between 80 and 90.

The data of this study are plotted beneath Chayes' data as Figure 39b. The plot illustrates a feature which has been previously emphasized: of the 32 analyses of Azores lavas presented in this study, there are no rock analyses with intermediate values of the Differentiation Index, i.e., with D.I. between 65 and 85. If these results were plotted with Chayes' data, the bimodality of Figure 39a would be reinforced.

Data from other Azores islands, including Sao Miguel have been plotted as Figure 39c. There is a range of values present, and a bimodal distribution of basalts and trachytes is indicated. This is weighted in favour of the trachytes because the rocks analysed by Schmincke and Weibel (1972) are chiefly trachytes. A plot of the data for analyses from Sao Miguel plotted for SiO_2 versus D.I. (Figure 40) shows that the data is weighted in favour of trachytes and basalts, with few analyses of intermediate compositions.
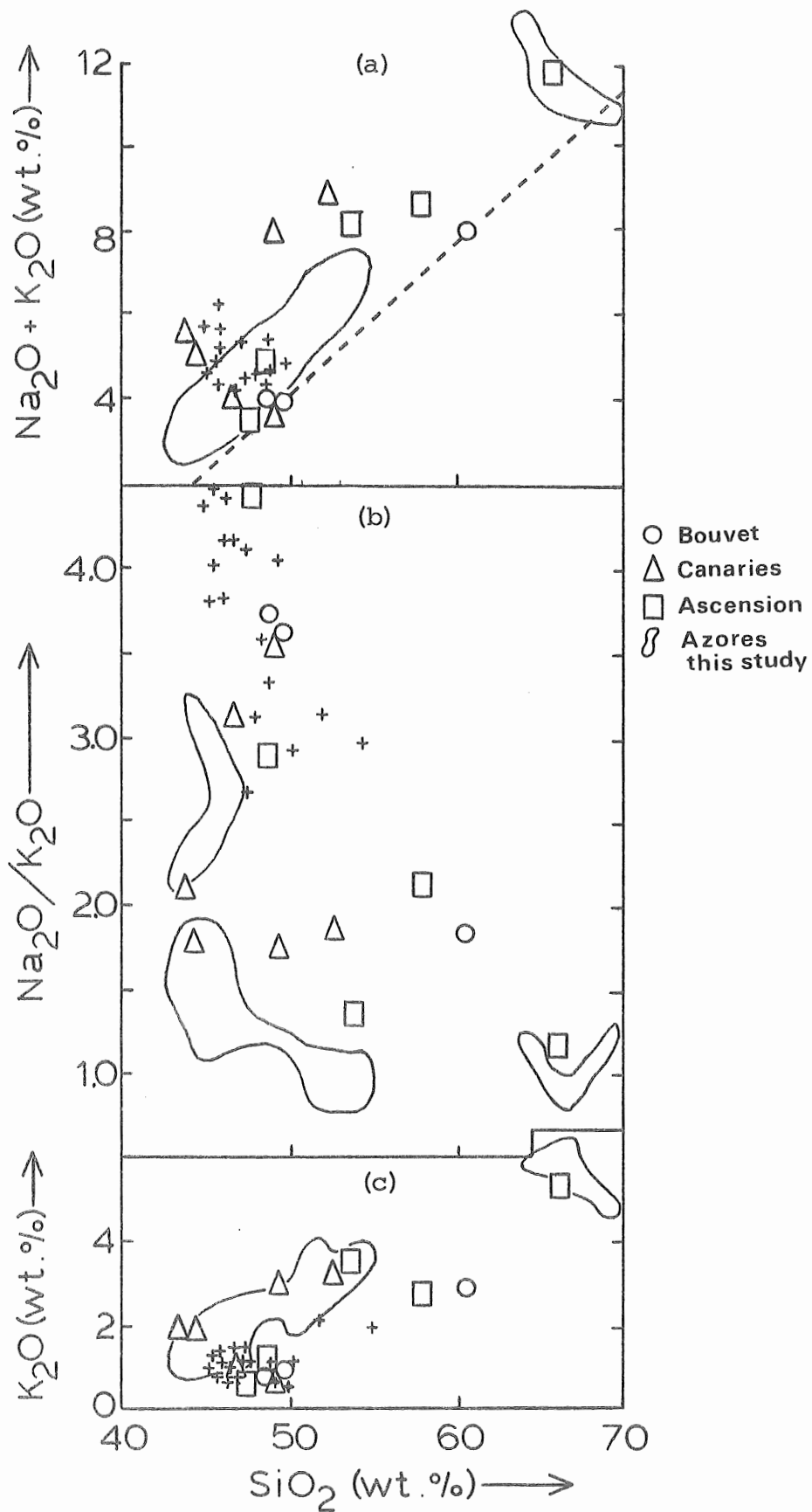
FIGURE 38: (a) $Na_2O + K_2O$ (wt.%), (b) Na_2O/K_2O, and (c) K_2O (wt.%)

plotted versus SiO_2 (wt.%) for sodic islands of the

Atlantic Ocean. Analyses from Daly [1925], Ibarrola[1969],

Hughes and Brown [1972], and Baker [1973].
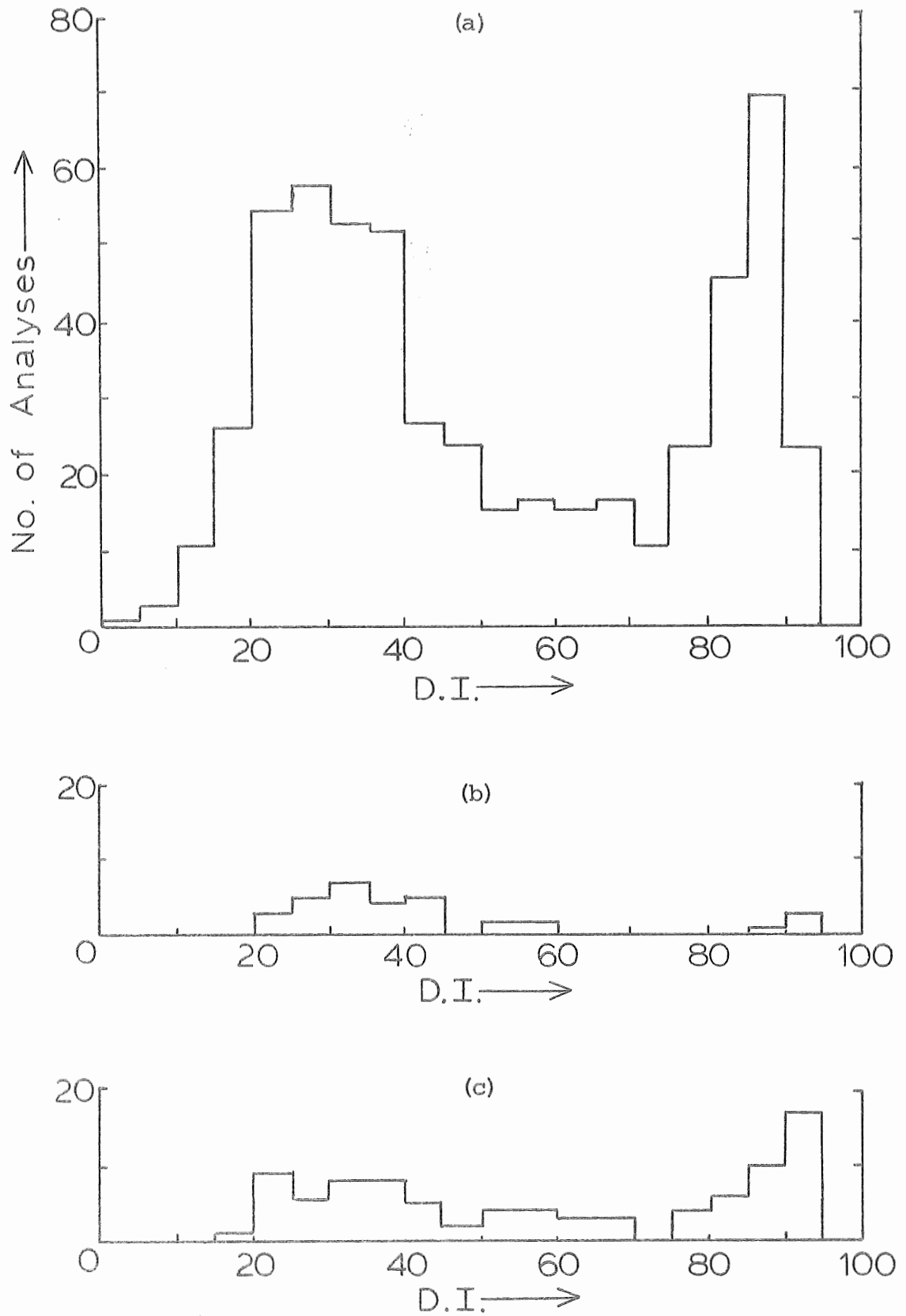
FIGURE 39: Number of analyses versus D.I. for (a) Chayes' data [1963], (b) analyses of this study, and (c) other analyses of Azores rocks.
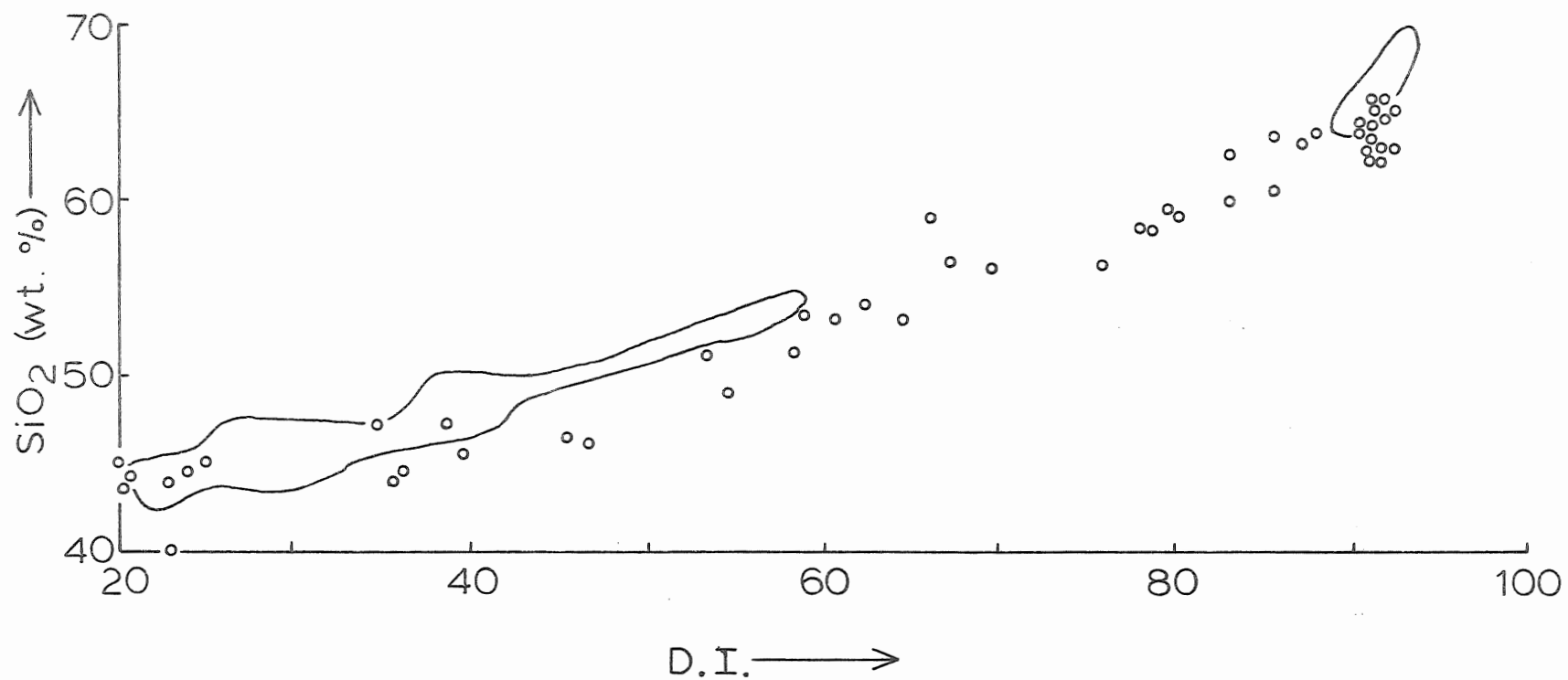
FIGURE 40: SiO$_2$ (wt.%) versus D.I. for other analyses of São Miguel volcanics. Field of this study is shown. Analyses from Machado [1967], Assunçao and Canilho [1970], and Schmincke and Weibel [1972].

If the Daly Gap is real, then one must either abandon basic concepts about crystal fractionation, or find some explanation for the discontinuity in the range of volcanic products within the framework of crystal fractionation.

One of the most obvious arguments against the validity of the gap is sampling bias. Baker (1968) has argued that petrologists have oversampled trachytic plugs because they offer variety in an area composed chiefly of relatively uniform basalts. His estimates of volumetric abundances on St. Helena are as follows: basalts = 70-80%, trachybasalts = 15-25%, trachyandesites = 4%, and trachytes and phonolites = 1%, but he has demonstrated that a bimodal distribution could be obtained by oversampling of trachytic plugs and smaller intrusions.

Similarly, Cann (1968) maintains that the mode of occurrence or rocks on volcanic islands influences the nature of the sampling. The basalts generally form large sheets while the more salic products are limited in extent. Thus, a geologist tends to sample on either side of a contact and in the process, overrepresents the trachytes.

In sampling the volcanics of the Azores borehole, an attempt was made to adequately represent the nature of the flow units in each of Subaerial Sequences I, II, and III, the Transition Sequence, and the Submarine Sequence. Thus there was no ignoring of the intermediate rock types among the flow units. If they had been present, they would have

been equally well-sampled with the basalts and trachytes.

It must be admitted that sampling bias is present here too: because the trachytes between 275 and 350 m appeared to be the only visible chemical variation of the lavas in the core, all three of the trachytes were sampled. However, if intermediate rocks were present among the basalts, they would have been as equally well-sampled as the basalts.

Thus, there remains the problem of explaining the lack of trachyandesites among the flow units. Why do we not see a complete profile of evolving magma products? Two possibilities exist: either the trachyandesites are produced and are not brought to the surface or, the magmatic evolution process is biased so that basalts and trachytes are produced with the exclusion of trachyandesites.

Cann (1968) has suggested that the final differentiates of a volcano are more water- and gaseous-rich, and therefore, final eruptions are biased in favour of the more explosively-extruded acid products. This results in a volumetric bimodal distribution of basalts and trachytes, to the detriment of the intermediate rock types.

If this argument is valid, then one can expect to find a residuum of chemically intermediate lavas somewhere beneath the 981 m of material uncovered in the drillcore. The only possibility of testing this theory is to drill deeper into the volcano.

Cann (1968) has also suggested that the earlier dif-

ferentiates are continually being re-melted and remobilized
by the passage of basalts through the volcanic pile. Thus,
while the actual volume of trachytic material is not great,
it appears to be more abundant because of its reappearance
at higher levels.

This reasoning still does not explain the absence of
trachyandesitic compositions among the flow units in the
drillhole since it is assumed that intermediate rocks have
been produced, and yet they are not seen in this core.

Yoder (1971) has used the system diopside-forsterite-
silica (Di-Fo-Qz) for P_{H_2O} = 20 kb to demonstrate that partial
melting of the mantle can preferentially produce basalts and
acid differentiates. This process could be used to explain
why there are no trachyandesites in the drillcore, but it
does not explain why, if this process is universal, trachy-
andesites are produced by other volcanic centres on Sao
Miguel.

In summary, it appears that there are three possi-
bilities: (1) the trachyandesites have been produced and
have not been brought to the surface, (2) the trachyandesites
have not been produced and thus are not found in the drill-
core, or (3) the intermediate rocks are represented in this
drillhole by the pyroclastics. The fact that trachyandesites
are found elsewhere on the island indicates that they are
being produced in the other volcanic centres and one would
expect a similar process to be in operation in this Agua de
Pau volcano.

However, the pyroclastic material has not as yet been considered with the analyses of the flow units. Table 17 compares the range in composition of some of the major oxides of the trachytes, the pyroclastics, and the trachybasalts and intrusives. From this table, it is apparent that the pyroclastics have SiO_2, TiO_2, MgO, CaO, and P_2O_5 intermediate to the compositions of the trachytes and the trachybasalts. Thus, it is a possibility that the pyroclastics represent the "missing link" in the range of lava compositions.

The difficulty arises in trying to assess exactly what has been analysed, since the pyroclastic units are all almost completely altered to clay minerals. The pyroclastic units could have been altered so that they appear more trachytic, or, conversely, altered to appear more trachy-andesitic. The Al_2O_3 values are high relative to the trachy-basalts and the trachytes.

However, it must be seriously considered that the pyroclastics represent the intermediate products in the drill-hole. A more extensive chemical study of these units could reveal further clues as to their chemical nature.

Therefore, while it can be shown that a Daly Gap exists for the lava units of this drillhole, the possibility exists that the pyroclastics provide the "missing" material of intermediate composition in this Agua de Pau volcano.

iv) Petrogenesis

Oceanic islands exist as volcanic "bulges" on the

TABLE 17: Comparison of the chemistry of the trachytes, pyroclastics, and trachybasalts.

	Trachytes	Pyroclastics	Trachybasalts
SiO_2	64.38-69.96	57.13-64.22	54.54-54.58
TiO_2	0.50- 0.74	0.71- 1.05	2.28- 2.26
Al_2O_3	14.41-16.76	17.10-22.00	17.57-17.97
Fe_2O_3	0.44- 0.52	2.40- 5.95	1.70- 3.41
FeO	2.51- 2.94	0.46- 1.09	3.02- 4.17
MnO	0.07- 0.21	0.02- 0.14	0.09- 0.15
MgO	0.09- 0.48	0.72- 1.95	2.13- 3.03
CaO	0.20- 0.74	0.78- 2.16	5.14- 6.56
Na_2O	5.25- 7.02	2.04- 5.29	3.29- 3.88
K_2O	4.79- 6.29	2.53- 4.41	3.49- 3.82
P_2O_5	0.03- 0.12	0.11- 0.19	0.89- 0.91
Nb	163-216	189-269	94-95
Y	56-88	71-77	54-56
Sr	6-57	100-358	1226-1315
Rb	147-214	96-122	63-67
Zr	823-1363	945-1227	405-419
Cr	N.D.	N.D.	12
Ni	1-2	2-10	17-18

floors of the ocean basins. In the case of the Azores islands, in addition to the active volcanism along the Mid-Atlantic Ridge, the Azores Platform appears to represent an anomalously high degree of magmatic activity. It is common practice to try to explain oceanic islands in terms of current theories about plate tectonics.

Morgan (1971) originally proposed that a mantle plume, i.e. upwelling of hot magma material from the earth's mantle, occurs beneath the Azores. This view has been expanded by Schilling (1975) who proposes the existence of a mantle "blob" beneath the Azores Platform on the basis of rare earth element variations. O'Hara (1973) explained Schilling's mantle plume under Iceland in terms of partial melting and crystal fractionation, arguments which can be applied to the Azores situation as well.

The following features have been observed by Schilling (1975) along the Mid-Atlantic Ridge south from the Azores Platform to the Atlantic Fracture Zone at 30°N latitude:

1) Towards the Azores, pyroxene becomes the more abundant phenocryst, with plagioclase (An_{73-89}) the second most common. Away from the Platform, plagioclase is the most common phenocryst, followed by olivine (Fo_{75-89}), then clinopyroxene. This same trend was observed along the Reykyanes Ridge south of Iceland (Schilling, 1973);

2) Analyses of dredged rock samples have shown that southwest along the Ridge from the Azores Platform, there is

a depletion of the light rare earth elements (REE), which is shown as a decrease in the La/Sm ratio (Schilling, 1975, Figure 4, p. 108). The ratio decreases from a maximum of La/Sm = 3 for a point on the Azores Platform to a value of less than 0.5 at 1000 km southwest of the Platform along the Ridge. South of 34°N latitude, a relatively constant low value of the La/Sm ratio is obtained which Schilling terms a "normal ridge" value. A similar feature was noted by Schilling (1973b, 1973a) for Iceland and for the Gulf of Aden;

3) There is no systematic variation of the FeO/ FeO + MgO with distance SW along the Ridge. The FeO/ FeO + MgO was found to increase along the Reykyanes Ridge towards Iceland (Schilling, 1973b);

4) There is a free air positive gravity anomaly relative to hydrostatic equilibrium over the Azores Platform;

5) The samples analysed by Schilling (1975) were either Ol- or Q-normative, in contrast to other published analyses presented for the Azores, which are alkaline (Ne-normative).

The above features have been explained by Schilling (1973, 1975) for both Iceland and the Azores as the result of a mantle "blob" or plume by which magma material upwells to the surface from the earth's mantle. Two different magma sources are proposed to exist beneath the Azores area: the mantle blob beneath the Azores Platform and a separate magma

source for the ridge south of 34°N latitude. The gradation
in values of La/Sm ratios from the Platform SW along the
Ridge results from a mixing of these two different magma
sources.

Thus, to produce the rare earth element pattern noted
by Schilling, the mantle blob theory proposes that there is
a mantle source which is rich in light rare earth elements
upwelling beneath the Azores Platform which, between 40° and
34°N latitude, mixes with a magma low in light REE whose
source is the low velocity layer of the mantle. Thus, a
somewhat consistent decrease in La/Sm ratio is observed
between the Azores Platform and 34°N latitude, assuming a
homogeneous mixing process has occurred.

In line with O'Hara's ideas, the two different magma
types and the gradation between them can be produced from
one magma with varying degrees of crystal fractionation.
The magma source for both the Azores Platform and the normal
ridge segment could be the base of the upper mantle, which
would imply a higher heat source from the lower mantle, but
would not require flow of the lower mantle as is necessary
in the plume model.

Once the magma is obtained from the mantle, the vary-
ing amounts of rare earth element contents can be generated
by crystal fractionation at different temperatures and pres-
sures. For example, a basalt depleted in the light rare
earth elements can be produced by clinopyroxene fractionation

(O'Hara, 1973; O'Hara et al., 1975). This is supported as a possibility by the fact that the lavas become increasingly depleted in the light REE as clinopyroxene becomes less common as a phenocryst in the lavas (Schilling, 1975). The question is whether the original mantle material contains sufficiently high concentrations of the light rare earth elements to produce such a difference between the samples of the Platform and those of the normal ridge.

Thus, both Schilling and O'Hara agree that Iceland and the Azores islands constitute unusual phenomena on the earth's surface. Both attribute these disturbances to the earth's mantle, Schilling as a flow of mantle material, and O'Hara as a flow of heat. Both of these theories do not consider how a change from oceanic tholeiitic basalts to the highly alkaline rocks found on the Azores islands can be effected. It must be assumed that either there is a second magma source (or a third magma source in Schilling's theory) which is alkaline or, at some pressure and temperature, the magma can cross a thermal divide and become alkaline in nature.

Figure 41 plots the chemical data of this study in the CMAS system of O'Hara (1968). In this type of projection, the components of basalts are represented by: $C = CaO$, $+ Na_2O$, K_2O, $-P_2O_5$; $M = MgO$, MnO, FeO, TiO_2; $A = Al_2O_3$, Fe_2O_3, Cr_2O_3; and $S = SiO_2$.

Figure 41 represents the diopside projection onto

C_3A - M - S for the basalts of this study. The olivine gabbro thermal divide and the hypersthene-gabbro thermal divide are included as well as the phase boundaries for P = 1 atm. and P = 20 kb.

The plotted positions suggest that the samples have undergone equilibration at 1 atm. pressure. There is an indication of an enrichment of plagioclase feldspar as phenocrysts, a feature also noticeable in Figure 42, which is the Quartz projection onto the Ol-Di-Pl plane within the normative basalt tetrahedron.

The samples straddle the olivine-gabbro thermal divide, a feature previously suggested by the C.I.P.W. norms. However, this could be the result of the altering conditions which has caused most of the basalts to plot in the Hy-normative field between the hypersthene-gabbro and olivine gabbro thermal divides.

The alkaline magma could be created by partial melting of spinel peridotite at 20 kb, or by fractional crystallization of a liquid from higher pressures at 20 kb, to produce a liquid lying somewhere along the cotectic curve A-B-C, depending on the degree of partial melting or fractional crystallization. Eruption of any liquid lying along the segment A-B, accompanied by polybaric fractionation of olivine en route to the surface (arrow 1) could produce bulk compositions at the surface lying along the one atmosphere

cotectic curve D-E. These would be Ne- normative alkali basalts, in accordance with the conclusion reached earlier in this chapter. However, the bulk compositions of the basaltic rocks do not now conform to the one atmosphere cotectic D-E. This suggests that they have been modified by two further processes. First, the displacement towards the cpx-plag piercing point (arrow 2) is indicative of plagioclase enrichment, probably as phenocrysts, and is confirmed by petrographic observations and Figure 42, where most of the compositions are displaced towards the plagioclase apex.

Secondly, P. Sarkar (personal communication) has suggested that addition of silica to these rocks has taken place during hydrothermal alteration. On Figure 41 this process is represented by a vector (arrow 3) which drives the compositions towards the SiO_2 apex, a result which could not be achieved by fractional crystallization at low pressure because of the olivine-gabbro thermal divide. This effect can account for the apparent tholeiitic nature of many of these rocks.

v) Significance of the Pearce and Cann Diagram

The Pearce and Cann diagram presented in Chapter 5 appears to be significant in terms of the local plate tectonics. The basalts plot in field D as within-plate basalts. This agrees with the present position of Sao Miguel

relative to the present plate boundaries, i.e., the island is situated on the Azores Platform approximately 450 km from the Mid-Atlantic Ridge and approximately 175 km from the East Azores Fracture Zone. In addition, the failure to find any rocks with chemical associations with plate margins (Field B) may suggest that the Terceira Trough which runs through Sao Miguel has not been a secondary spreading centre.
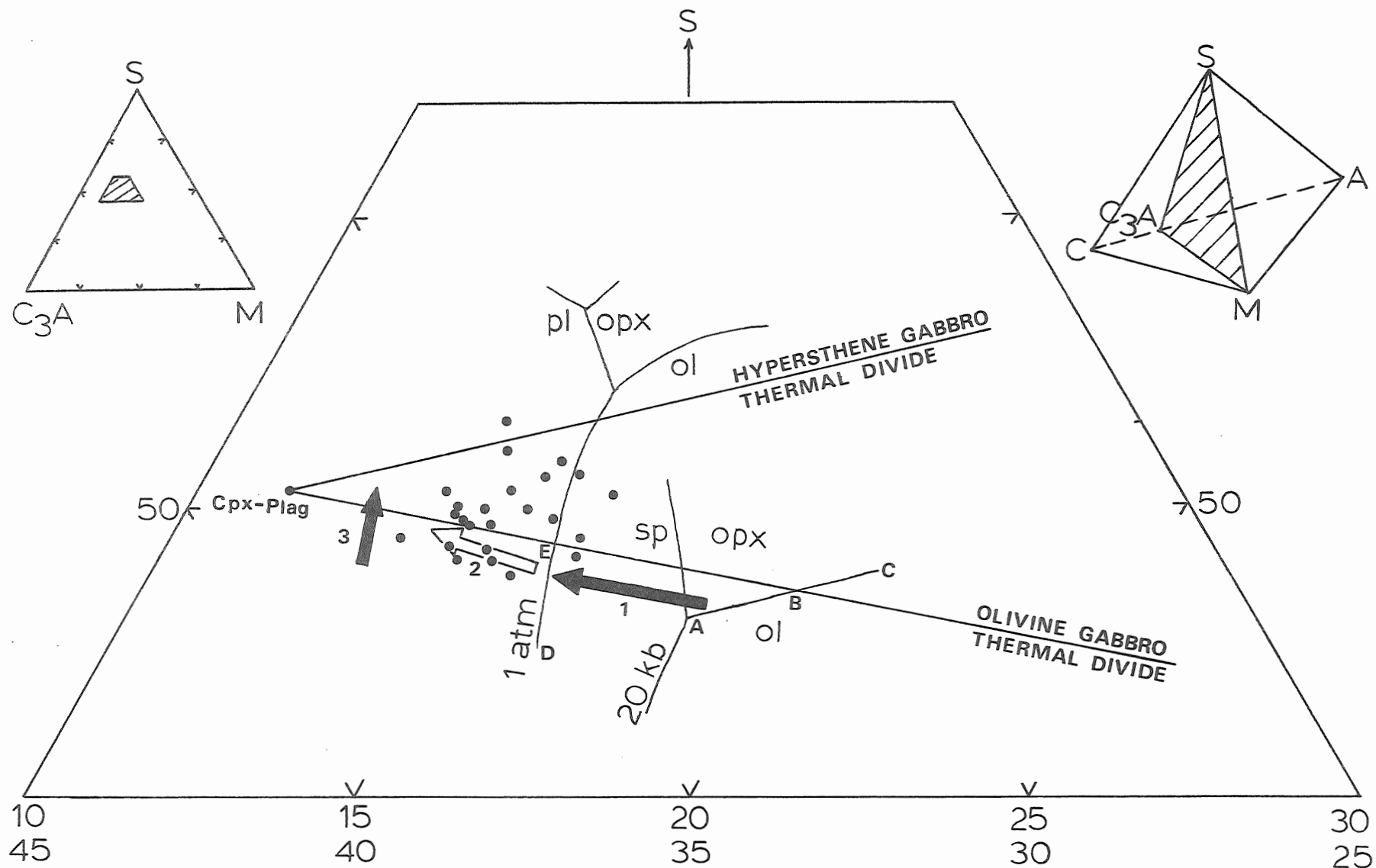
FIGURE 41: Diopside projection onto C₃A-M-S for basalts of this study. Phase boundaries for 1 atm. and 20 kb. pressure shown. Explanation in text.
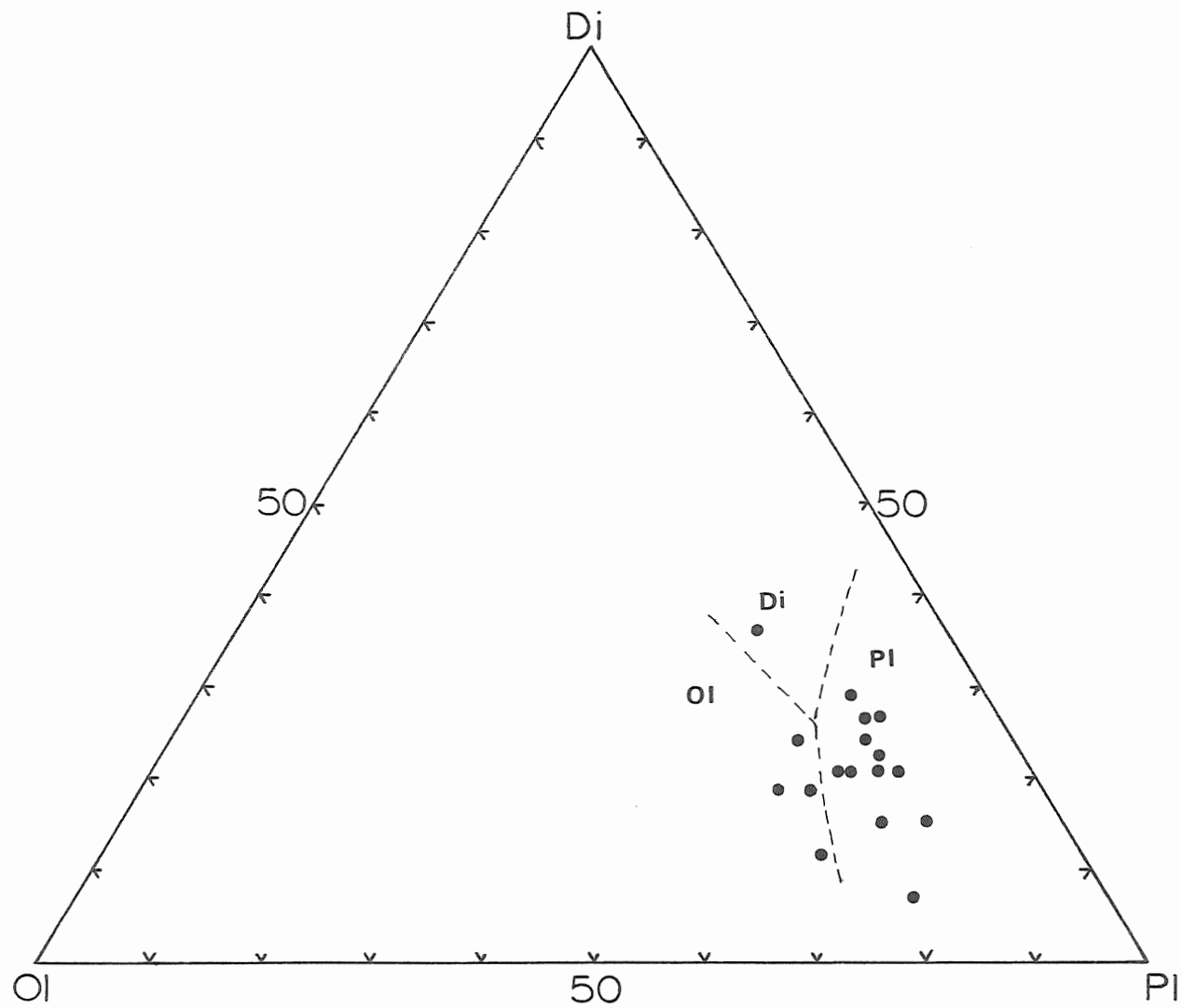
FIGURE 42: Projection in normative basalt tetrahedron from Q onto Ol-Di-Pl.

CHAPTER 8: SUMMARY

The material and ideas presented in this study can be summarized as follows:

1) Of the thirty flow units analysed in this study, 24 are basaltic in chemistry and mineralogy, 2 are trachy-basaltic, and 4 are trachytic. The 2 intrusive units are similar in chemistry to the trachybasalts.

2) For the basalts, Al_2O_3, Nb, and Zr increase with depth in the drillhole; CaO, TiO_2, and MgO decrease; FeO_T, Cr, and Ni vary randomly; and K_2O, Na_2O, SiO_2, Sr, Rb, and Y show no significant increase or decrease.

3) The four pyroclastic units analysed have SiO_2, TiO_2, MgO, CaO, and P_2O_5 concentrations intermediate to the values recorded for the trachytes and the trachybasalts.

4) The sequences recognized in the core are not reflected by the chemistry of the analysed rock units.

5) The magmatism appears to have been alkaline in nature, with some of the alkaline characteristics obscured by hydrothermal alteration.

6) The lavas of this study contain high K_2O, P_2O_5, and TiO_2, but are not the most potassic nor the most alkaline of the rocks found on the islands of the Atlantic Ocean.

7) The absence of lavas of intermediate composition (trachyandesites with D.I. = 60-80) has been observed in this study and is considered to represent the Daly Gap of Chayes

(1963) for the flow units of this drillhole; however, the pyroclastic units analysed have a chemistry intermediate to the trachytes and trachybasalts, and could represent the missing material of intermediate chemistry.

8) CMAS projection of the analyses of this study indicate that the basalts have probably undergone equilibration at 1 atm. pressure, and have been enriched in phenocrysts of plagioclase feldspar.

9) Analysis of the flow units of the drillcore has been useful in outlining the present chemistry of the core. However, the value of a petrological study has been limited by the occurrence of hydrothermal alteration.

FUTURE WORK

The plots of Nb and Zr versus depth have shown correlation coefficients for the basalts of + 0.76 and + 0.71, respectively. This suggests that for these elements, which are considered to be immobile during alteration, there is a somewhat regular decrease with evolution of the volcano. If red, this decrease is incompatible with the basalts having been successive eruptions from a single magma batch undergoing normal fractional crystallization. The further significance of these trends would be useful to investigate.

REFERENCES

Abbey, Sydney (1973): Studies in "Standard Samples" of silicate rocks and minerals Part 3: 1973 extension and revision of "usable" values. Geol. Surv. Can. Paper 73-36, 25 pp.

Abdel-Monem, A., Fernandez, L.A., and Boone, G.A. (1968): Pliocene-Pleistocene minimum K-Ar ages of the older eruptive centers, Eastern Azores. Am. Geophys. Union Trans. 49, p. 363.

Abdel-Monem, A.A., Fernandez, L.A., and Boone, G.M. (1975): K-Ar ages from the eastern Azores group (Santa Maria, Sao Miguel, and the Formigas Islands). Lithos 8, pp. 247-254.

Assunçao, Torre de, C.F., and Canilho, M.H. (1970): Notas sobra petrografia comparada das ilhas Atlanticas. Lisboa Univ. Fac. Cienc. Mus. e Lab. Mineral. e Geol. Bol. 11, pp. 305-342.

Baker, I. (1968): Intermediate oceanic volcanic rocks and the "Daly Gap". Earth Plan. Sci. Let. 4, pp. 103-106.

Baker, I. (1969): Petrology of the volcanic rocks of St. Helena Island, South Atlantic. Bull. Geol. Soc. Am. 80, pp. 1283-1310.

Baker, P.E. (1967): Historical and geological notes on Bouvetøya. Br. Antarct. Surv. Bull. 13, pp. 71-84.

Baker, P.E. (1973): Islands of the South Atlantic in "The Ocean Basins and Margins, V. I: The South Atlantic", Nairn, Alan, E.M., and Stehli, Francis G., Eds., pp. 493-553. Plenum Press, N.Y.

Baker, P.E., Gass, I.G., Harris, P.G., and Le Maitre, R.W. (1964): The volcanological report of the Royal Society Expedition to Tristan da Cunha, 1962. R. Soc. (London) Phil. Trans. A256, No. 1075, pp. 439-578.

Barberi, F., Bizouard, H., and Varet, J. (1971): Nature of the clinopyroxenes and iron enrichment in alkalic and transitional basaltic magmas. Contr. Miner. Petrology 33, pp. 93-107.

Boone, G.M., and Fernandez, L.A. (1971): Phenocrystic olivines from the eastern Azores. Mineralog. Mag. 38, pp. 165-178.

Borley, G.D. (1974): Oceanic islands in "The Alkaline Rocks", Sorensen, H., Ed. John Wiley and Sons, N.Y., pp. 311-330.

Bouvier, J.L., Gupta, J.G. Sen, and Abbey, Sydney (1972): Use of an "Automatic Sulphur Titrator" in rock and mineral analysis: determination of sulphur, total carbon, carbonate, and ferrous iron. Geol. Surv. Can., Paper 72-31, 22 pp.

Cann, J.R. (1967): A second occurrence of dalyite and the petrology of some ejected syenite blocks from Sao Miguel, Azores. Mineralog. Mag 36, pp. 227-232.

Cann, J.R. (1968): Bimodal distribution of rocks from volcanic islands. Earth Plan. Sci. Let. 4, pp. 497-480.

Chayes, F. (1963): Relative abundance of intermediate members of the oceanic basalt-trachyte association. J. Geophys. Res. 68, pp. 1519-1534.

Chayes, F. (1965): Titania and alumina content of oceanic and circumoceanic basalts. Mineralog. Mag. (Tilley Vol.) 34, pp. 126-131.

Coombs, D.S. (1963): Trends and affinities of basaltic magmas and pyroxenes as illustrated on the diopside-olivine-silica diagram. Mineral. Soc. Am. Spec. Paper 1, pp. 227-250.

Daly, R.A. (1925): The geology of Ascension Island. Proc. Am. Acad. Arts Sci. 60, pp. 1-80.

Flanagan, F.J. (1973): 1972 values for international geochemical reference samples; Geochim. Cosmochim. Acta 37, pp. 1189-1200.

Gibb, Fergus G.F. (1973): The zoned clinopyroxene of the Shiant Isles Sill, Scotland. J. Petrology 14, Pt. 2, pp. 203-230.

Glassley, W. (1975): Geochemistry and tectonics of the Crescent volcanic rocks, Olympic Peninsula, Washington. Bull. Geol. Soc. Am. 85, pp. 785-794.

Gunn, B.M., Coy-Yll, R., Watkins, N.D., Abramson, C.E., and
    Nougier, J. (1970): Geochemistry of an oceanite
    ankaramite basalt suite from East Island, Crozet
    Archipelago. Contr. Miner. Petrology 28, pp. 319-339.

Heezen, B.C. (1962): The deep sea floor in "Continental
    Drift", S.K. Runcorn, Ed., Academic Press, N.Y.,
    pp. 235-288.

Hughes, D.J., and Brown, G.C. (1972): Basalts from Madeira:
    A petrochemical contribution to the genesis of oceanic
    alkali rock series. Contr. Miner. Petrology 37, pp.
    91-109.

Hyndman, D.W. (1972): Petrology of Igneous and Metamorphic
    Rocks. McGraw-Hill, N.Y. 533 pp.

Ibarrola, E. (1969): Variation trends in basaltic rocks of
    the Canary Islands. Bull. Volc. 33, Pt. 2, pp. 729-
    777.

Irvine, T.N., and Baragar, W.R.A. (1971): A guide to the
    chemical classification of the common volcanic rocks.
    Can. J. Earth Sci. 8, pp. 523-548.

Jeffery, Paul Geoffrey (1970): Chemical Methods of Rock
    Analysis, First Edition. Oxford, N.Y. Pergamon Press.
    509 pp.

Kaula, W.M. (1972): Global gravity and mantle convection,
    Tectonophysics 13, pp. 341-359.

Krause, Dale C. (1965): East and West Azores Fracture Zones
    in the North Atlantic in "Submarine Geology and Geo-
    physics, 17th Colston Symposium", Bristol, 1965.
    pp. 163-173.

Krause, D.C., and Watkins, N.D. (1970): North Atlantic
    crustal genesis in the vicinity of the Azores.
    Geophys. J. 19, pp. 261-283.

Kuno, H. (1968): Differentiation of basalt magmas in
    "Basalts, V. 2", Hess, H.H., and Poldervaart, A., Eds.,
    Interscience, N.Y. pp. 623-688.

Lambert, Richard St. John, and Holland, James Grenville,
    (1974): Yttrium geochemistry applied to petrogenesis
    utilizing calcium-yttrium relationships in minerals
    and rocks. Geochim. Cosmochim. Acta 38, pp. 1393-
    1414.

Le Maitre, R.W. (1962): Petrology of volcanic rocks, Gough
    Island, South Atlantic. Bull. Geol. Soc. Am. 73,
    pp. 1309-1340.

Lessing, Peter, Decker, Robert W., Reynolds, Robert C. Jr.
    (1963): Potassium and rubidium distribution in
    Hawaiian lavas. J. Geophys. Res. 68, pt. 5, pp.
    5851-5855.

MacDonald, G.A. (1968): Composition and origin of Hawaiian
    lavas. Geol. Soc. Am. Mem. 116, pp. 477-522.

Machado, F. (1967): Active volcanoes of the Azores in
    "Catalogue of the Active Volcanoes of the World.
    Part XXI, Atlantic Ocean". Van Padang, M.N., and
    others, pp. 7-52.

Maxwell, John Alfred (1968): Rock And Mineral Analysis.
    New York, Interscience, 584 pp.

McBirney, R., and Gass, I.G. (1967): Relations of oceanic
    volcanic rocks to mid-oceanic rises and heat flow.
    Earth Plan. Sci. Let. 2, pp. 265-276.

Morgan, W.J. (1971): Convection plumes in the lower Mantle.
    Nature 230, pp. 42-43.

Muecke, G.K., Ade-Hall, J.M., Aumento, F., MacDonald, A.,
    Reynolds, P.H., Hyndman, R.D., Quintino, J., Opdyke,
    N., and Lowrie, W. (1974): Deep drilling in an
    active geothermal area in the Azores. Nature 252,
    pp. 281-285.

Noe-Nygaard, A. (1974): Cenozoic to Recent volcanism in
    and around the North Atlantic Basin. In "The Ocean
    Basins and Margins Vol. 2: The North Atlantic".
    Nairn, Alan E.M., and Stehli, Francis G., Eds., Plenum
    Press, N.Y., pp. 391-443.

O'Hara, M.J. (1968): The bearing of phase equilibria studies
    on the origin and evolution of basic and ultrabasic
    rocks. Earth Sci. Rev. 4, pp. 69-133.

O'Hara, M.J. (1973): Non-primary magmas and dubious mantle
    plume beneath Iceland. Nature 243, p. 507.

O'Hara, M.J., Saunders, M.J., and Mercy, E.L.P. (1975):
    Garnet-peridotite, primary ultrabasic magma and
    eclogite: interpretation of upper mantle processes
    in kimberlite. Phys. Chem. Earth 9, pp. 571-604.

Pearce, J.A., and Cann, J.R. (1973): Tectonic setting of basic volcanic rocks determined using trace element analyses. Earth Plan. Sci. Let. 19, pp. 290-300.

Poldervaart, A. (1964): Chemical definition of alkali basalts and tholeiites. Bull. Geol. Soc. Am. 75, pp. 229-232.

Ridley, W.I., Watkins, N.D., and MacFarlane, D.J. (1974): The Oceanic Islands: Azores. In "The Ocean Basins and Margins, Vol. 1: The North Atlantic", Nairn, A.E.M., and Stehli, F.G., Eds., Plenum Press, N.Y. pp. 445-483.

Saggerson, E.P., and Williams, L.A.V. (1964): Ngurumanite from Southern Kenya and its bearing on the origin of rocks in the northern Tanganyika alkaline district. J. Petrology 5, pp. 40-81.

Schilling, J.G. (1973a): Afar mantle plume: rare-earth evidence. Nature Phys. Sci. 242, p. 2.

Schilling, J.G. (1973b): Iceland mantle plume. Nature 242 pp. 565-571.

Schilling, J.G. (1975): Azores mantle blob: Rare-earth evidence. Earth Plan. Sci. Let. 25, pp. 103-115.

Schmincke, H.U. (1973): Magmatic evolution and tectonic regime in the Canary, Madeira, and Azores Island groups. Bull. Geol. Soc. Am. 84 pp. 633-648.

Schmincke, H.U., and Weibel, M. (1972): Chemical study of rocks from Madeira, Porto Santo, Sao Miguel, and Terceira. Jeues Jahrb. Mineralog. Abh. 117, pp. 253-281.

Schwarzer, R.R., and Rogers, John J.W. (1974): A worldwide comparison of alkali olivine basalts and their differentiation trends. Earth Plan. Sci. Let. 23, pp. 286-296.

Stice, G.D. (1968): Petrography of the Manu'a Islands, Samoa. Contr. Miner. Petrology 19, pp. 343-357.

Thornton, C.P., and Tuttle, O.F. (1960): Chemistry of igneous rocks I: Differentiation Index. Am. J. Sci. 258, pp. 664-684.

Upton, B.G., and Wadsworth, W.J. (1966): The basalts of Reunion Island, Indian Ocean. Bull. Volc. 29 pp. 7-23.

Volborth, Alexis (1969): Elemental Analysis in Geochemistry.
    Elsevier, Amsterdam, N.Y. 373 pp.

Walker, G.P.H., and Croasdale, R. (1970): Two Plinian-type
    eruptions in the Azores. J. Geol. Soc. London 127,
    pp. 17-55.

Weston, F.S. (1964): List of recorded volcanic eruptions in
    the Azores with brief reports. Boletim. do Museu e
    Lab. Mineral. e Geol. Lisboa 10, pp. 3-18.

Wilkinson, J.F.G. (1974): The mineralogy and petrography of
    alkali basaltic rocks in "The Alkaline Rocks", Soren-
    sen, H., Ed. John Wiley and Sons, N.Y. pp. 67-95.

Yoder, H.S. (1971): Contemporaneous rhyolite and basalt.
    Carnegie Inst. Washington Yr. Book 69, pp. 141-145.

APPENDIX I: ANALYTICAL METHODS

i) Preparation of Sample Powders

Approximately eight small one-inch diameter cores were taken from each rock unit and combined to form a composite sample for that unit. The cores were crushed in a ceramic jaw crusher and subsequently ground in a tungsten carbide swing mill. The powders were then processed for 10 minutes in a twin shell dry blender to ensure their homogeneity.

ii) Atomic Absorption Analysis

The following elements were analysed by atomic absorption: Al, Fe, Mg, Ca, K, Na, and Mn.

Sample solutions were prepared by the digestion of 0.5 g of sample powder in nitric, perchloric, and hydrofluoric acid on a water bath. The hydrofluoric acid and water were fumed off by placing the crucibles in a sand bath, after which, the samples were acidified with hydrofluoric acid and diluted to 250 c.c. and stored in polyethylene bottles. These sample solutions were then diluted as required to bring the elemental concentrations within a linear working range for atomic absorption. A 20% lanthanum solution was added to each dilution to reduce interferences.

Sample blanks, JB-1 (a standard rock), and duplicates were prepared by the same procedure and analysed with the sample solutions.

The analyses were made on a Beckmann Model Number 503 Atomic Absorption Spectrophotometer. Five standard concentrations and a standard blank were made up for the analysis of each element. A plot of absorption reading versus concentration (ppm) was made for each element to ascertain linearity, and thus, the accuracy of the standard solutions.

iii) Phosphorus Determination

To determine the concentration of P_2O_5 in the samples, a colorimetric method involving the formation of a "molybdenum blue" complex was used after the method of Jeffery, (1970, pp. 367-371).

A 5 cc aliquot of the sample solution prepared for the atomic absorption analysis was added to specially treated 50 cc volumetric flasks. A 20 cc aliquot of a reducing solution composed of sulphuric acid, ammonium molybdate solution, and ascorbic acid was added to each flask, and the solutions diluted to volume. The flasks were allowed to stand overnight to develop the colour. Standard solutions were prepared by the same method.

A Bausch and Lomb Spectronic 70 Spectrophotometer was used to read sample and standard absorbances at a wavelength of 830 nm, using sample and standard blanks as references. The sample concentrations of P_2O_5 were then calculated by comparison with the standard absorbances.

iv) Water Determinations

Total water was determined using a modified Pen-field method after Volborth (1969, pp. 119-123). A 0.5g portion of sample powder was transferred to a specially designed Penfield tube along with 2.5 - 3 g of flux composed of lead dioxide, lead chromate, and sodium tungstate. The end of the tube was heated gently for 10 minutes and then heated strongly for 5 minutes. The bottom bulb containing the powder and the flux was then twisted off using an acetylene torch. The tube was allowed to come to room temperature, was weighed, and then was dried in an oven at $110^{\circ}C$ for 4 hours. The tube was then re-weighed at room temperature and the weight change calculated as weight per cent total water.

H_2O^- was determined on the same day as total water. Approximately 1.0 g of sample powder was weighed into a glass weighing bottle and dried in an oven at $110^{\circ}C$ for 4 hours. The bottles were then covered and removed to a dessicator and allowed to come to room temperature. The bottles were re-weighed and the weight change calculated as weight per cent H_2O^-. H_2O^+ was calculated by subtracting this H_2O^- value from the total water determination.

v) Titanium Determination

Two different methods were used in the analysis of TiO_2: a hydrogen peroxide method (Maxwell, 1968), and

the method of Rigg and Wagenbauer using Tiron (Maxwell, 1968). Both involve the use of the undiluted sample solutions prepared for atomic absorption and the measurement of the absorbance of a yellow titanium complex at a wavelength of 380 mμ.

In the Tiron method, a 3 cc aliquot of sample solution was added to a 50 cc flask. A sodium acetate-acetic acid buffer solution was added along with the Tiron solution and thioglycolic acid. The flask was diluted to volume and allowed to stand for approximately 2 hours to develop the colour. Standard solutions and blanks were prepared at the same time using standard stock solution. The absorbance of the samples at 380 mμ was measured with a Bausch and Lomb Spectronic Spectrophotometer and compared with the standards, and a weight per cent TiO_2 calculated.

The hydrogen peroxide method involved the pipetting of 20 cc of sample solution into 100 cc flasks. A hydrogen peroxide solution was added to each flask, and the flasks were heated on a water bath for 20 minutes. The flasks were cooled, and diluted to volume. The colour was allowed to develop for 2 hours, and the absorbance of standards and samples was measured on the spectrophotometer and compared to obtain a weight per cent TiO_2.

vi) FeO Determination

The method of Wilson (Maxwell, 1968) was used to determine the weight per cent of iron as FeO. A 0.5 g portion of sample powder was weighed out and transferred to a special polyethylene flask. Ammonium metavanadate solution and hydrofluoric acid were added and the flask was covered and agitated at 150 to 200 rpm for 2 days until no gritty particles were visible. An acid mix was then added and the contents of the flask transferred to a 400 cc beaker by washing with a 5% boric acid solution. Ferrous ammonium sulphate was added with an automatic pipette, barium diphenylamine indicator was added, and the solution was titrated with potassium dichromate to a grey end-point. The weight per cent of FeO for each sample was then calculated.

vii) CO_2 Determination

The CO_2 concentration was determined using an automatic CO_2 titrator similar to that used by the Geological Survey of Canada (Bouvier, 1972). CO_2 was evolved by heating 0.25 to 0.5 g of sample with hydrochloric acid for 5 minutes. The evolved gases were passed through a series of traps to remove water and sulphur dioxide, and then trapped in a titrating cell. The CO_2 gas was automatically titrated by a solution of sodium methylate as an electronic eye detected a change

in the blue colour of the trapping solution. The burette readings for the samples were recorded and compared with those of standard rocks to determine the concentration of CO_2.

viii) SiO_2 Determination

SiO_2 was determined by neutron activation analysis using a Dallas counter and sampling system. Sample powders were packed in special plastic rabbits and the weight of the powder recorded. A water (H_2O^-) analysis was determined at the same time, and the recorded weights corrected to dry weight. The samples were paired with standard rocks and both were irradiated for 30 sec. with a 15 Mev source. After a 30 sec. delay, the sample and standard were counted at the 1.78 Mev peak of Al-28 for 200 sec. Each sample-standard pair was irradiated 12 times and counted 6 times by detector A, 6 times by detector B. The SiO_2 concentrations of the samples were calculated by comparison of sample counts to standard counts. Corrections were made for Na_2O, MgO, P_2O_5, Al_2O_3, and total iron as Fe_2O_3.

ix) Trace Element Analysis

The trace element analyses were performed by Dr. Ian Gibson, Bedford College, London by means of X-ray fluorescence analysis on pressed pellets of the sample powders.

APPENDIX II: DISCUSSION OF ERRORS

i) Major Elements

Analyses of these rocks were made at three different times: May, 1974; August, 1974, and February, 1975. With each batch of analyses, a standard rock was run, and comparisons were made with the "accepted" values as a check on the validity of the analyses.

The standard rock, GSJ-JB-1, a basalt, was analysed at three different times. The results are presented in Table A-1, along with the accepted values of Flanagan (1973) and Abbey (1973). The results of Abbey (1973) are on an H_2O^--free basis and therefore are not directly comparable to the values determined in this study for which H_2O^- was not determined. However, Flanagan's (1973) results contain an analysis of H_2O^-. An average of the three values obtained in this study has been calculated, and a percentage difference with the accepted value of Flanagan (1973) has been calculated and presented in Table A-1.

The standard rock, USGS-W-1, a diabase was analysed with the sample batch in February, 1975. The analysed results are presented in Table A-2 with the accepted values of Flanagan (1973) and Abbey (1973). A percentage difference between the values obtained from this study and the values of Flanagan (1973) has also been calculated and included in Table A-2.

TABLE A-1: Comparison of analyses of standard rock GSJ-JB-1

with "accepted" values.

	Flanagan (1973)	Abbey (1973)	May,1974	August 1974	February 1975	Avg. Value	Avg.% Differ.
TiO_2	1.34	1.35	1.34	1.30	–	1.32	1.492
Al_2O_3	14.53	14.67	14.48	14.50	14.48	14.49	0.27
MnO	0.16	0.16	0.15	0.15	0.15	0.15	6.25
MgO	7.70	7.78	7.80	7.74	7.79	7.78	1.039
CaO	9.21	9.30	9.15	9.13	9.26	9.18	0.325
Na_2O	2.79	2.82	2.76	2.74	2.71	2.74	1.792
K_2O	1.42	1.43	1.43	1.41	1.45	1.43	0.704
P_2O_5	0.26	0.26	0.26	0.24	0.25	0.25	3.846
H_2O^+	1.00	1.01	–	–	–		
H_2O^-	0.98	0.00	–	–	–		
CO_2	0.19	0.19	–	–	–		
Total Fe as Fe_2O_3	9.04	9.13	9.17	9.10	8.99	9.09	0.553

TABLE A-2: Comparison of analyses of standard rock USGS-W-1

with "accepted" values.

	Flanagan (1973)	Abbey (1973)	February 1975	Per Cent Difference
TiO_2	1.07	1.07	–	
Al_2O_3	15.00	14.87	14.81	1.27
MnO	0.17	0.17	0.17	0
MgO	6.62	6.63	6.60	0.30
CaO	10.96	10.98	10.90	0.55
Na_2O	2.15	2.15	2.19	1.86
K_2O	0.64	0.64	0.65	1.56
P_2O_5	0.14	0.14	0.13	7.14
H_2O^+	0.53	0.53	–	
H_2O^-	0.16	–	–	
CO_2	0.06	0.06	–	
Total Fe as Fe_2O_3	11.09	11.11	10.97	1.08

In addition to the use of standard rocks, duplicates of some of the samples were analysed to check the precision of the analyses. Table A-3 presents values obtained for duplicates of sample AUL 124.1, and a calculation of the standard deviation.

Original and duplicate values were averaged in cases where the results were similar. However, when the values differed greatly, the result which gave a better total for the whole rock analysis was chosen.

For the silica analysis by gamma-ray Spectrommetry, each sample was counted against a standard five times, and an average value calculated. The maximum acceptable standard deviation was 0.5; although for most samples, standard deviation was less than 0.3.

ii) Trace Elements

Several standard rocks were included with the samples analysed by Dr. Ian Gibson for trace elements. Table A-4 compares the results of Gibson with the accepted values of Flanagan (1973) and Abbey (1973). All values are in ppm.

TABLE A-3:　　Standard deviation of duplicate analyses of
AUL 124.1

	"A"	"B"	Aug. of A + B	Standard Dev.
TiO_2	5.53	3.52	3.52(5)	0.007
Al_2O_3	16.12	16.18	16.15	0.04
Fe_2O_3	10.61	10.59	10.60	0.014
MnO	0.18	0.17	0.17(5)	0.007
MgO	3.17	3.15	3.16	0.014
CaO	8.45	8.53	8.49	0.06
Na_2O	2.95	3.01	2.98	0.04
K_2O	2.36	2.38	2.37	0.01
P_2O_5	0.76	0.74	0.75	0.01

TABLE A-4: Comparison of trace element analyses by Gibson on standard rocks included with Azores Samples with "accepted" values.

		Gibson (1975)	Flanagan (1973)	Abbey (1973)
AGV-1	Nb	15	15	15
	Y	20	21.3	26
	Sr	655	657	660
	Rb	68	67	67
	Zr	197	225	220
BCR-1	Nb	14	13.5	14
	Y	40	37.1	46
	Sr	317	330	330
	Rb	46	46.6	47
	Zr	157	190	185
G-2	Nb	10	13.5	14
	Y	10	12	12
	Sr	475	479	480
	Rb	168	168	170
	Zr	303	300	300
G5P-1	Nb	18 (?)	29	29
	Y	29	30.4	32
	Sr	231	233	230
	Rb	246	254	250
	Zr	512	500	500
W-1	Nb	9	9.5	9.5
	Y	23	21	25
	Sr	185	190	190
	Rb	20	21	21
	Zr	91	105	105

APPENDIX III: PHOTOMICROGRAPHS

PLATE A-1:   AUL 001.2.   A trachyte showing sanidine pheno-
             crysts, small augite phenocrysts. and fluidal
             texture of the feldspar microlites in the
             groundmass.   The dark elongated grains included
             in the sanidine are biotite.   Crossed nicols.
             Magnification: 1.25 X 2.5.

PLATE A-2:   AUL 020.3.   Clinopyroxene accumulate in basalt
             showing inclusion of opaque grains within the
             rim of the large clinopyroxene.   Crossed nicols.
             Magnification: 1.25 X 2.5.
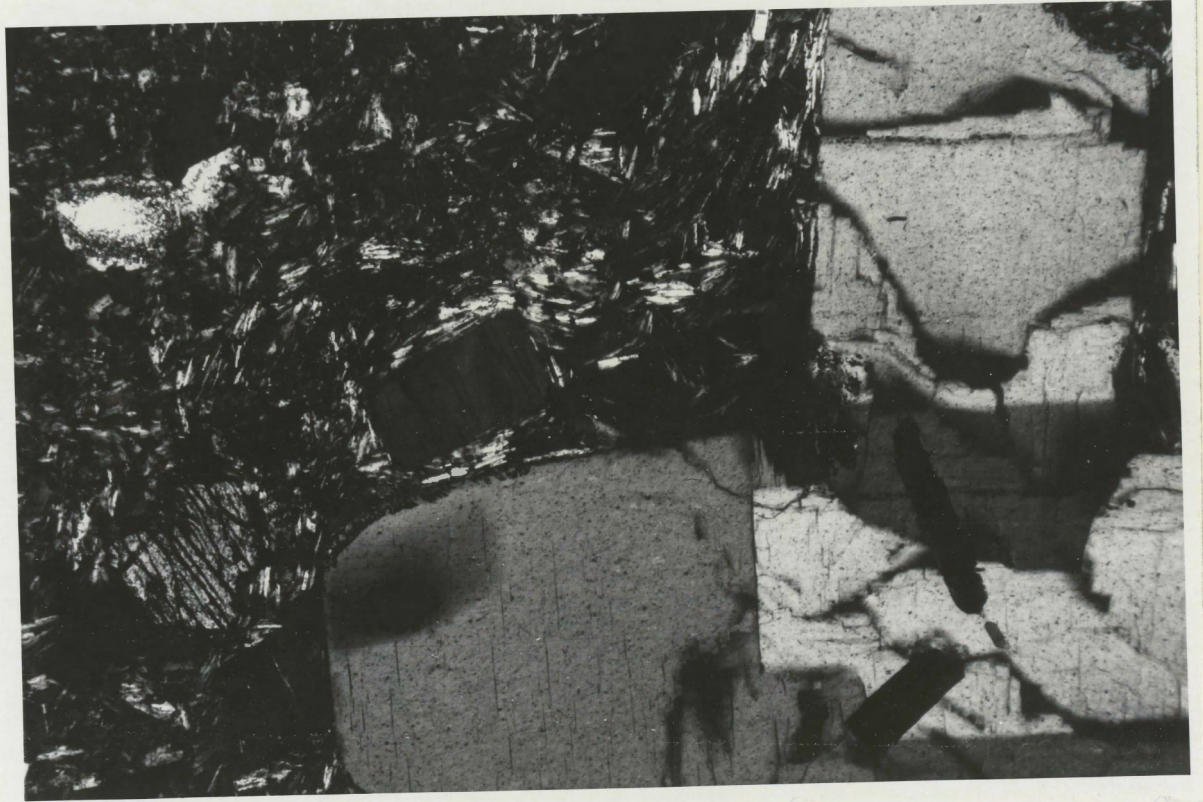
PLATE A-3: AUL 020.3. Serpentinized olivine in basalt
with zoned plaqioclase phenocryst. Crossed
nicols. Maqnification: 1.25 X 2.5.

PLATE A-4: AUL 030.4. Fluidal aliqnment of feldspar
microlites in the qroundmass of a trachyte.
Crossed Nicols. Magnification: 1.25 X 2.5.

PLATE A-5: AUL 051.2. Large zoned clinopyroxene phenocryst.
The core of the phenocryst is green and the rim
purple in plane polarised light. Crossed
nicols. Magnification: 1.25 X 2.5.

PLATE A-6: AUL 098.2. Subfluidal alignment of feldspar
microlites in a trachybasalt. Zoned plagioclase
phenocrysts also present. Crossed Nicols.
Magnification: 1.25 X 2.5.
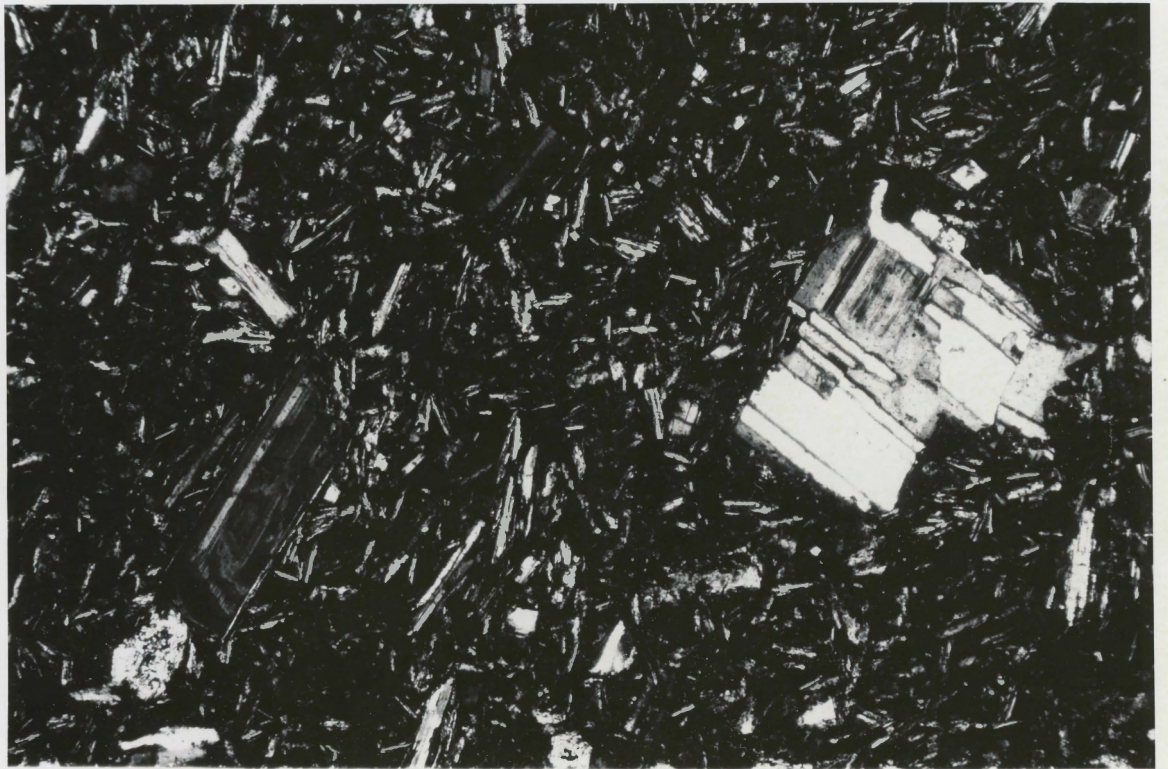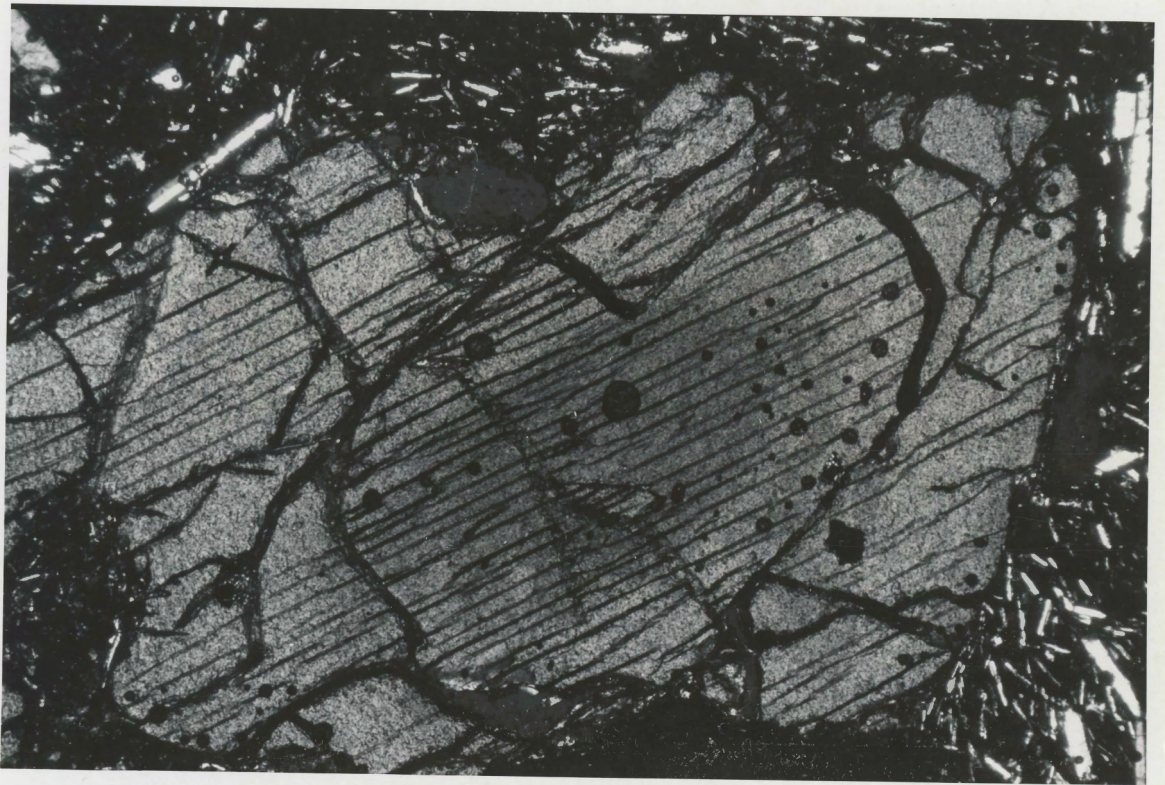
PLATE A-7: AUL 124.1. Fluidal texture in basalt from
           the transition sequence showing plagioclase
           aggregate. Crossed nicols. Magnification:
           1.25 X 2.5.

PLATE A-8: AUL 124.1. Groundmass fluidal texture showing
           alignment of feldspar microlites. Crossed
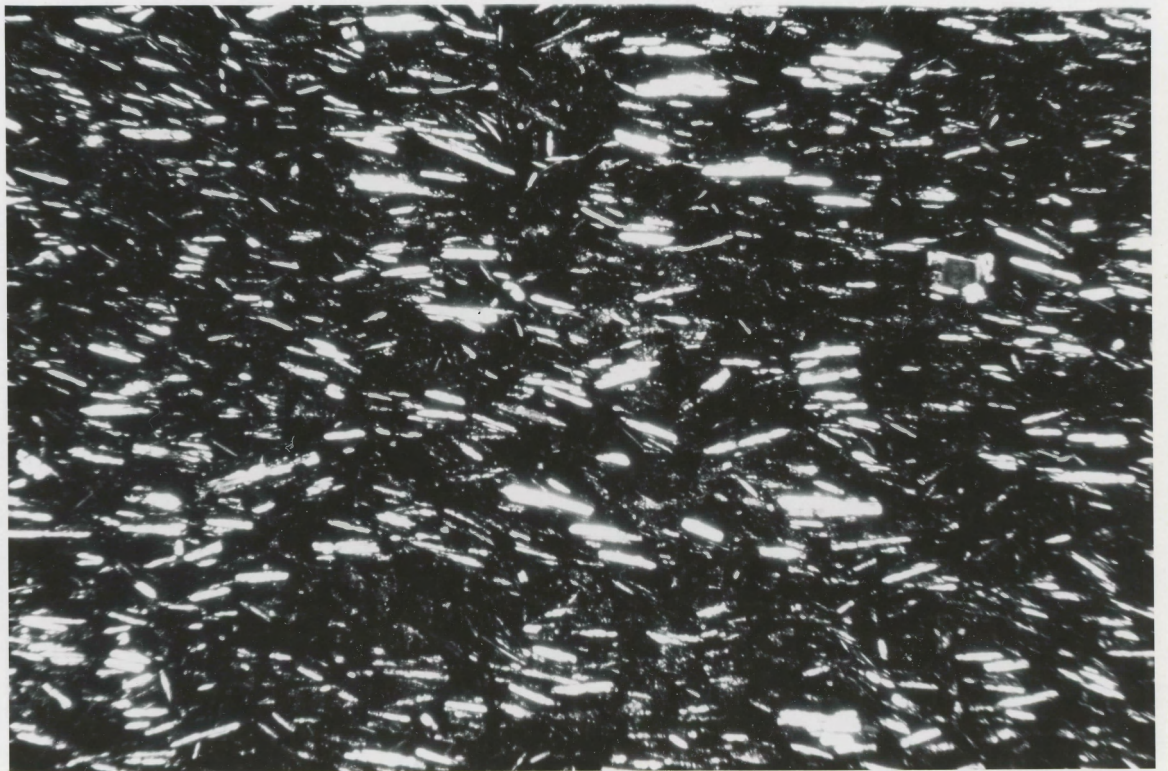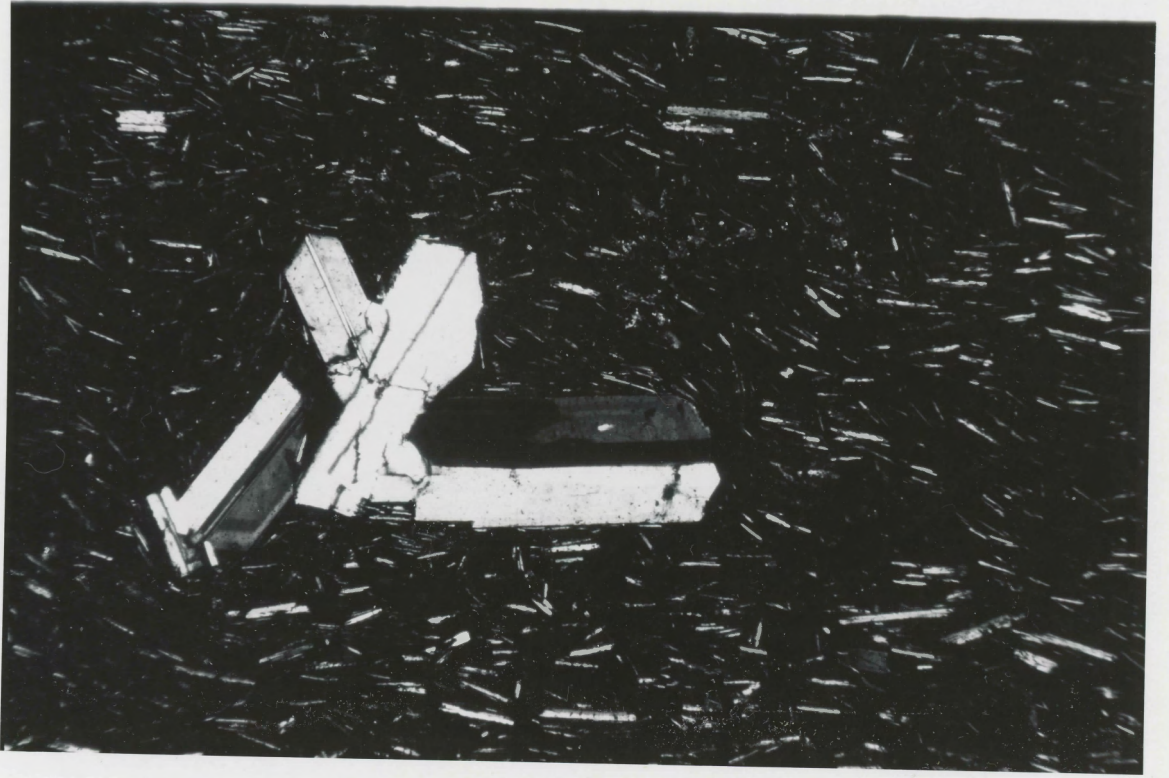   nicols. Magnification: 1.25 X 2.5.

PLATE A-9:   AUL 134.1.   Groundmass texture of a submarine
             basalt.   Crossed nicols.   Magnification:
             1.25 X 2.5.

PLATE A-10:   AUL 030.4.   Sanidine phenocryst and alignment
              of feldspar microlites in the groundmass of
              a trachyte.   Crossed nicols.   Magnification:
              1.25 X 2.5.

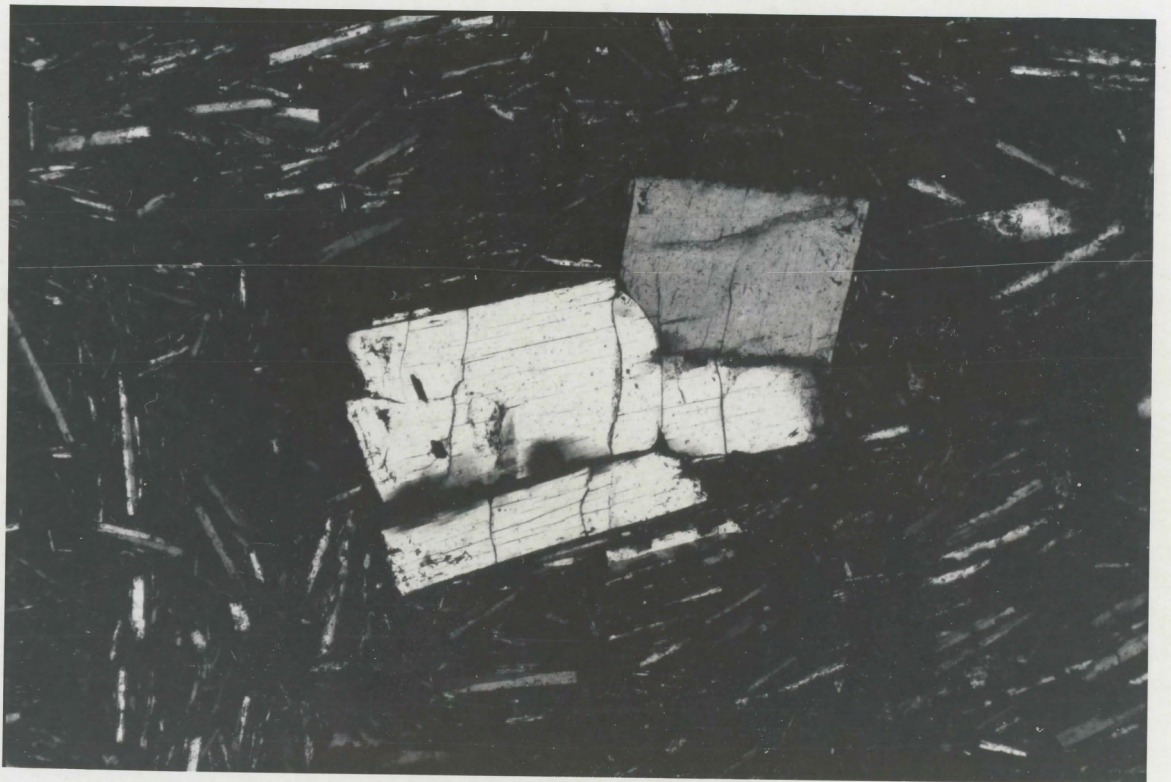PLATE A-11:   AUL 098.2.   Subfluidal texture in a trachy-
              basalt. Crossed nicols. Magnification:
              1.25 X 2.5.